In vitro evaluation of the enzyme inhibition and membrane permeation properties of benzophenones extracted from honeybush

M Raaths

22416498

(B. Pharm)

Dissertation submitted in fulfillment of the requirements for the degree *Magister Scientiae* in Pharmaceutics at the Potchefstroom Campus of the North-West University

Supervisor: Prof JH Hamman

Co-supervisor: Dr CJ Malherbe

November 2016

Luke 1:37
“For nothing will be impossible with God.”

ACKNOWLEDGEMENTS

First and foremostly, I want to say a thank you prayer to my *Heavenly Father* for all the blessings and love He has shown and provided in my life and for giving me the ability and the strength to be where I am today and for always leading me in the right direction where He wants me to be and not where I want to be. I am so thankful for Him for being with me throughout all of these years especially the past two years because although the completion of this dissertation seemed impossible at first it would not have been possible without Him.

To my supervisor Prof JH Hamman, I would like to express my deepest gratitude for all your time, effort, guidance towards the formulation and transport studies and especially your patience towards me, because the process of writing and completing this dissertation could not have been possible without you. I have learned so much from you and I couldn't have asked for a better supervisor. I also want to thank you specially, for providing the rest of the funds and excipients needed for my project.

I would also like to extend my gratitude to my co-supervisor, Dr CJ Malherbe, for providing me with a bursary and for all of your help and generosity when I visited the ARC at Stellenbosch. I am extremely grateful for your assistance in showing me how enzyme inhibition procedures work, I have learned so much from you and I am thankful to have you as my co-supervisor to help me to complete my dissertation. I would also want to thank you sincerely for conducting the analytical procedures including the rest of the enzyme inhibition work and for providing the rest of the funds needed for the research project from your NRF Thuthuka fund.

Prof L.H. du Plessis, thank you so much for your kindness and input with GraphPad Prism, for helping me to understand it better.

To my mom, I am grateful for the time I had with you. I still miss you a lot and you will always be in my heart. Whenever life seems tough, I just think of you and just know it will get better. I am also thankful for my father for guiding me into becoming the person I am today.

To my wonderful husband, Werner, who has always been my pillar of strength, motivating and supporting me through everything and never having any lack of faith in my capabilities and always being by my side and for his kindness and for loving me through it all. You mean the world to me. Love you so much.

I am particularly grateful for my mother and father in law, Wilna and Willie, I would not have come this far if it hadn't been for you. Although you are not my blood family, you are the parents I never had and you are the ones who've always been there for me and accepting me for whom I am and

loving me unconditionally and helping me through some tough times. I really appreciate everything you have done for me and I love you infinitely so.

Grandma Rina, I cannot express in words how much you mean to me, I am so fortunate to have you in my life. Thank you for always supporting me with your loving heart and motivating words and for all your encouragement over the years. I love you very much.

My dearest friends Daneille, Esmerelda, Eljane, Lizel and Trunelle you are like angels sent from above. Thank you for your friendship, for always being there for me, cheering me up in difficult times, encouraging me and always listening to me when I needed you the most.

Last, but not the least, everyone else whom I've encountered the last two years, acquaintances and my colleagues at the NWU with whom I have formed new friendship bonds. Each one of you have a special place in my heart and your friendship means a lot to me and you will never be forgotten.

ABSTRACT

Tea prepared from the honeybush (*Cyclopia spp.)* plant has become a popular beverage and has been shown to possess medicinal properties. Honeybush plants contain phytochemicals that can contribute to the prevention of certain diseases. One mechanism through which glucose and fat uptake can be controlled by honeybush tea is enzyme inhibition in the gastrointestinal tract. The aim of this study was to determine the enzyme inhibition (i.e. lipase and α-glucosidase) effect of crude honeybush extracts, benzophenone rich fractions and xanthone rich fractions from *Cyclopia genistoides*. The *in vitro* permeation of marker molecules (i.e. benzophenone and xanthone molecules) after application of the crude extracts and fractions across excised intestinal epithelial tissues was also investigated. In addition, a non-effervescent, floating gastro-retentive drug delivery system containing honeybush extract was developed and evaluated.

The lipase and α-glucosidase inhibition activity of the crude extracts and isolated rich fractions was determined through various fluorometric methods. The transport experiments were conducted across excised pig intestinal tissues in Sweetana Grass diffusion chambers. Gastro-retentive tablets were compressed from beads consisting of low-density polymers (i.e. polypropylene and polystyrene divinylbenzene), which were prepared by means of extrusion spheronisation. The tablets were evaluated in terms of buoyancy, disintegration, friability, hardness and dissolution. Samples obtained from the transport and dissolution experiments were analysed by means of ultra-high performance liquid chromatography (UHPLC).

The crude extract ARC188 has presented with better inhibition against the rat α-glucosidase and pig lipase enzymes (IC_{50} = 150 µg/ml and IC_{50} = 198 µg/ml, respectively) than the crude extract ARC189 (IC_{50} = 186 µg/ml and IC_{50} = 730 µg/ml, respectively). In addition, the crude extracts and fractions presented with better inhibitory activity against the α-glucosidase than against the lipase.

Relatively low transport in the apical-to-basolateral (A-B) direction was obtained for the honeybush marker molecules across excised pig intestinal tissues from both the crude extracts (ARC188 P_{app}: 3-β-D-glucopyranosyl-4-β-D-glucopyranosyloxyiriflophenone (IDG) = $4.95x10^{-7}$ cm/s; 3-β-D-glucopyranosyliriflophenone (I3G) = $2.38x10^{-7}$ cm/s; mangiferin = $2.09x10^{-7}$ cm/s and isomangiferin = $3.49x10^{-7}$ cm/s; ARC189 P_{app}: IDG = $1.00x10^{-7}$ cm/s; I3G = $3.18x10^{-7}$ cm/s; mangiferin = $3.92x10^{-7}$ cm/s and isomangiferin = $5.40x10^{-7}$ cm/s), but efflux transport occurred in almost all the groups showing higher P_{app} values for the basolateral-to-apical (B-A) direction (ARC188 P_{app}: IDG = $6.74x10^{-7}$ cm/s; I3G = $4.52x10^{-7}$ cm/s; mangiferin = $3.00x10^{-7}$ cm/s and isomangiferin = $4.55x10^{-7}$ cm/s; ARC189 P_{app}: IDG = $1.10x10^{-7}$ cm/s; I3G = $1.22x10^{-7}$ cm/s; mangiferin = $3.90x10^{-7}$ cm/s and isomangiferin = $6.44x10^{-7}$ cm/s).

A gastro-retentive dosage form was successfully produced that showed acceptable buoyancy and release of marker molecules. The relatively low intestinal epithelial permeation of phytochemicals from honeybush is beneficial for local effects in the gastrointestinal tract and may prevent downstream side effects, while the moderate enzyme inhibition combined with a gastro-retentive delivery system has potential in preventing and alleviating diseases such as diabetes mellitus type 2 and obesity.

Key words: Honeybush; *Cyclopia genistoides*; enzyme inhibition; lipase; α-glucosidase; *in vitro* permeation; Sweetana Grass diffusion chambers; non-effervescent; gastro-retentive drug delivery system; polypropylene; polystyrene divinylbenzene

Uittreksel

Tee wat voorberei word met heuningbos (Cyclopia *spp.*) plante het 'n gewilde drankie geword en daar is bestaande bewyse dat hierdie plant spesie medisinale eienskappe besit. Heuningbos plante bevat fitochemiese komponente wat kan bydra tot die voorkoming van sekere siektetoestande. Een van die meganismes waardeur glukose en vetopname beheer kan word deur heuningbostee is deur middel van ensiem inhibisie eienskappe in die spysverteringskanaal. Die doel van hierdie studie was om die ensiem inhibitoriese (lipase en α-glucosidase) effek te bepaal van die ru-ekstrakte, bensofenoon ryk fraksies en xantoon ryk fraksies van *Cyclopia genistoides*. Die *in vitro* deurlaatbaarheid van die enkel bensofenoon en xantoon komponente na toediening van hierdie ru-ekstrakte en fraksies oor uitgesnyde gastrointestinale kanaal epiteelweefsels is ook ondersoek. Verder is 'n nie-bruisende, gastro-retentiewe geneesmiddelafleweringsisteem wat heuningbos ekstrak bevat ontwikkel en geëvalueer.

Die lipase en α-glukosidase inhibitoriese aktiwiteit van die ru-ekstrakte en geïsoleerde fraksies was bepaal deur verskeie fluorometriese metodes. Die transport eksperimente was uitgevoer op varkdermweefsel op die Sweetana Grass diffusie-apparaat. Gastro-retentiewe tablette was saamgepers uit krale wat bestaan het uit lae-digtheid polimere (d.i. polipropileen en polistireen divinielbenseen), wat berei was deur ekstrusie sferonisasie. Die tablette was geëvalueer in terme van hul dryfbaarheid, disintegrasie, brosheid, hardheid en vrystellingseienskappe. Monsters wat verkry was uit die transport en dissolusie eksperimente was ontleed deur middel van ultra-hoë verrigtings vloeistof chromatografie (UHPLC).

Die ru-ekstrak ARC188 het beter inhibisie getoon teenoor die rot alfa-glukosidase en vark lipase (IC_{50} = 150 µg/ml en IC_{50} = 198 µg/ml, respektiewelik) in vergelyking met die ARC189 ru-ekstrak (IC_{50} = 186 µg/ml en IC_{50} = 730 µg/ml, respektiewelik). Die geïsoleerde fraksies het ook beter inhibitoriese aktiwiteit getoon teenoor die rot α-glucosidase in vergelyking met die varklipase.

Relatiewe lae transport was verkry in die apikaal-tot-basolaterale (AB) rigting vir die heuningbos merkermolekules oor die varkderm weefsel vir beide die ru-ekstrakte (ARC188 P_{app}: 3-β-D-glucopyranosyl-4-β-D-glucopyranosyloxyiriflophenone (IDG) = $4.95x10^{-7}$ cm/s; 3-β-D-glucopyranosyliriflophenone (I3G) = $2.38x10^{-7}$ cm/s; mangiferin = $2.09x10^{-7}$ cm/s and isomangiferin = $3.49x10^{-7}$ cm/s; ARC189 P_{app}: IDG = $1.00x10^{-7}$ cm/s; I3G = $3.18x10^{-7}$ cm/s; mangiferin = $3.92x10^{-7}$ cm/s and isomangiferin = $5.40x10^{-7}$ cm/s), maar effluks transport was ook verkry in amper al die groepe (ARC188 P_{app}: IDG = $6.74x10^{-7}$ cm/s; I3G = $4.52x10^{-7}$ cm/s; mangiferin = $3.00x10^{-7}$ cm/s and isomangiferin = $4.55x10^{-7}$ cm/s; ARC189 P_{app}: IDG = $1.10x10^{-7}$ cm/s; I3G = $1.22x10^{-7}$ cm/s; mangiferin = $3.90x10^{-7}$ cm/s and isomangiferin = $6.44x10^{-7}$ cm/s).

’n Gastro-retentiewe doseervorm was suksesvol ontwerp wat aanvaarbare dryfvermoë en vrystelling van merker molekules getoon het. Die relatiewe lae dermepiteel deurlaatbaarheid van die fitochemiese komponente van heuningbos is veral voordelig vir plaaslike effekte in die gastrointestinale kanaal en kan verdere newe-effekte dalk voorkom, terwyl die matige ensiem inhibitoriese eienskappe wat gekombineer word in 'n gastro-retentiewe afleweringstelsel die potensiaal besit om siektes soos diabetes mellitus tipe 2 en vetsug se simptome te kan verlig en voorkom.

Sleutelterme: Heuningbos; *Cyclopia genistoides*; ensiem inhibisie; lipase; α-glukosidase; *in vitro* deurlaatbaarheid; Sweetana-Grass diffusieapparaat; nie-bruisende; gastro-retentiewe geneesmiddel aflewering sisteem; polipropileen; polistireen divinielbenseen

CONFERENCE PROCEEDINGS

Madelaine Raaths, Lissinda H. du Plessis, Christiaan J. Malherbe, Josias H. Hamman. 2016. *In vitro* evaluation of the enzyme inhibition and membrane permeation properties of benzophenones extracted from honeybush. Poster presented at the All Africa Congress on Pharmacology and Pharmacy (Misty Hills conference centre, Muldersdrift, Johannesburg).

The event was jointly hosted by the Tshwane University of Technology and the Sefako Makgatho Health Sciences University.

Herewith the awards received for the poster at the congress: a) Runner-Up of the best poster prize – APSSA and b) Separations prize for the best poster with a chromatography element (See Appendix A)

TABLE OF CONTENTS

CHAPTER 3

METHODS AND MATERIALS

CHAPTER 4

RESULTS AND DISCUSSION

CHAPTER 5

FINAL CONCLUSIONS AND FUTURE RECOMMENDATIONS

LIST OF TABLES

LIST OF FIGURES

LIST OF ABBREVIATIONS

AMPK	Adenosine 5′-monophosphate-activated protein kinase
AOR	Angle of repose
AP-BL	Apical to basolateral
API	Active pharmaceutical ingredients
BL-AP	Basolateral to apical
Caco-2	Human caucasian colon adenocarcinoma cell lines
CI	Confidence interval
CO_2	Carbon dioxide
DMSO	Dimethyl sulfoxide
ER	Efflux ratio
HBA	Hydrogen bond acceptors
HBD	Hydrogen bond donors
HCl	Hydrochloric acid
HPLC	High performance liquid chromatography
HPLC-DAD	High performance liquid chromatography with diode array detection
I3G	3-β-D-glucopyranosyliriflophenone
IDG	3-β-D-glucopyranosyl-4-β -D-glucopyranosyloxyiriflophenone
KH_2PO_4	Potassium phosphate buffer
KOH	Potassium hydroxide
KRB	Krebs-Ringer bicarbonate
LC/MS	Liquid chromatography linked to mass spectrometry
M3G	3-β-D-glucopyranosylmaclurin

MCC	Microcrystalline cellulose
MDT	Mean dissolution time
MUB	4-Methylumbelliferyl butyrate
MUG	4-Methylumbelliferyl-α-D-glucopyranoside
MUPS	Multi-unit pellet systems
MW	Molecular weight
NetFL	Net fluorescence
O_2	Oxygen
PAMPA	Parallel artificial membrane permeability
P_{app}	Apparent permeability coefficient
PDC	Polystyrene divinylbenzene
P-gp	P-glycoprotein
PP	Polypropylene
PPL	Porcine pancreatic lipase
PSA	Polar surface area
RB	Rotatable bonds
RFUs	Relative fluorescence units
RIAP	Rat intestinal acetone powder
ROS	Reactive oxygen species
SD	Standard deviation
T2DM	Type 2 diabetes mellitus
TEER	Transepithelial electrical resistance
UHPLC	Ultra-high performance liquid chromatography

UHPLC-DAD	Ultra-high performance liquid chromatography with diode array detection
USA	United States of America
UV	Ultra violet

CHAPTER 1
INTRODUCTION

1.1 BACKGROUND INFORMATION

For centuries, many cultural groups around the world relied on medicinal plants to help promote health, mainly because people tend to believe natural products have lesser side-effects than synthetic drugs. An estimated amount of about 20 000 medicinal plants are currently used in cosmetic and medicinal products over a wide spread of industries, which has led to substantial investment in ethnobotany research of herbal medicine for the assurance of high quality and safety of these products. The majority of modern medicines have been derived from medicinal plants, which contain phytochemicals as secondary metabolites in different plant parts (Bahadur *et al*., 2007; Cragg and Newman, 2013). Mehta *et al*. (2015) mentions that over 50% of all drugs recorded in the Western pharmacopoeia are of herb and plant origin, which were either isolated or chemically modified for therapeutic use. It is also known that the economy benefits on a large scale globally and nationally from medicinal plants.

Ethnobotany is a well-known source to find new cures for metabolic diseases such as diabetes and obesity also known as “diabesity” (Astrup and Finer, 2000). The International Diabetes Federation have supporting evidence that indicates over 2 million of the South African population suffer from diabetes and 61% of the people are corpulent (Baleta and Mitchell, 2014). Shaw *et al*. (2010) predicted that over the coming decade, there will be an approximate 70% increase in people diagnosed with diabetes in countries with developing economies and a 20% increase in countries with developed economies.

Diabetes is considered a great health risk as it can lead to microvascular and macrovascular complications because it is a chronic disease that people are struggling to manage. A few key concepts associated with people suffering from type 2 diabetes mellitus (T2DM) include the following: people are resistant against insulin uptake in the skeletal muscle, liver and adipose tissue which are the main insulin responsive tissues; they suffer from abnormal insulin secretion causing their β-cell function to decrease and they have a higher hepatic gluconeogenesis. Other factors also relevant to T2DM include an increase in lipolysis, a decrease in incretin, hyperglucagonemia and an increase in renal glucose reabsorption (Powers and D´Alessio, 2011). Several suggestions have stated that insulin resistance can lead to the development of T2DM and can be triggered from an increase of reactive oxygen

species (ROS) levels, which can be suppressed through anti-oxidant therapy (Houstis *et al.,* 2006).

"Diabesity" is a great concern and affects the global population at a high prevalence. The International Diabetes Federation (2015) mentions that there are approximately 415 million people (between the age of 20-79) struggling with this disease, which will increase with 227 million people in the next 25 years. The fact that approximately 42 million children (under the age of 5 years) are struggling with obesity might be due to an increased exposure to an obesogenic environment, which are becoming more of an epidemic problem. Therefore, global strategies need to be in place to help manage and prevent "diabesity" through the implementation of a healthy lifestyle or utilising traditional herbal products known to be safe and of good quality (WHO, 2016).

Insulin resistance is the cause of more than 80% of T2DM and one of the main factors contributing to obesity. A high glucose intake and a state of inactivity are major factors contributing to "diabesity" leading to uncontrolled plasma glucose concentrations. Glucose is an import energy source for your brain to be able to function normally and during an exercise session the skeletal muscles requires energy, which is obtained from glucose after it's produced through hepatic gluconeogenesis (glucose produced by the liver) (Powers and D´Alessio, 2011).

Although potent synthetic enzyme inhibitors are available, natural inhibitors such as benzophenones and xanthones present in honeybush tea may be considered a safer option. Surya *et al*. (2014) stated that there are approximately 350 plant species utilized as traditional medicine for potential treatment of "diabesity". The InterAct Consortium (2012) have concluded that if a person drinks approximately 4 cups of tea per day (i.e. either black, herbal or green tea) containing flavonoids they might have a 16% less chance to develop T2DM in comparison to people who don't drink any tea. Extracts such as benzophenones and xanthones present in honeybush tea may help to prevent or manage "diabesity" (De Beer *et al*., 2012; Jo *et al*., 2013; Matkowski *et al*., 2013; Muller *et al*., 2011).

In order to determine by which mechanism the benzophenones and xanthones present in honeybush tea can prevent "diabesity", it is very important to evaluate their enzyme inhibition properties (e.g. lipase and α-glucosidase activity). Of subsequent importance are their membrane permeation properties since some biological activities occur locally in the gastrointestinal tract (e.g. enzyme inhibition) and some biological activities occur systemically (e.g. anti-oxidant activities).

1.2 RESEARCH PROBLEM

Honeybush tea is a health promoting beverage for the prevention of certain diseases, but information regarding the mechanisms of action of honeybush tea active chemical components is still incomplete. Furthermore, very little information is available on the bioavailability of phytochemicals in honeybush tea and controlled delivery of these phytochemicals may contribute to improved action. This study is therefore needed to identify the potential inhibiting effects of crude extracts, benzophenone rich fractions and xanthone rich fractions from honeybush (*Cyclopia genistoides*) on selected gastro-intestinal enzymes. It is also important to evaluate the *in vitro* epithelial permeability of honeybush phytochemicals in order to get an indication of their absorption and bioavailability after oral intake.

Honeybush is often ingested in the form of a tea or infusion that may not provide optimum levels of the active constituents in the gastro-intestinal tract or in the systemic circulation for long periods of time. After intake of immediate release dosage forms, a relatively quick rise in concentration of the active substances over a short period of time in the systemic circulation does not provide biological activity over prolonged time periods. One way to overcome this problem is to formulate the honeybush extract into a gastro-retentive dosage form that releases the extract over an extended period of time and thereby could maintain concentration levels over an extended period of time in the gastro-intestinal tract and/or systemic circulation.

1.3 AIM AND OBJECTIVES OF STUDY

The aim of this study involves three aspects of honeybush extracts, namely to determine their lipase and α-glucosidase inhibition properties, to investigate the intestinal epithelial permeation of marker molecules from the honeybush extracts and to develop a gastro-retentive delivery system containing honeybush extract.

In order to reach this aim, the following objectives need to be achieved:

- To chemically characterise honeybush extracts (i.e. crude extract, benzophenone rich fraction and xanthone rich fraction) by means of high performance liquid chromatography with diode-array detection (HPLC-DAD).
- To determine the lipase and α-glucosidase enzyme inhibition activity of the different honeybush extracts, by means of various fluorometric methods.

- To conduct bi-directional *in vitro* permeation studies on the different honeybush extracts across excised pig intestinal tissues using the Sweetana-Grass diffusion apparatus.

- To determine whether efflux transport occurred for all the marker molecules analysed in the transport studies.

- To develop and evaluate a gastro-retentive delivery system for sustained release of honeybush tea extract.

- To analyse marker molecules (i.e. selected benzophenones and xanthones) in the transport and dissolution samples by means of ultra-high performance liquid chromatography (UHPLC) method.

1.4 ETHICAL ASPECTS OF RESEARCH

The intestinal excised tissue was directly obtained from slaughtered pigs at the local abattoir (Potch Abattoir, Potchefstroom, South Africa). The excised tissues were disposed after the experiments by means of approved procedure. Since pigs are slaughtered for meat production purposes at the abattoir, there are no ethical aspects related directly to the animals, but an application was submitted to the Animal Ethics Committee of the North-West University for the use of excised pig tissues in the *in vitro* pharmacokinetic studies, which has been approved (NWU-00025-15-A5) (Appendix A).

1.5 CONTRIBUTION OF CANDIDATE, OUTSOURCING AND CONTRACTING

The candidate was responsible for the following experimental procedures:

- Partial section of the α-glucosidase enzyme inhibition studies
- Bi-directional *in vitro* permeation studies
- Development of a sustained release non-effervescent gastro-retentive delivery system of honeybush tea extract.

Dr. CJ Malherbe at the Agricultural Research Council, Infruitec-Nietvoorbij at Stellenbosch supplied the chromatograms, preformed the extraction of chemical compounds from honeybush plant and fractionations of the extracts including the lipase enzyme inhibition and the rest of the α-glucosidase inhibition studies as well as the ultra-high performance liquid chromatography with diode array detection (UHPLC-DAD) and high performance liquid chromatography with diode array detection (HPLC-DAD).

CHAPTER 2

LITERATURE OVERVIEW

2.1 INTRODUCTION

Tea is a hot beverage that can be prepared from different plant species and can be distinguished into two groups, namely “regular teas” and “herbal teas”. Conventionally consumed tea (i.e. black, green, white, yellow and oolong tea) originates from the shrub *Camellia sinensis,* whereas herbal teas are prepared from a different plant species than *Camellia sinensis* (e.g. honeybush tea is prepared from various *Cyclopia* species, while rooibos tea is prepared from *Aspalathus linearis*) (Desideri *et al*., 2011; Joubert and De Beer, 2011; Joubert *et al*., 2011; Van Wyk and Wink, 2009; Zhao *et al*., 2013). Herbal teas not only have enticing flavours and smells, but preparation time is relatively quick with minor possibility of side effects (Tschiggerl and Bucar, 2012).

According to Quispe *et al*. (2012), certain properties of herbal teas are of great significance for human health and they should be considered as a daily supplement considering they are a rich source of anti-oxidant components. Paddy *et al*. (2015) reported that there are several herbal tea products on the market that are sold to benefit people with health problems including metabolic diseases such as diabetes and obesity (also known as “diabesity”). Honeybush is one of the herbal teas which may help prevent and treat this disease.

2.2 BOTANY OF HONEYBUSH (*CYCLOPIA* SPECIES)

The name “honeybush” has originally been derived from the flowers of the plant from which honeybush tea is prepared that smell like honey (Herbst, 2014; Iwu, 2014; Van Wyk and Wink, 2009). There are approximately 25 different *Cyclopia* species that are referred to as “honeybush”, but two of the species are extinct (*C. filiformis and C. laxiflora*) and the remaining 23 species consist of *C. alopecuroides, C. alpina, C. aurescens, C. bolusii, C. bowieana, C. burtonii, C. buxifolia, C. falcata, C. filiformis, C. galioides, C. genistoides, C. glabra, C. intermedia, C. latifolia, C. laxiflora, C. longifolia, C. maculata, C. meyeriana, C. plicata, C. pubescens, C. sessiliflora, C. subternata* and *C. squamosa* (Kies, 1951; Schutte, 2012). Each of these *Cyclopia* species has its own unique characteristics by which it can be identified as summarised in Table 2.1.

Honeybush species have wooden stalks with relatively small leaves attached to it (Du Toit and Joubert, 1998). The individual plant species have different leaf-shapes and flower petals with

prominent grooves, but in general they are all recognizable by their flowers which have a resplendent yellow colour (because of the luteolin pigment). Their leaves are divided into three leaflets that can be distinguish from a cylindrical shape to an almost flattened shape (Du Toit *et al*., 1998; Herbst, 2014; Joubert *et al*., 2011; Kies, 1951; Van Wyk and Wink, 2009).

Table 2.1: Description of the different *Cyclopia* species including their blooming period and geological region of occurrence (Harvey, 1868; Joubert *et al*., 2011; Kies, 1951; Schutte, 1997; Schutte, 2012)

Species	Plant description	Geological region of occurrence	Blooming period
C. alopecuroides	• Rigidly upright • Re-sprouting or re-seeding plant specie • Grows ± 60 cm • Yellow flowers	• Found in Subalpine mountain fynbos • Between Swartberg and Kammanassie mountain • Distributed ± 1500-2000 m at high altitude	• Sept-Dec
C. alpina	• Sprawling and re-sprouting plant species • Grows ± 30 cm • Yellow flowers	• Found in sandstone slopes at high altitude • From Hex River to Hottentots Holland to Kammanassie mountains • Distributed ± 1170-2070 m at high altitude	• Nov-Dec
C. aurescens	• Rigidly upright and resprouting plant species • Rich scent • Grows ± 70 cm • Yellow flowers	• Found in Subalpine mountain fynbos • Klein Swartberg • Distributed 1800 m above high altitude	• Oct-Dec
C. bolusii	• Sprawling and re-sprouting plant species • Grows ± 30 cm • Yellow flowers	• Found in Subalpine mountain fynbos • Groot Swartberg • Distributed ±1900-2270 m at high altitude	• Nov-Jan
C. bowieana	• Rigidly upright • Sturdy scent • Prolifically re-sprouting or re-seeding plant species • Grows ± 1.8 m Yellow flower colour with the bracts attached to base of calyx	• Found in mountain fynbos in upper slopes • Between Langeberg and Outeniqua mountains • Distributed ± 1220-1830 m at high altitude	• Oct-Dec

C. burtonii	• Reseeding plant species • Rich scent • Grows ± 80 cm • Yellow flowers	• Found in Subalpine mountain fynbos in sandstone slopes • Groot Swartberg • Distributed ± 1600-2070 m at high altitude	• Oct-Dec
C. buxifolia	• Rigidly upright almost flat re-sprouting plant species • Rich scent • Grows ± 2 m • Yellow flowers	• Found in mountain fynbos in sandstone slopes • From Cold Bokkeveld to Outeniqua mountains Distributed ± 830-1670 m at high altitude	• Sept
C. falcata	• Rigidly upright and re-sprouting plant species • Rich scent • Grows ± 1.5 m • Yellow flowers	• Found in mountain fynbos in sandstone slopes • From Cold Bokkeveld mountains to Caledon Swartberg Distributed ± 550-1600 m at high altitude	• Sept-Nov
C. filiformis	• Rigidly upright, not known if it is a reseeding plant specie Yellow flower colour with the calyx lobes three-sided to a point	• Found in lowland fynbos in sandy flats • Van Staden's mountains • Distributed for about 100 m at high altitude	• Oct
C. galioides	• Rich scent, • Covered with soft hairs, • Re-sprouting plant species • Grows ± 1 m • Yellow flowers	• Found in lowland fynbos between flats and slopes • Cape Peninsula • Distributed ± 160-700 m at high altitude	• Jan-May
C. genistoides	• Rigidly upright, Re-sprouting plant species • Rich scent • Grows ± 2 m • Yellow flowers	• Found in lowland fynbos between flats and slopes • Cape Peninsula • Distributed ± 160-700 m at high altitude	• Aug-Sept
C. glabra	• Rich scent, • Re-sprouting plant species • Grows ± 1.2 m Yellow flower with the bracts attached to base of calyx	• Found in Subalpine mountain fynbos • Hex River mountains • Distributed ± 1660-2249 m at high altitude	• Nov-Dec
C. intermedia	• Rigidly upright re-sprouting plant species • Rich scent • Grows ± 2 m • Yellow flowers	• Found in mountain fynbos in sandstone slopes • From Witteberg and Langeberg to Van Staden's mountains • Distributed ± 500-1700 m at high altitude	• Sept-Nov

C. latifolia	• Rigidly upright and re-seeding plant species • Grows ± 1 m • Yellow flowers	• Found in mountain fynbos in sandstone slopes • Cape Peninsula • Distributed ± 900-1000 m at high altitude	• Sept-Nov
C. laxiflora	• Rigidly upright, not known if it is a re-seeding plant species • Yellow flowers	• Found in lowland fynbos in sandy flats • In Knysna and Plettenberg Bay	• Sept
C. longifolia	• Rigidly upright and re-seeding plant species • Grows ± 3 m • Bright yellow flowers	• Found in lowland fynbos in sandy slopes and flats • Van Staden's mountains • Distributed ± 300-360 m at high altitude	• Sept-Oct
C. maculata	• Rigidly upright and re-seeding plant species • Grows ± 3.5 m • Yellow flowers	• Found at stream-sides in lowland fynbos • From Bain's Kloof to Riversdale • Distributed ± 150-830 m at high altitude	• Aug-Sept
C. meyeriana	• Rigidly upright and re-seeding plant species • Grows ± 2 m Yellow flower colour with the bracts attached to base of calyx	• Found in mountain fynbos in upper slopes • From Cedarberg to Riviersonderend mountains • Distributed ± 1000-1800 m at high altitude	• Sept-Dec
C. plicata	• Rigidly upright and re-seeding plant that are branched widely • Grows ± 1.7 m • Yellow flower colour with the bracts clearly pleated with circular apices and the calyx lobes clearly bi-lobed and dense.	• Emerge from shale bands on sandstone slopes in mountain fynbos • Between Kammanassie and Kouga mountains • Distributed ± 1000-1700 m at high altitude	• Sept
C. pubescens	• Rigidly upright and re-seeding plant species • Grows ± 1.7 m • Yellow flower colour with the bracts pleated with rounded apices and the calyx lobes dense and narrowed	• Found in marshes and seeps in lowland fynbos • In Port Elizabeth • Distributed for about 300 m at high altitude	• Sept
C. sessiliflora	• Rigidly upright, re-sprouting plant species	• Found in mountain fynbos in sandstone slopes	• May-Jun

	• Rich scent • Grows ± 1 m • Pale yellow flowers	• Between Warmwaterberg and Langeberg • Distributed ± 300-1500 m at high altitude	
C. subternata	• Rigidly upright and re-seeding plant species • Grows ± 3.5 m • Yellow flowers	• Found in mountain fynbos in sandstone slopes • From Langeberg to Tsitsikamma mountains • Distributed ± 160-1000 m at high altitude	• Sept
C. squamosa	• Re-seeding plant species • Yellow flowers	• Found in mountain fynbos between the southern slopes and deep peaty soils • Wemmershoek mountains • Distributed ± 1700 m at high altitude	• Oct

The genus *Cyclopia* is part of the legume family (Fabaceae), which thrives mainly in the "fynbos biome" of the Eastern and Western regions of the Cape Province of South Africa (Anon., 2014; De Nysschen *et al*., 1996; Du Toit and Joubert, 1998; Iwu, 2014; Le Roux *et al*., 2008; Marnewick, 2009; Van Wyk, 2008). Herbal infusions with a sweet honey-like taste are commercially made from the leaves and twigs of *Cyclopia* species and are commonly referred to as 'honeybush tea'.

The flowers such as shown in Figure 2.1 are not required as an ingredient in honeybush tea, but can enhance the flavour if included (Du Toit *et al.*, 1998; Le Roux *et al.*, 2012; McKay and Blumberg, 2007).

Figure 2.1: Photographs showing honeybush flowers of *Cyclopia genistoides* (SAHTA, 2016b)

The utilisation of herbal teas for health purposes has increased drastically because people tend more and more to include organic foods and drinks in their diets and this resulted in honeybush tea becoming a popular “hot or cold” beverage together with other herbal teas. The tea contains very small quantities of tannins with a total lack of caffeine, which may be beneficial to people with sleeping disorders (Du Toit *et al*., 1998; McKay and Blumberg, 2007). Honeybush also contains phytochemicals with anti-oxidant activities, which may defend the body against free radicals and thereby may delay or prevent cell damage (Marnewick, 2009; Van Wyk and Wink, 2009).

2.3 GEOGRAPHICAL DISTRIBUTION OF HONEYBUSH

Honeybush is an endemic plant, which can be found in the Cape region known as the Cape Floristic Kingdom or Core Cape Sub-region shown in Figure 2.2. The Cape Floristic Kingdom region (90760 km^2) inhabits approximately 4% of the sub-continent of South Africa that includes an extraordinary rich flora. Two different types of soil can be found in this region: (1) clay rich soils consisting of important nutrients and (2) coarse-grained sandy soils with low levels of important nutrients (Manning and Goldblatt, 2012).

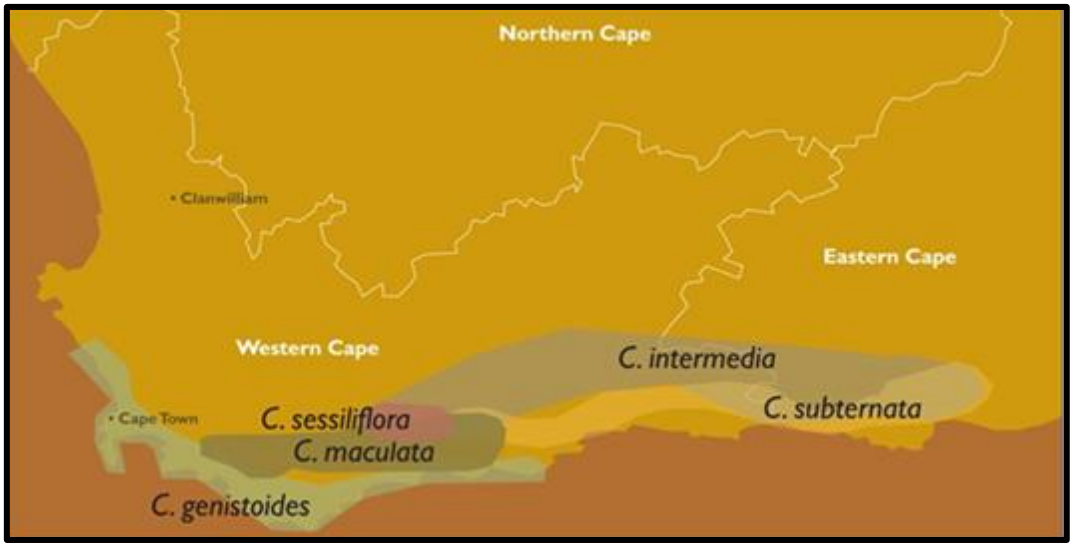

Figure 2.2: Map of the Western and Eastern Cape provinces of South Africa with the distribution of various *Cyclopia* species (SAHTA, 2016a)

According to Joubert *et al.* (2007), honeybush plants grow in acidic, low phosphorus sandy soils, but gains advantage from fertilization materials such as those from organic sources like sawdust and from phosphate supplementation. Sawdust is beneficial by maintaining the soil structure, helps to regulate the underlying soil temperatures and helps to ensure that the moisture loss from the surface is reduced (Barney and Colt, 1991). Rainfall patterns which contributes to the fynbos vegetation is present throughout the year, ranging from 100 - 2000 mm, thus benefitting the growth rate of each honeybush species, which blooms in different months of the season as shown in Table 2.1 (Harvey, 1868; Kies, 1951; Manning and Goldblatt, 2012; Schutte, 2012). Fire outbreaks arise annually in the Cape region, which may have a positive impact on the fynbos vegetation. Bergh and Compton (2015) concludes that after a year's regrowth of the vegetation where a fire occurred, the nutrients present in the ashes are beneficial to the fynbos vegetation.

2.4 BIOLOGICAL ACTIVITIES OF HONEYBUSH CONSTITUENTS

There is a wide variety of different biological active compounds in each honeybush species that were identified such as coumestans (e.g. flemichapparin C, medicagol, sophora-coumestan B), flavanes (e.g. epigallocatechin 3-*O*-gallate, 5,7,3′,4′-tetrahydroxyflavane-5-*O*-glucoside), flavanones (e.g. butin, eriocitrin, eriodictyol, hesperitin, hesperidin, isosakuranetin, naringenin, narirutin, prutin), flavones (e.g. diosmetin, 5-deoxyluteolin, luteolin, vicenin II), flavonols (e.g. glucoside derivatives of kaempherol), isoflavones (e.g. afrormosin, calycosin, formononetin, fujikinetin, orobol, pseudobaptigen, wistin), xanthones (e.g. hydroxyisomangiferin, hydroxymangiferin, isomangiferin, mangiferin) and other compounds like organic acids, 4-hydroxycinnamic acid, inositol and tyrosol/4-hydroxybenzaldehyde derivatives (De Beer *et al.*, 2012; Ferreira *et al.*, 1998; Joubert *et al.*, 2008b; Kamara *et al.*, 2003; Kamara *et al.*, 2004; Kokotkiewicz and Luczkiewicz, 2009; Le Roux *et al.*, 2012). Other phytochemicals were also identified in honeybush species such as dihydrochalcones (e.g. 3-Hydroxyphloretin-3',5'-di-C-hexoside, phloretin-3',5'-di-C-glucoside), benzophenones (e.g. 3-*β*-D-glucopyranosyliriflophenone(I3G) and 3-*β*-D-glucopyranosylmaclurin (M3G)) (Beelders *et al.*, 2014a; Schulze *et al.*, 2014) and terpenoids (Le Roux *et al.*, 2012).

Growing evidence exists that benzophenones as well as xanthones contribute to the alleviation of diabetes, obesity and rheumatoid arthritis. Compounds from these chemical groups also showed potent anti-oxidant activity and may have possible anti-osteoclastogenic effects (Kokotkiewicz *et al.*, 2015; Malherbe *et al.*, 2014; Misra, 2008; Visagie *et al*., 2015).

The honeybush species, *C. genistoides,* was selected for this study because it contains the highest concentration of xanthones and benzophenone phytoconstituents relative to other commercial species e.g. *C. maculata*, *C. subternata* and *C. intermedia* (Kokotkiewicz *et al*., 2015; Schulze *et al*., 2015).

2.4.1 Benzophenones

Benzophenones have a 13-carbon basic chemical structure, which contains two benzene rings connected with a double oxygen chain as shown in Figure 2.3. Benzophenones may further be cyclized (i.e. formation of an adjoining ring structure when compounds or molecules become linked) or prenylated (i.e. when a compound gains a hydrophobic molecule) to be able to form new compounds which have alternative biological activities (Baggett *et al*., 2005; Oxford dictionaries, 2016).

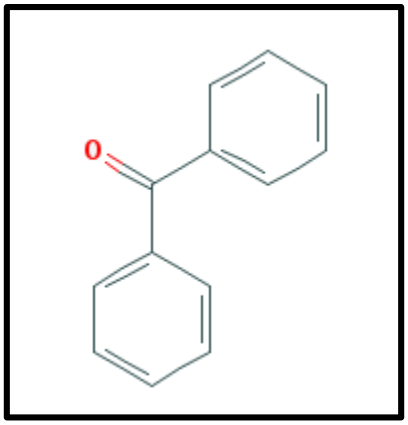

Figure 2.3: Basic chemical structure of benzophenones

Different benzophenone classes have been discovered and isolated, which include over 300 natural benzophenones that can be divided into: polyprenylated benzophenones (PPBS, which are benzophenones formed when isoprenyl groups intervene and alter the benzene ring after completion of the acetate reaction pathway) and basic benzophenone skeletons (BBS). Some benzophenones such as of benzophenone *O*-glycosides in the *ortho* position may be the pre-cursors of some xanthone structures (El-Seedi *et al*., 2010; Kitanov and Nedialkov, 2001).

Benzophenones found particular in honeybush species include 3-β-D-glucopyranosyliriflophenone (I3G), 3-β-D-glucopyranosyl-4-β-D-glucopyranosyloxyiriflophenone (IDG) and 3-β-D-glucopyranosylmaclurin (M3G) (Figure 2.4). I3G may be a potential anti-oxidant although it may not be as effective as the xanthones, mangiferin and isomangiferin (Malherbe *et al*., 2014). M3G showed potential anti-metastatic effects to protect the body against human non-small-cell lung cancer cells by inhibiting the signal pathway of the Src/FAK-ERK-β-catenin and may contribute to successful transplantation procedures affecting mesenchymal stem cells by protecting the mesenchymal stem cells against hydroxyl radical scavenging effects (Ku *et al*., 2015; Li *et al*., 2014).

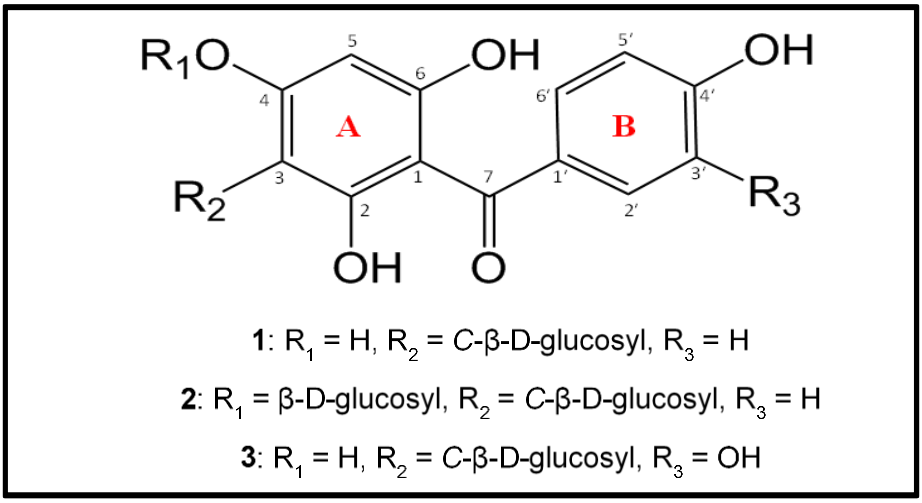

Figure 2.4: Chemical structure of benzophenone marker molecules (1) I3G, (2) IDG and (3) M3G

Benzophenones have exhibited the ability to protect human skin against UV irradiation after topical application (Vela-Soria *et al*., 2011). The benzophenones, I3G and xanthones such as isomangiferin are potent compounds for pro-apoptotic action in active rheumatoid arthritis, whereas hesperidin and mangiferin appears to have potential to inhibit synoviocyte activity (Kokotkiewicz *et al*., 2013).

Inhibitory effects on lipid accumulation, through the adenosine 5′-monophosphate-activated protein kinase (AMPK) signalling pathway, have also been reported for some of the benzophenones (Zhang *et al.*, 2013). Activation of AMPK results in a reduction of body weight due to metabolism of stored fat in adipose tissue. In addition, AMPK activation in the liver leads to increased fatty acid oxidation, which results in decreased plasma glucose, cholesterol and triglyceride levels (Misra, 2008). Another important effect of benzophenones isolated from honeybush species is their α-glucosidase inhibitory effect (Beelders *et al*., 2014a), which influences the digestion process of carbohydrates and fat that can assist with treatment of diabetes and other diseases (Hamden *et al*., 2012).

2.4.2 Xanthones

Diderot *et al.* (2006) described xanthones as dibenzo-γ-pyrone chemical compounds, which include heterocyclic groups with oxygen molecules. The basic chemical structure of xanthones is illustrated in Figure 2.5.

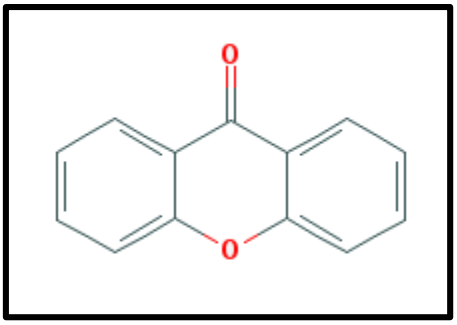

Figure 2.5: Basic chemical structure of xanthones

El-Seedi *et al*. (2010) reported that xanthones have important pharmacological effects, which are summarised in Figure 2.6.

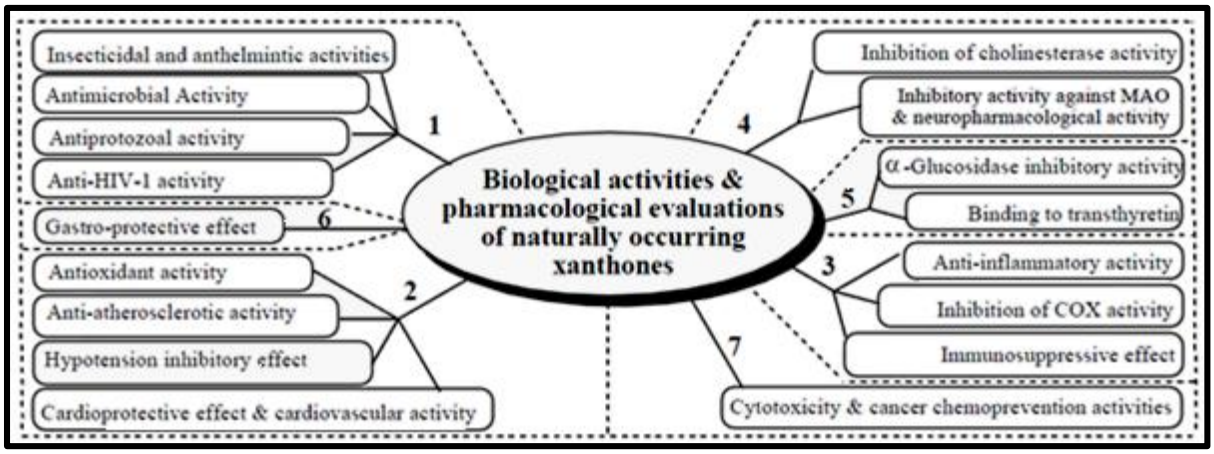

Figure 2.6: Important biological and pharmacological effects of natural xanthones (El-Seedi *et al*., 2010)

Kokotkiewicz *et al.* (2013) developed a method to isolate *C*-glucosidated xanthones (i.e. mangiferin and isomangiferin) with their chemical structures shown in Figure 2.7 from *Cyclopia genistoides*. Mangiferin had a lower percentage pro-apoptotic action than isomangiferin, but both may be utilized for treatment of rheumatoid arthritis. Luczkiewicz *et al*. (2014) stated that mangiferin found in herbal medicines has hardly any side-effects and does not show any toxicity.

A xanthone analogue has been synthesised by Chae *et al*. (2015), which was shown to be beneficial in terms of the oral uptake of P-gp substrates, especially for anti-cancer medicines. Xanthones which have been isolated from *Garcinia mangostan* have shown significant importance through the inhibition of digestive enzymes such as α-glucosidases (IC_{50} = 1.5 – 63.5 µM) and may be able to lower a person's postprandial glucose levels (Ryu *et al*., 2011).

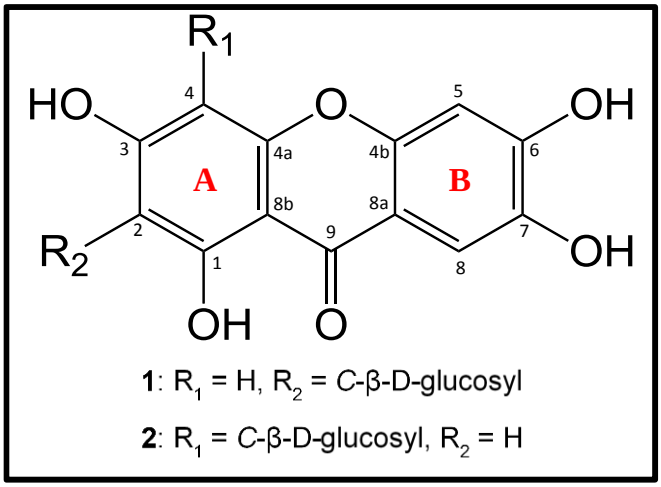

Figure 2.7: Chemical structures of 1) mangiferin and 2) isomangiferin

2.5 ENZYMES AS TARGETS FOR DRUG TREATMENT

2.5.1 Enzyme function

Enzymes can be defined as functional proteins that operate as biological catalysts to accelerate intra-cellular chemical and metabolic reactions (Palmer and Bonner, 2007). Enzymes catalyse reactions between substances (i.e. substrates) with which they are in contact with, which enter the body or are already present in the body in order to elicit a certain activity (Berg *et al*., 2002; Fromm and Hargrove, 2012; Guyton and Hall, 2011). The reaction model described by Leonor Michaelis and Maude Menten illustrates the function of enzyme-catalysed reactions, which can be described by the following equation (Berg *et al*., 2002; Demeester, 1997; Harvey *et al*., 2011):

$$E+S \underset{k_{-1}}{\overset{k_1}{\rightleftarrows}} ES \xrightarrow{k_2} E+P \qquad \textbf{[2.1]}$$

Where:

k_1, k_{-1}, and k_2 = Rate constants

E = Enzyme

S = Substrate

ES = Enzyme-Substrate complex

P = Product

Active sites of enzymes are essential domains where catalytic reactions occur and represent the sites where substrate molecules will bind specifically to an enzyme to release a product by means of two different type of models, namely the lock and key model and the induced fit

model. The lock and key model illustrates the perfect three dimensional fit between the substrate (key) and the enzyme (lock). The induced fit model describes the conformational changes the enzymes active site undergoes when binding occurs between the substrate and the enzyme to assure a perfect fit (Atkins and De Paula, 2011; Berg *et al*., 2002; Cooper, 2000; Fromm and Hargrove, 2012; Klazema, 2014; Palmer and Bonner, 2007; Telleen, 2015).

The graph in Figure 2.8 illustrates the free energy needed for a reaction between molecules. The reaction initially requires activation energy (i.e. transition state). The product that is finally formed will have a lower energy state. Catalysts (e.g. enzymes) speed up the reaction rate by lowering the activation energy.

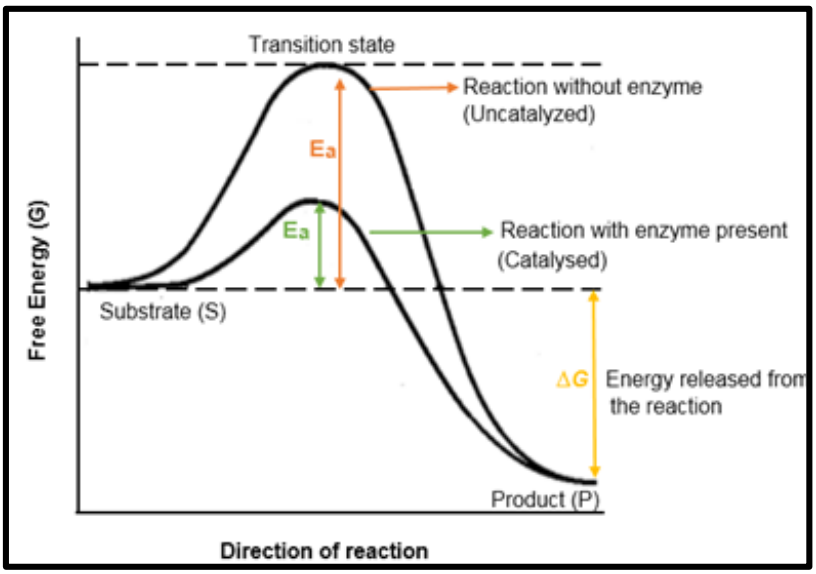

Figure 2.8: The influence of enzymes on activation energy in a catalysed chemical reaction (Cooper, 2000; Harvey *et al*., 2011; Ragoonanan, 2013)

Other enzyme functions include generation of energy for cells to function normally through oxidative reactions, detoxification of certain substances through coagulation and conjugation with glucuronic acid, but also through oxidation and hydrolysis reactions and promotion of the synthesis of certain substrates (Guyton and Hall, 2011).

It is known that certain drugs function by inhibiting enzymes and therefore enzyme inhibition can be seen as an important mechanism to regulate and maintain biological systems, which will further be discussed below.

2.5.2 Enzyme inhibition

Enzyme inhibition causes a decrease in the rate of the reaction that is catalysed by the enzymes (Harvey *et al*., 2011; Johnson, 2015). Enzyme inhibitors can be classified as

irreversible and reversible inhibitors. Irreversible inhibitors are substrates which bind irreversible to a target enzyme through a mechanism called covalent binding. The effect of these inhibitors can only be overcome by production of new enzymes. Reversible inhibitors, on the other hand, bind in such a way to the enzyme that they can be replaced and include competitive, uncompetitive and non-competitive inhibition. Competitive inhibition takes place when an inhibitor (appearing to have the same structural characteristics as a specific substrate) attaches to the enzyme's active site to prevent the binding of a substrate leading to a diminished catalytic effect. This can be overcome if the substrate concentration is increased. Uncompetitive inhibition takes place when the inhibitor anchors on the enzyme-substrate complex. Non-competitive inhibition takes place when a substrate binds on the active site of an enzyme and the inhibitor binds on the same enzyme, but to a site other than the active site (Atkins and De Paula, 2011; Berg *et al*., 2002; Fromm and Hargrove, 2012).

Enzymes are important to assure our body gets the proper nutrients to be absorbed, but sometimes it is beneficial to inhibit specific enzymes especially digestive enzymes to help prevent certain diseases.

2.5.2.1 Inhibition of digestive enzymes

Inhibition of digestive enzymes has been identified as an important target for drug development for the prevention and treatment of T2DM and obesity. The enzymes of interest include amylases, lipases and glucosidases (Bellamakondi *et al*., 2014; Bischoff, 1994; Hamden *et al.,* 2012; Liu *et al*., 2013; Rabasa-Lhoret and Chiasson, 2004). According to Boath *et al.* (2012), polyphenol-rich extracts can cause *in vitro* inhibition of α-amylase and α-glucosidase at very low levels. Their study also showed that tannin-like components can inhibit α-amylase and lipase successfully, but not α-glucosidase. On the other hand, research by Liu *et al.* (2013) showed that flavonoid enriched extracts could inhibit all three enzymes.

2.5.2.1.1 Amylase

Amylases are enzymes that are present in the saliva and intestinal fluids of humans together with malto-glucoamylase and sucrase-isomaltase (a pair of brush-border enzymes). These enzymes rapidly initiate the saccharification of starch to glucose monomers so that they can be easily absorbed (Carai *et al.,* 2009; Lo Piparo *et al*., 2008; Vermaak *et al*., 2011a).

A distinction can be made between two different types of amylase enzymes, which initiate the breakdown of glycogen and starch, namely endo-amylase (α-amylase or α-1,4-glucan-4-glucanohydrolase) and exo-amylase (beta-amylase or 1,4-α-D-glucan maltohydrolase). The composition of endo-amylase includes glycoproteins that cause the total breakdown of starch

molecules to allow for the subsequent absorption of sugar molecules (Beaupoil-Abadie *et al*., 1973; Kandra, 2003). A large variety of animals, microorganisms and plants contain these specific endo-amylases to assure that glucose is released steadily from starch. The α-1,4-glucan bonds present in the starch molecule are hydrolysed particular by endo-amylase as illustrated in Figure 2.9 (Richardson and Gorton, 2003). The exo-amylase, on the other hand, commences its action within the plant before it is consumed, e.g. in dormant seeds (Dhital *et al*., 2015; Highley, 1997).

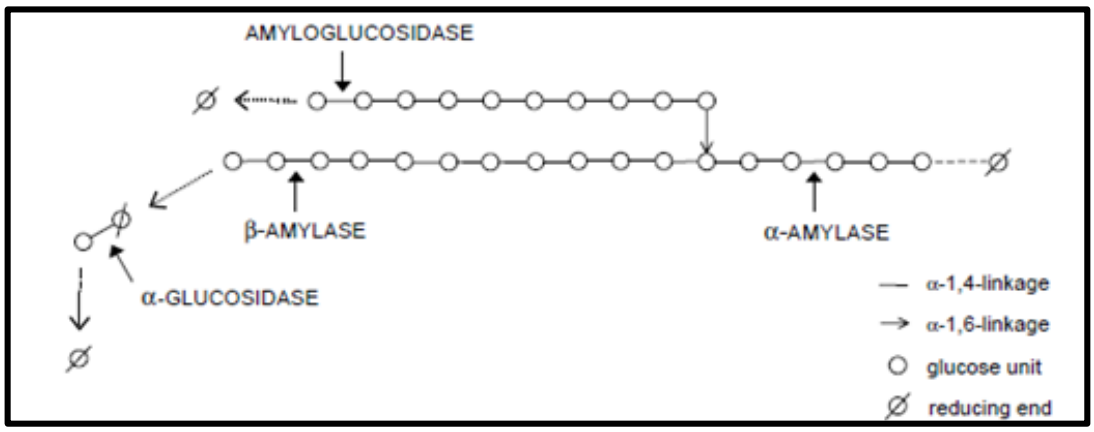

Figure 2.9: Schematic illustration of the mechanism of action of α-amylase, β-amylase, amyloglucosidase and α-glucosidase enzymes (Richardson and Gorton, 2003)

To determine the enzyme activity of amylase enzymes, a suitable starch source such as starch-azure can be utilised for both endo- and exo-amylases because it is a substrate for both these enzymes (Highley, 1997).

2.5.2.1.2 α-Glucosidase

α-Glucosidase enzymes play an important role in the digestion of carbohydrates. They are secreted primarily by the brush border epithelium in the jejunum (Kalra and Bhutani, 2014; Matsumoto *et al*., 2003; Nolte, 2009; Odaci *et al*., 2010; Schmidt *et al*., 2014; Sfetcu, 2014; Soumyanath, 2006). α-Glucosidase can be categorised as an "exo-group" of enzymes called "carbohydrases", which causes α-glucose to be released from the substrate's non-reducing end position. In addition, they have the ability to hydrolyse α-glucans like glycogen and soluble complex carbohydrates including molecules which consist of α-glucosidic bonds like oligosaccharides (Nelson and Cox, 2005; Peng *et al*., 2016; Schmidt *et al*., 2014; Chiba, 1988; Van de Laar *et al*., 2005).

By inhibiting this enzyme, glucose uptake in the small intestine would be reduced because the total number of simple glucose molecules from carbohydrate sources will be lowered (Azuma

et al., 2011; Bischoff, 1994; Sfetcu, 2014; Tadera *et al*., 2006). According to Kumar *et al.* (2011), research on plants has led to the isolation of phytoconstituents that act as inhibitors for α-glucosidase enzymes, which are also present in *Cyclopia* species. Acarbose, miglitol and voglibose are synthetic inhibitors to ensure inhibition of α-glucosidase in the intestinal brush border of the gastrointestinal system to provide effective anti-hypoglycaemic therapy. Some side-effects of the synthetic inhibitors may include abdominal bloating, diarrhoea, flatulence and malabsorption. Further research is required to determine whether honeybush extracts presents with the same side-effects (Powers and D´Alessio, 2011).

2.5.2.1.3 Lipase

Lipases are produced by the liver, pancreas and other organs, which are responsible for hydrolysis of ester bonds of water-insoluble substrates such as dietary lipids also known as triacylglycerols. Humans consume a lot of food consisting of natural lipids and thereby containing these triacylglycerols. Pancreatic lipase is an important digestive enzyme regarding fat digestion from our daily dietary choices. They are secreted by the pancreatic juices at the acinar cells of the pancreas and delivered into the small intestine by pancreatic ducts to accomplish fat digestion (Gilham and Lehner, 2005; Mansbach *et al*., 2001; Mukherjee, 2003; Scharpé *et al*., 1997; Quiroga and Lehner, 2011).

Orlistat is an inhibitor of gastrointestinal lipase and is an example of a drug that is used to prevent uptake of dietary fat by blocking the digestion process (Corelli, 2009). Extracts of plants such as those of *C. maculata and C. subternata* have shown significant inhibition regarding the intracellular fat accumulation and triglycerides. They are investigated as alternative treatments against “diabesity” because they might not present the unpleasant side effects such as those resulting from orlistat, which causes fatty stools and stomach pain due to high-fat diets ingested during orlistat therapy (Dudhia *et al*., 2013; Filippatos *et al.,* 2008; SAMF, 2012).

To quantify the inhibitory effects of plant extracts on specific enzymes, activity assays, e.g. fluorometric methods can be utilized. Andlauer *et al*. (2009) made use of optical absorption of fluorescence at an emitted state of 445 nm upon excitation at 365 nm to detect lipase inhibitory activity whereas Azuma *et al*., (2011) determine the α-glucosidase inhibitory activity at an optical absorption of fluorescence at an emitted sate of 460 nm upon excitation at 355 nm.

2.6 POSSIBLE UNDESIRED EFFECTS OF HONEYBUSH CONSTITUENTS

Most patients tend to believe that if a product is of natural origin, they are safe for consumption and therefore don't always see the need to notify their physicians about the natural products they consume together with their prescribed medicines (Bressler, 2005). On the contrary, natural products or compounds can be as harmful as any conventional drug (Seeff *et al*., 2015). However, results obtained from experiments done on rats with extracts from fermented and unfermented honeybush have not shown any side effects or damage to the kidneys and the liver if ingested chronically over a 10 week period (Joubert *et al*., 2008a). Research conducted by Marnewick *et al*. (2003) also have shown no signs of negative side-effects on the kidney and liver organs of rats when they ingested honeybush extract solutions which were dissolved in water. Therefore, honeybush extracts might be considered safe and can be incorporated into a desirable sustained release type of dosage form ready for consumption.

2.7 BIOPHARMACEUTICAL PRINCIPLES

Determination of membrane permeability properties of pharmacologically active compounds is an important aspect of the medicinal product development process (Balimane *et al*., 2000). To determine whether drugs from oral dosage forms do cross the intestinal epithelium, permeation studies can be conducted, which includes the use of methods categorised as biological, computational and physicochemical methods. *In vivo*, *in vitro* and *in situ* models all fall within the category of the biological methods (Ashford, 2007).

The aim of drug delivery is to reach and maintain therapeutic blood levels of the active compound, except for compounds that are targeted to specific sites (Varma *et al*., 2003). Therapeutics can be targeted to specific sites in the gastrointestinal tract to exhibit a systemic or local effect (Singhal *et al*., 2012). As an example, targeting the colon can be used to treat diseases such as irritable bowel syndrome including Chrone's disease and ulcerative colitis (Yang *et al*., 2002). Another example is prevention and treatment of T2DM by controlling the absorption of glucose, which can be done by inhibiting carbohydrate-hydrolyzing enzymes (Ali *et al*., 2016).

Pathways of drug absorption across the intestinal epithelium include transcellular pathways (e.g. passive diffusion, carrier mediated transport and active transport which consist of facilitated diffusion, endocytosis, pinocytosis, receptor-mediated endocytosis, phagocytosis and transcytosis), paracellular pathways and efflux transporters (e.g. P-glycoprotein) (Ashford, 2007).

P-glycoprotein (P-gp) is found in the columnar cells of the intestinal epithelium on the brush border membrane (Figure 2.10) at high concentrations and also on other cell surfaces including on tumour cells. P-gp is an efflux protein, which causes counter transport of drugs back into the lumen of the gastrointestinal tract after absorption took place (Ashford, 2007; Linardi and Natalini, 2006). For most drugs this is not a desirable outcome because P-gp can cause unsatisfactory bioavailability through alternation of drug absorption (Varma *et al*., 2003). Most enzymes (e.g. lipases and glucosidases) targeted for enzyme inhibition to help treat "diabesity" are located in the lumen of the gastrointestinal tract and therefore systemic bioavailability is not necessary for this particular mechanism of treatment (Ashford, 2007).

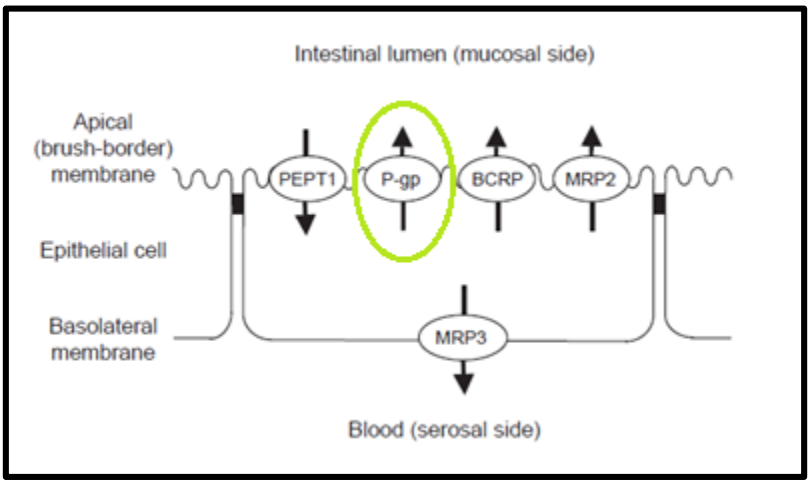

Figure 2.10: P-gp expression in the epithelial cells of the intestine (Takano *et al*., 2006)

2.7.1 Permeability testing techniques

Intestinal absorption and simulation techniques that can be used to evaluate drug permeation are outlined in Figure 2.11. The most frequently used techniques include excised tissue based *ex vivo* models (e.g. Ussing type diffusion chambers, everted sac technique*), in vitro* artificial membrane models (e.g. parallel artificial membrane permeability (PAMPA)), *in situ* methods (e.g. single pass perfusion studies) and cell-based *in vitro* models (e.g. Caco-2 cell monolayers) (Balimane *et al*., 2000).

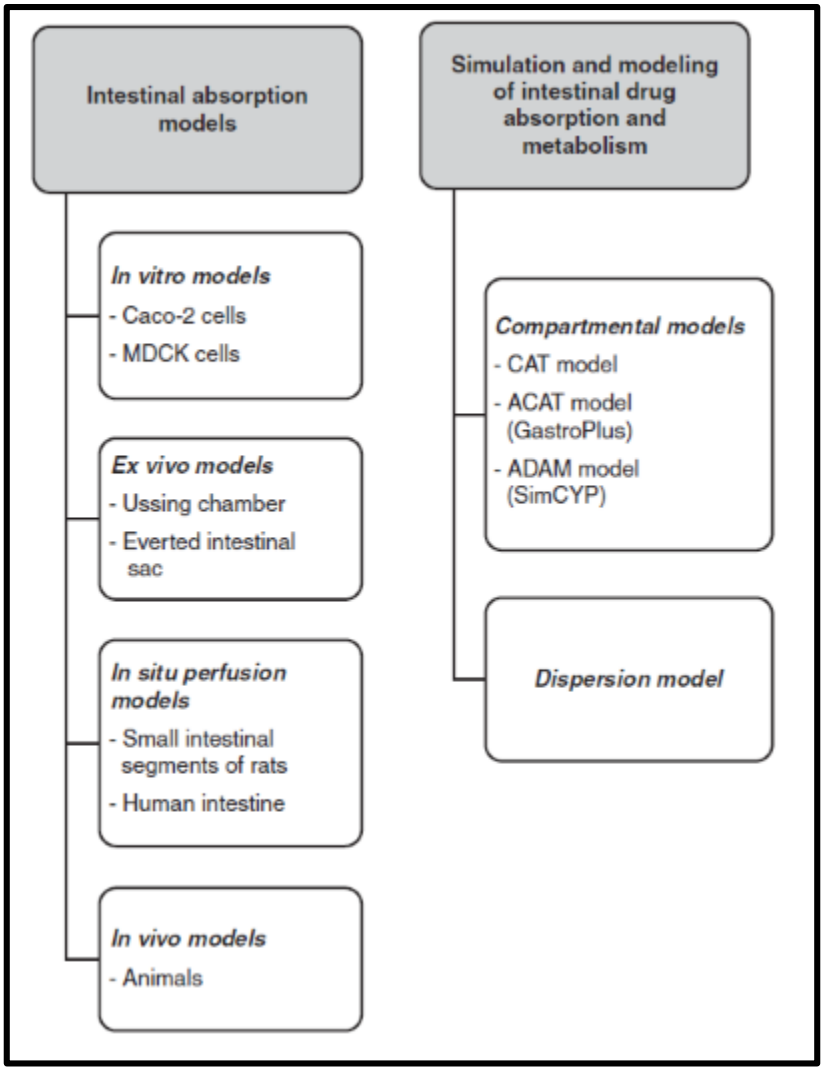

Figure 2.11: Summary of models for permeation studies (adapted from Alqahtani *et al*., 2013)

In vitro methods are more cost-effective and less laborious than *in vivo* studies, but many variables can influence the results. Other disadvantages include lack of mimicking physiological conditions such as gastrointestinal pH, gastric emptying, mucus layer secretions and blood supply (Balimane *et al.*, 2000; Volpe, 2010).

2.7.1.1 Cell culture models

One of the most commonly used *in vitro* cell culture models is the Caco-2 cell line, which resembles the structure of the small intestinal epithelium of humans. This cell line expresses cytochrome P450 enzymes and efflux transporters and contains microvilli (Awortwe *et al*., 2014; Le Ferrec *et al*., 2001; Peng *et al*., 2014). This cell line can be grown in monolayers on filter membranes in Transwell plates as illustrated in Figure 2.12.

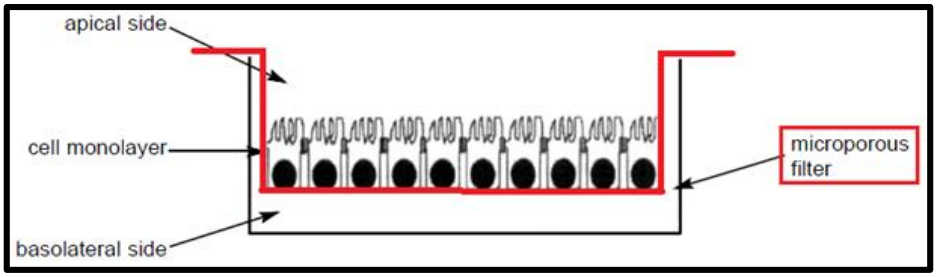

Figure 2.12: Caco-2 cell monolayer illustrated in a single well of a Transwell® plate (Le Ferrec *et al*., 2001)

The advantages and disadvantages of the Caco-2 cell line as *in vitro* permeability model are summarised in Table 2.2.

Table 2.2: Caco-2 model advantages and disadvantages (Ashford, 2007; Le Ferrec *et al*., 2001)

Advantages	Disadvantages
Straightforward method that can be grown in a reasonable time frame.	Physiology conditions are not 100% resembled because bile salts, cholesterol and mucus are not present.
The test solution can be added either in apical or basolateral side of the well.	It is static.
Human cell line.	Human cells being used are from tumoral source.
High throughput screening is possible.	Consists of only one cell type (lack diversity of the epithelium e.g. goblet cells).
Small quantity of drug can be utilized.	P-gp interference are not easy to determine.
Toxicity of drugs towards cells can be tested as well.	Originates from the colon.

2.7.1.2 Excised tissue models

The Ussing chamber that was originally used for permeability studies consisted of *in vitro* short-circuit methods of ion transport across frog skin, which was originally created by Hans Ussing. Certain shortcomings in the Ussing type chamber apparatus led to the development of an improved apparatus, namely the Sweetana Grass diffusion apparatus (illustrated in Figure 2.13). The diffusion apparatus has a reservoir volume of 7 ml compared to the 10 ml volume of the Ussing chamber. The surface area available for absorption in this diffusion

apparatus is larger than that of the Ussing chamber and temperature can be better managed and it is much more effortless to clean the half cells of the diffusion appartaus than to disconnect the reservoirs of the Ussing apparatus (Berggren, 2006; Grass and Sweetana, 1988).

Diffusion chambers based on the Sweetana Grass apparatus are currently used for drug permeability studies across excised tissues. Animal excised tissues of dogs, hamsters, mice, monkeys, pigs, snakes have been utilized to perform experiments on the diffusion chamber apparatus (Barry, 2007).

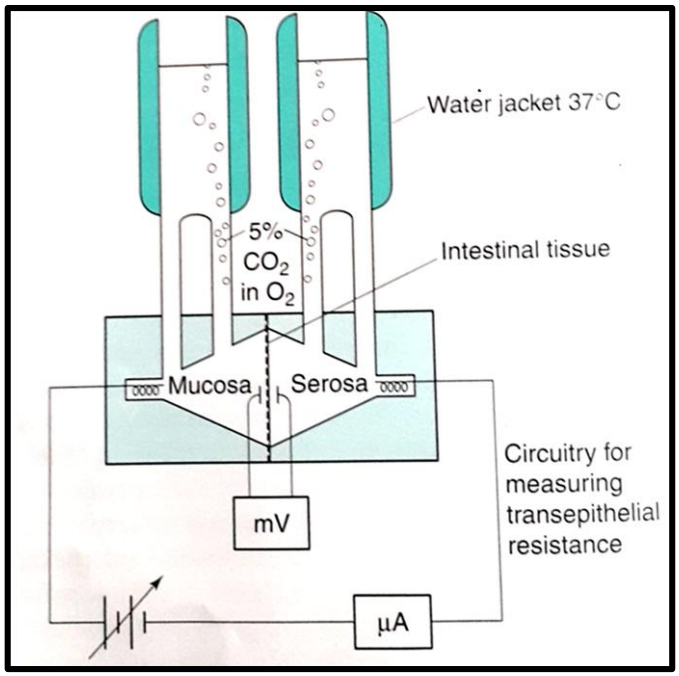

Figure 2.13: Schematic illustration of Sweetana Grass diffusion chamber (Ashford, 2007)

The advantages and disadvantages of isolated sheets of animal intestinal tissue as well as everted intestinal rings are summarised in Table 2.3 (Ashford, 2007).

Table 2.3: Differences, advantages and disadvantages of intestinal rings and isolated intestinal mucosa sheets mounted onto diffusion chamber apparatus (Ashford, 2007).

Everted intestinal rings		**Isolated sheets**	
Entire piece of intestinal segment can be utilized.		Only pieces of intestinal mucosa can be utilized.	
Musculature stays intact and does not need to be removed.		Musculature is removed.	
Placed onto a glass rod.		Mounted onto diffusion chamber half cells spikes.	
Advantage	**Disadvantage**	**Advantage**	**Disadvantage**
Fast and straightforward experiment to conduct.	Extended preparation time needed for samples which can complicate the assay procedure being followed.	Permeability can be determined across various regions of the gastro-intestinal tract.	Tissues are not viable for long periods, all experiments must be completed within a 2 h period from departure from the abattoir.
A great quantity of rings from the intestine segment can be assembled.	Tissues are not viable for too long.	Fluxes between apical-basolateral and basolateral-apical side can be determined due to tissue being independently sampled.	Working with biological material, ethical disposal is costly.
Animal can act as their own control.	Working with biological material, ethical disposal is costly.	The transport pH dependence can be assessed by changing the buffers' pH ranges.	
	Considered an uptake method, since efflux and polarity cannot be evaluated.	Active transport can be analysed.	

According to Ashford (2007), the rat intestinal tissue is the more favourable model to evaluate permeability, because it is corresponds highly with the human intestinal properties. Experiments done by Nejdfors *et al*. (2000) showed that the pig model permeation data corresponded better to those of humans than the rat model.

To determine whether efflux of the compound under investigation occurred, the apparent permeability coefficient (P_{app}) values in the apical to basolateral direction (AP-BL) are compared to that in the basolateral to apical (BL-AP) direction (Ashford, 2007). When P_{app}

(BL-AP) = P_{app} (AP-BL), then no efflux occurred, while when P_{app} (B-A) > P_{app} (A-B), then the compound is effluxed (Ashford, 2007; Ozeki *et al*., 2015).

A study done by Artursson and Karlsson (1991) on the Caco-2 intestinal cell line showed that drugs which are totally absorbed presented with an apparent permeability coefficient (P_{app}) value of > 1 $\times 10^{-6}$ cm/s, whereas drugs having an absorption range between 1% and 100% consisted of P_{app} values of 0.1−1.0$\times 10^{-6}$ cm/s. If drugs had absorption range of < 1%, their P_{app} values were ≤ 1$\times 10^{-7}$cm/s. In a study done by Franco *et al*. (2008) utilising a frog model on the intestinal sac system determined that the P_{app} values for drugs being fully absorbed presented with values >3$\times 10^{-6}$ cm/s and drugs having absorption of less than 90% presented with P_{app} values < 1$\times 10^{-6}$ cm/s. It is therefore clear that there is still variation in terms of permeability ranges and results between *in vitro* models and different laboratories.

2.8 DOSAGE FORMS

For a drug to be administered to the body and to be therapeutically active, a suitable dosage form (Table 2.4) need to be selected. Whether the drug will be available from its dosage form can be established through *in vitro* and/or *in vivo* study methods (Ansel, 2010).

Table 2.4: Types of dosage forms, delivery systems and site of action (Ansel, 2010)

Route of administration	Site of action	Dosage forms/Drug delivery systems
Oral	Mouth Gastro-intestinal tract	Tablets, capsules, oral solutions, drops, syrups, elixirs, suspensions, magmas, gels, powders, troches and lozenges (last two, oral cavity)
Sublingual	Under the tongue	Tablets
Parental Intravenous Intra-arterial Intracardiac Intraspinal/Intrathecal Intraosseous Intra-articular Intrasynovial Intracutaneous/Intradermal/Subcutaneous Intramuscular	 Vein Artery Heart Spine Bone Joint Joint fluid Skin Muscle	Solutions, suspensions

Epicutaneous	Skin surface	Ointments, creams, pastes, plasters, powders, aerosols, lotions, transdermal patches, solutions (topical)
Conjunctival	Eye conjunctiva	Ointments
Intraocular	Eye	Solutions, suspensions
Intranasal	Nose	Solutions, ointments
Aural	Ear	Solutions and suspensions (drops)
Intrarespiratory	Lung	Solutions (aerosols)
Rectal	Rectum	Solutions, ointments, suppositories
Vaginal	Vagina	Solutions, ointments, emulsion foams, gels, tablets/inserts
Urethral	Urethra	Solutions and suppositories

Dosage forms ensure the drug reaches a specific site of action either systemically or locally to function properly, whereas modified drug delivery systems (Table 2.5) help to control the plasma concentration of the drug after administration (Collett and Moreton, 2007). The onset of action may differ for every single dosage form and people prefer oral type of dosage form that are solid rather than a liquid (York, 2007). Drugs or active pharmaceutical ingredients (API) together with excipients are combined into a dosage form to ensure improved performance, to help with manufacturing of the final product and/or to obtain suitable bioavailability of the drug (Collett and Moreton, 2007; WHO, 2010).

Table 2.5: Description of different types of modified release drug delivery systems (Chandana *et al*., 2013; Collett and Moreton, 2007)

Type of delivery system	Description
• Controlled release	• The drug is released at a constant rate to establish invariable plasma concentrations.
• Delayed release	• The drug release is delayed after it has been administered and is only starting to be released on a later stadium (e.g. enteric-coated dosage forms).

• Extended release	• The drug concentration is released at a slower state to achieve relatively stable plasma concentration for 8 – 12 hours.
• Prolonged release	• These dosage form differ from conventional dosage forms because they prolong the release and absorption period.
• Repeat action	• More doses are released from the dosage form after administration at certain time periods.
• Sustained release	• The active ingredients are slowly released from the dosage form over an extended time period to reduce the number of doses that need to be taken by the patient.
• Site specific targeting	• Drugs are delivered at a specific site or region within the gastrointestinal tract.

Immediate release type of solid oral dosage forms disintegrate rapidly and possess a dissolution rate within 30 min time period after administration. They present with high patient compliance, cost-effectiveness and a stable type of dosage form, because they are easily administered to a patient. However, they may exhibit a variable time of onset because they rely on disintegration (Jaimini *et al*., 2013; Rathod *et al*., 2014; Sandeep *et al*., 2013). A more preferable type of dosage form is modified release drug delivery systems. Modified drug delivery systems are attractive due to the fact that patient compliance is improved as a result of less frequent dosing and fluctuations of blood concentrations are minimized with fewer side effects (Chandana *et al*., 2013).

Modified release drug delivery systems ensure the release of a single drug dose at a certain rate to achieve prolonged therapeutic action over a predictable period of time. They are primarily designed to provide drug plasma concentrations within the desired therapeutic range over an extended period of time. It is difficult to design a dosage form that can deliver a drug at a precise absorption window or at the exact desired release rate. Certain factors such as enzyme activity, different transit rates through the gastrointestinal tract, different types of drugs, potential overdose because of larger drug concentrations present and a person's state of health can have an impact on the formulation of a modified dosage forms (Collett and Moreton, 2007). However, the disadvantages can be outweighed by the advantages. Certain modified release drug delivery systems are gaining attention due to the fact that they can help to deliver drugs to specific regions of the small intestine. Jigar *et al*., (2013) designed a sustained release gastro-retentive dosage form to treat T2DM with less frequent dosing, which contributes to optimal patient compliance. Gastro-retentive systems are maintained in the

stomach while sustaining drug release over an extended period of time. The released drug is continuously moving to the rest of the gastrointestinal region, which helps to maintain the drug in the absorption window and can assist to achieve optimal bioavailability (Dave *et al*., 2004).

2.8.1 Multi-unit pellet systems (MUPS)

A distinction can be made between single-unit dosage forms and multiple-unit dosage forms. Single-unit dosage forms consist of a single "body" in which the entire drug dose is contained. (Sarojini and Manavalan, 2012). Multiple-unit drug delivery systems, on the other hand, are composed of multiple "bodies" each containing a portion of the drug dose (Collett and Moreton, 2007). Multiple-unit pellet systems (MUPS) can be prepared by compressing spherical beads (or pellets) into tablets (illustrated in Figure 2.14) or loading beads into hard gelatine capsules. This is an ideal approach for extended drug release and combining it with a gastro-retentive dosage form may be an ideal drug delivery system for specific applications. They have favourable drug delivery and bioavailability properties making them efficient drug delivery systems (Jyothi and Doniparthi, 2014). Beads are mainly utilized in MUPS because they present with suitable flow properties and don't have the issue of interparticulate contact points such as non-uniform shaped particles. They are prepared through a process called extrusion spheronisation (Hoag and Lim, 2008; Newton, 2008).

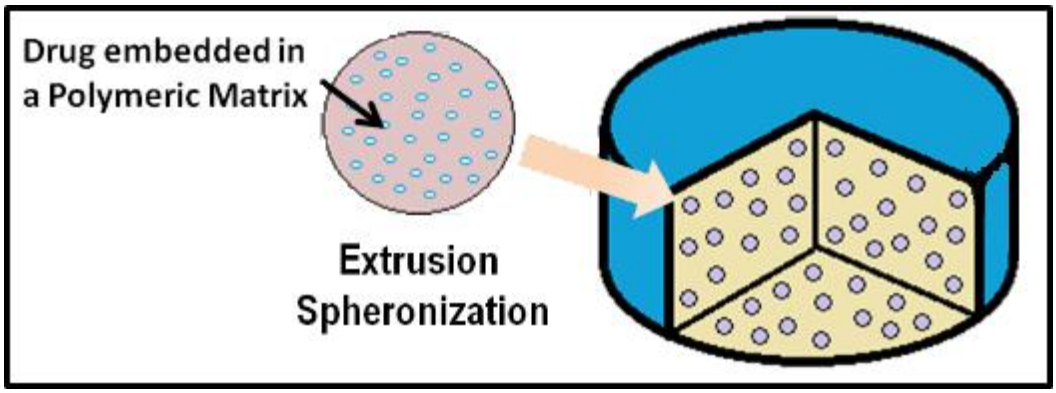

Figure 2.14: Illustration of a multiple-unit pellet system where beads are prepared through a processed called extrusion spheronization and then compressed into a tablet (Pinto *et al*., 2013)

MUPS present with resilient drug release patterns and they also don't have the risk of dose dumping such as conventional single-unit immediate release type of dosage forms (Roy and Shahiwala, 2009). Sustained release dosage forms have the advantage over conventional immediate release dosage forms that doses can be taken less frequently. Another advantage of MUPS is the evenly distributed spherical beads in the gastrointestinal tract after administration and disintegration of the MUPS (Dwibhashyam and Ratna, 2008).

2.8.2 Extrusion spheronisation as a technique to prepare beads

Extrusion spheronisation is one of the most widely used methods for the production of beads (or spherical pellets) as multiple-unit oral controlled drug delivery systems (Bhaskaran and Lakshmi, 2010). Other methods used to prepare beads include the powder layering technique, suspension/solution layering technique, spherical agglomeration, spray drying, spray congealing, melt spheronization and cryopelletization (Bhaskaran and Lakshmi, 2010; Dash *et al*., 2012; Kandukuri *et al*., 2009; Kumari *et al*., 2013). The extrusion spheronisation technique consists of a process with four steps to prepare spherical beads (Dukić-Ott *et al*., 2009). These four steps are: wetting (wet mass preparation), extrusion (wet mass shaped into cylinders), spheronisation (disintegration of extrudate and shaping particles into spheres) and drying (Gandhi *et al*., 1999).

Figure 2.15 illustrates the steps in the formation of beads during the spheronisation process. After the wetted powder mass is extruded to form rod shaped cylinders, they are broken up into shorter pieces in the spheronizer, which are then rounded into spherical beads.

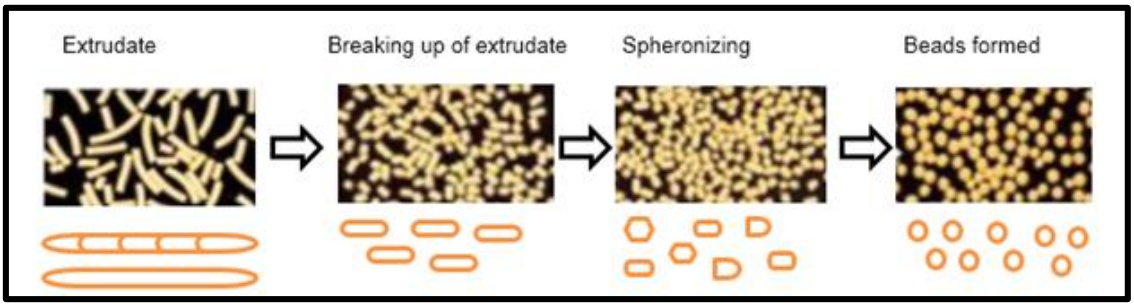

Figure 2.15: Formation of beads during the extrusion spheronisation process (adapted from Sachdeva *et al*., 2013)

The advantages of using the extrusion spheronization technique include having more uniform size and spherical shaped beads or pellets. It is relatively easy to operate the equipment and desirable drug-release outcomes can be achieved. It is also possible to achieve enhancement of bioavailability, efficiency and safety with this multiple-unit solid oral dosage forms (Bhaskaran and Lakshmi, 2010; Gandhi *et al*., 1999).

2.8.3 Gastro-retentive drug delivery

Klausner *et al.* (2003) stated that formulating drugs in such a way as to target a specific window of absorption (i.e. a target area in the gastrointestinal tract) can be done with gastro-retentive dosage forms. This type of dosage form can significantly lengthen the absorption time of a drug from the gastrointestinal tract and thereby ensure maintaining blood levels over an

extended period of time after a single dose. Gastro-retentive drug delivery systems aim to keep the dosage form in the stomach and thereby extend the gastric emptying time (Rao and Pavan, 2012) by means of different mechanisms. The rate of gastric emptying can be affected by the density of a dosage form and can influence where the delivery system will end up in the stomach (Gautam and Deva, 2012). The mechanisms to retain dosage forms within the stomach include high density systems, muco-adhesion, swelling and expanding systems beyond the pylorus valve dimensions, inclusion of delaying excipients and floating on the stomach contents (Narang *et al.,* 2010a). The high density gastro-retentive systems are not influenced by peristaltic waves and remains in the bottom of internal surface of the stomach (i.e. the gastric rugae) when a person is standing/sitting in an upright position (Bardonnet *et al*., 2006). Plug type systems (i.e. expanding and swelling systems) become too large to move through the pyloric sphincter due to the osmotic water absorption (Bardonnet *et al.*, 2006; Narang *et al.,* 2011b). Muco-adhesive systems are able to attach themselves to the mucosal surface of the stomach (Bardonnet *et al.,* 2006).

This study involves development of a floating gastro-retentive drug delivery system (i.e. a system with a density lower than gastric fluid), which will be able to float on the surface of the stomach causing the dosage form to be isolated from the pylorus region. Gastro-retentive drugs of this kind can be divided into effervescent and non-effervescent systems and are based on the buoyancy mechanism (Narang, 2010a; Singh and Kim, 2000). Our study will focus on non-effervescent floating spherical bead type drug delivery systems as a means to obtain sustained release of honeybush extracts within the stomach.

The non-effervescent gastro-retentive floating systems can further be divided into four approaches namely: colloidal gel barrier systems, micro-porous compartment systems, multi-particulate systems such as floating beads and micro-balloons (Arora *et al*., 2005; Narang *et al*., 2011b; Sharma *et al*., 2011). The colloidal gel barrier systems consist of certain gel forming, swellable cellulose type of polysaccharides, hydrocolloids and polymers. They can be incorporated into floating beads together with the active compound. When this particular system is swallowed and reaches the stomach area containing gastric fluids, it begins to form a colloidal gel barrier, which results in release of the active components controlled by the rate of fluid entering the system (Sharma *et al*., 2011).

Many advantages make the floating gastro-retentive drug delivery system an ideal system because drug absorption can be improved, controlled drug delivery can be achieved, many different diseases/disorders can be treated and the equipment needed to produce these dosage forms are easy to use. The disadvantages, on the other hand, include variable factors

(e.g. gastric motility, presence of food and pH changes), which makes it difficult to predict the buoyancy and gastric emptying time (Sharma *et al.*, 2011).

To overcome some of the disadvantages, specialised excipients can be incorporated into the formulation. Excipients help to ensure the dosage form function according to the design of formulation and to achieve the desired outcome (Dwibhashyam and Ratna, 2008). Jämstorp *et al*. (2012) mentions that polymer excipients show beneficial sustained release properties which are not effected by intestinal or gastric conditions and are therefore beneficial when added into an oral type of dosage form together with an active ingredient.

Microcrystalline cellulose (MCC) is considered of great value when utilized as an excipient in tablet formulation because of its exceptionally good properties in dry binding making direct compression possible in tablet formulations. MCC can also serve as a filler-binder, which helps to enhance the compactibility during direct compression methods (Thoorensa *et al*., 2014). Polymer excipients such as polypropylene (Figure 2.16) are flexible polymers, and are considered hydrophobic polymers having low density which helps to achieve buoyancy properties and can be combined with ethylene/propylene copolymers (Taylor, 2007). Polystyrene polymers such as Dow styrene-DVB consist of orbicular shaped particles and are basically free flowing. They are composed of styrenic polymers, which have been linked to divinylbenzene components exhibiting more effective hydrodynamic and mechanical characteristics (Figure 2.17) (Galia *et al*., 1994). Polystyrene polymers are usually utilized to help achieve a non-effervescent floating delivery system by allowing air to be held tightly in the polymer to achieve buoyancy (Gautam and Deva, 2012).

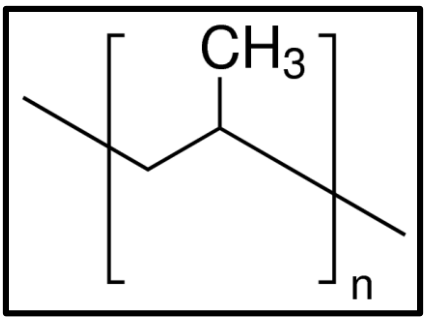

Figure 2.16: Polypropylene basic chemical structure

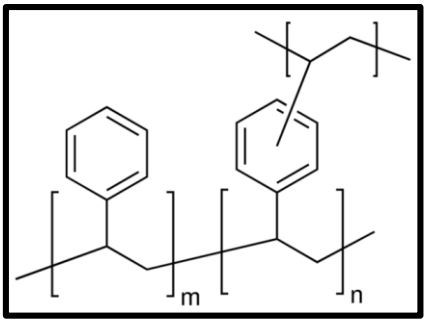

Figure 2.17: Polystyrene divinylbenzene basic chemical structure

To ensure the desired buoyancy is achieved, sublimating components can also be incorporated to help achieve lower density dosage forms with improved buoyance. When camphor is incorporated into a formulation, the camphor starts to sublimate that leads to a better or more porous formulation helping to be less dense and to float more easily. Oh *et al.* (2013) designed a floating gastro-retentive tablet by utilising camphor as a sublimation material to help achieve floatability of the tablets, no lag time was presented during the study and the tablets presented with desired buoyancy properties that lasted a whole day.

CHAPTER 3

METHODS AND MATERIALS

3.1 PREPARATION AND CHEMICAL CHARACTERISATION OF HONEYBUSH EXTRACTS

3.1.1 Source, collection and identification of the plant material

Cyclopia genistoides plant material for both the crude extracts were sourced from two different locations. The unfermented plant material of the ARC188 crude extract was sourced from the *Cyclopia* gene bank of the ARC at Nietvoorbij in Stellenbosch, whereas the unfermented plant material for the ARC189 crude extract was harvested from a commercial plantation in the Pearly Beach area of the Western Cape of South Africa. For both extracts, the unfermented shoots were dried utilising a cross-flow drying tunnel which were set at 40 °C for 16 h to obtain less than 10% moisture content. For ARC188, the leaves and fine stems were collected and the thick shoots were removed. For ARC189, the shoots remained intact before milling the plant material in a Retsch rotary mill (1.0 mm sieve; Retsch GmbH, Haan, Germany) to obtain a fine powder.

3.1.2 Preparation of crude extracts and enriched fractions

Several honeybush (*Cyclopia genistoides*) crude extracts and benzophenone or xanthone enriched fractions were prepared and evaluated based on preliminary mini-scale extractions that were characterised and the plant materials were pooled according to their phytochemical composition. The crude extracts and enriched fractions that were used in this study are summarised in Table 3.1.

Table 3.1: Honeybush crude extracts and enriched fractions investigated in this study

Crude extract/fraction	Abbreviation	Description	Marker molecules present
ARC188	ARC188	Crude extract with relative high benzophenone content	IDG, M3G, I3G, mangiferin and isomangiferin
ARC189	ARC189	Crude extract with relative high iriflophenone dihexoside content	IDG, M3G, I3G, mangiferin and isomangiferin
ARC188 Benzophenone	ARC188 Benz	Fraction of ARC188 containing mainly benzophenones	IDG, M3G and I3G
ARC188 Xanthone	ARC188 Xanth	Fraction of ARC188 containing xanthones and one benzophenone	Mangiferin, isomangiferin and I3G (benzophenone)
ARC189 Iriflophenone dihexoside	ARC189 IdH	Fraction of ARC189 containing mainly two benzophenones	IDG and M3G
ARC189 Benzophenone	ARC189 Benz	Fraction of ARC189 containing mainly benzophenones	IDG, M3G and I3G
ARC189 Xanthone	ARC189 Xanth	Fraction of ARC189 containing xanthones and one benzophenone	Mangiferin, isomangiferin and I3G (benzophenone)

All extracts and fractions were chemically characterised in terms of marker molecule (benzophenones and xanthones) content. These selected marker molecules were quantified in each of the extracts and fractions as listed in Table 3.1 with high performance liquid chromatography with diode-array detection (HPLC-DAD), which are shown in Table 3.2.

Table 3.2: Honeybush rich fractions utilized in experiments

Rich fraction	Marker molecules present				
	Benzophenones			Xanthones	
	IDG	M3G	I3G	Mangiferin	Isomangiferin
ARC 188	√	√	√	√	√
ARC 188 Benzophenone	√	√	√	x	x
ARC 188 Xanthone	x	x	√	√	√
ARC 189	√	√	√	√	√
ARC 189 Iriflophenone dihexoside	√	√	x	x	x
ARC 189 Benzophenone	√	√	√	x	x
ARC 189 Xanthone	x	x	√	√	√

*√=Marker molecule present; x=Marker molecule not present at detectable levels

3.1.3 Characterisation of extracts and analysis of samples

The honeybush extracts were chemically characterised by means of high performance liquid chromatography (HPLC) equipped with a diode-array detector (DAD). The transport and dissolution samples were analysed by means of ultra-high performance chromatography (UHPLC) to determine the concentration of marker molecules.

3.1.3.1 Extraction and fractionation

To select honeybush plant material from which extracts and fractionations, enriched in the selected benzophenones and xanthones, could be produced, extractions were performed on a mini-scale before accordingly. Subsequently, extracts on a “bulk” scale were performed on the selected plant material. For the mini-scale extractions, clean 5 ml Reactivials (Sigma Aldrich, Missouri, USA) were utlized to weigh 40 mg of plant material in. An ethanolic solvent (40% ethanol:water) was prepared in a 500 ml volumetric flask by which 200 ml 99% ethanol (Servochem (Pty) Ltd, Johannesburg, South Africa) was added and further diluted with deionised water to make up to volume. From this solvent, a volume of 4 ml was withdrawn and added to each Reactivial and closed tightley. After pre-heating a Stuart SBH200D/3 block heater (Bibby Scientific, Staffordshire, UK), the samples were placed on the heater and mixed every 5 min for an hour at 93 ˚C. Thereafter, the samples were cooled off and filtrated through

a 0.45 micron Millipore Millex PVDF syringe driven filters (Nerck-Millipore, Darmstadt, Germany). In separate 20 ml volumetric flasks, an amount of 2 ml from each sample was added and further diluted with deionised water up to volume (meniscus mark) from which 1.5 ml aliquots were stored at -20 ˚C. Chemical characterization and quantification of major phenolic compounds were done by HPLC-DAD after a preservative (e.g. ascorbic acid) was added to prevent oxidation to occur.

For the “bulk” scale extraction process, the plant material samples were separated into two groups (Group 1: high in total benzophenones and total xanthones, Group 2: Rich in IDG) based on their phenolic content as determined by the mini-scale screening process. An amount of 150 g of plant material was obtained from each group, which was weighed into clean 2 l glass bottles. An ethanolic solvent (40% ethanol:water) was prepared in a 5 l volumetric flask and 2 l ethanol (99%, Servochem (Pty) Ltd, Johannesburg, South Africa) was added and further diluted with deionised water up to volume. In the 2 l glass botlles, a volume of 1.5 l of the solvent was added to the plant material, which were tightly closed. Thereafter, the samples were mixed every 5 min after being placed in a pre-heated waterbath for 30 min at 93 ˚C. The extractions were filtrated (Whatman #4 filter, Whatman plc, Maidstone, UK) under vacuum after being poured through a 200 mesh stainless steel sieve. A Büchi Rotavapor R-215 (BÜCHI Labortechnik, Flawil, Switzerland) was utilized to evaporate the ethanol from the extraction solutions.

3.1.3.2 XAD fractionation

Approximately 1.2 kg XAD1180 polymeric resin was prepared a day in advance in 100% methanol (Merck-Millipore, Darmstadt, Germany) to be able to expand and swell. Thereafter an open glass column with a large bore was filled with the prepared XAD1180 resin (Sigma-Aldrich, Missouri, USA) to create a column with the following dimensions: 70 mm internal diameter, 550 mm height. The column solvent was changed from 100% methanol to 100% deionised water (Millipore Advantage water purification system, Merck-Millipore, Darmstadt, Germany) before elution commenced by an elution “wash step” using 8 litres of deionised water. Thereafter, 20 grams of the benzophenone rich extract (ARC188), suspended in 40 mL of deionised water, was applied to the top of the column. The elution rate was controlled at 19 ml/min with a Gilson Minipuls 3 peristaltic pump (Gilson Inc., Wisconsin, USA), at room temperature, followed by a stepwise elution, consisting of 4 L each of 100% water (H2O), 10% MeOH:H20, 20% MeOH:H20, 30% MeOH:H20, 40% MeOH:H20, 50% MeOH:H20 and 100% MeOH. Fractions of 1 L volume were collected for the duration of the fractionation. Thereafter, a Thermo Scientific Savant SPD2010 SpeedVac (ThermoFisher Scientific, Waltham, Massachusetts, USA) was utilised to ensure 500 µl samples of each fraction collected and

concentrated from the 1 L fractions by centrifugal concentration. Reconstitution of the concentrated fractions commenced using 10% DMSO, which were then analysed for phenolic content by HPLC with diode-array detection (HPLC-DAD). Based on their phenolic profiles, the remainder of the 1 L fractions were then pooled into a benzophenone rich and a xanthone rich fraction where after the methanol was evaporated using a Büchi Rotavapor R-215 (BÜCHI Labortechnik, Flawil, Switzerland). This XAD fractionation process was repeated for the IDG rich extract (ARC189) from which an IDG-rich fraction was pooled separately from the benzophenone rich and xanthone rich fractions. Lastly a Virtis AdVantage Plus freeze dryer (SP Industries, Pennsylvania, USA) was utilized to ensure the pooled fractions were lyophilized, which were stored under desiccation.

3.1.3.3 High performance liquid chromatography with diode-array detection (HPLC-DAD)

Using the described validated method of Beelders *et al*. (2014b), marker molecules in the crude extracts and rich fractions of *Cyclopia genistoides* were analysed with HPLC-DAD to ensure adequate separation of constituents. HPLC-DAD was performed on an Agilent 1200 series system consisting of an in-line degasser, quaternary pump, autosampler, column thermostat and diode-array detector. Instrument control and data analysis was performed using Openlab Chemstation software (Agilent Technologies Inc., Santa Clara, CA, USA). A Kinetex column protected with an HPLC Krudkratcher Ultra in-line filter (0.5 µm; Phenomenex) was used. The column temperature was maintained at 30 °C. The mobile phase was made up of (A) 1% aq. formic acid (v/v), (B) methanol and (C) acetonitrile. For this analysis a 1.0 mL/min flow rate was set and a multi-linear gradient was performed as follows: 0 min (95.0% A, 2.5% B, 2.5% C), 5 min (95.0% A, 2.5% B, 2.5% C), 45 min (75% A, 12.5% B, 12.5% C), 55 min (50% A, 25.0% B, 25.0% C), 56 min (50% A, 25.0% B, 25.0% C), 57 min (95.0% A, 2.5% B, 2.5% C), 65 min (95.0% A, 2.5% B, 2.5% C). UV-Vis spectra were recorded between 200–700 nm with selective wavelength monitoring at 288 and 320 nm. The benzophenones, IDG and I3G, were monitored at 288 nm, while the xanthones, mangiferin and isomangiferin, and the benzophenone, maclurin, were monitored at 320 nm. Quantification of samples was based on the six-point calibration curves, spanning the expected concentration ranges, using mixtures of authentic standards. Authentic standards in these mixtures were limited to IDG (isolated by the ARC), I3G (Fluka from Sigma-Aldrich), Maclurin (Sigma-Aldrich) and Mangiferin (Sigma-Aldrich). Isomangiferin and M3G was quantified based on response factors calculated relative to mangiferin and maclurin, respectively, as limited amounts of pure compounds were available.

3.1.3.4 Quantification of phenolic compounds in samples with ultra-high performance liquid chromatography with diode-array detection (UHPLC-DAD)

Samples from the in vitro transport studies and dissolution studies were quantified using an unpublished, but validated, UHPLC-DAD method (Beelders, 2015). The high number of samples required a much more rapid analysis system and this led to the use of UHPLC-DAD for this purpose. The analyses were conducted on an Agilent 1290 UHPLC instrument (maximum pressure 1000 bar), consisting of an in-line degasser, binary pump, autosampler, column thermostat and diode-array detector controlled by OpenLab Chemstation software (Agilent Technologies Inc., Santa Clara, CA, USA). A quantitative analyses was performed on an Agilent Zorbax Eclipse Plus C18 column (Rapid Resolution HD; 1.8 µm, 2.1 × 50 mm) with temperature set at 23 °C. The mobile phase comprised of (A) 0.1% formic acid in water (v/v) and (B) acetonitrile. The flow rate was maintained at 0.7 mL/min and a multi-linear gradient was performed as follows: 5-22% B (0-2.2 min), 22-50% B (2.2-2.6 min), 50% B (2.6-4.1 min), 50-5% B (4.1-4.6 min). The column was re-equilibrated for 2 min. UV-Vis spectra were recorded between 200-500 nm at an acquisition rate of 20 Hz, with selective wavelength monitoring at 288 and 320 nm. IDG and I3G were monitored at 288 nm, while M3G, mangiferin and isomangiferin were monitored at 320 nm. A 10-point calibration curve was analysed to cover the range of quantities expected in the various samples.

3.2 ENZYME INHIBITION

Fluorometric methods are often used as suitable analysing methods for enzyme activity assays, but can also be used when determining the enzyme inhibitory potential of compounds. In this study, two fluorometric methods for enzyme inhibition were adapted from Azuma *et al.* (2011) and Sancheti *et al.* (2011), for rat α-glucosidases, and from Andlauer *et al*. (2009) and Slanc *et al*. (2009), for porcine pancreatic lipases. For both types of assays, the activity determination as well as the enzyme inhibition assay itself were performed on a BioTek SynergyHT microplate reader equipped with an in-line dispenser (BioTek, Winooski, USA). Fluorescence (λ_{EX}: 360 nm; λ_{EM}: 460 nm) were used to monitor the release of fluorescent 4-methylumbelliferone from the substrates as a measure of enzyme activity. All samples were analysed in triplicate and on triplicate days. The adapted methods are described below.

3.3 PANCREATIC LIPASE INHIBITION ASSAY

3.3.1 Preparation of buffer

A 75 mM potassium phosphate buffer solution was prepared a day in advance of the enzyme inhibition experiment by weighing approximately 10.2 g KH_2PO_4 (Merck: 1.04873.0250,

Billerica, USA) in a 800 ml glass beaker after which 600 ml HPLC-grade deionised water were added to dissolve the KH_2PO_4. This solution was then adjusted to a pH of 7.4 with a 2 M KOH (Merck, Billerica, USA) solution. Thereafter, the solution was poured into a 1 l volumetric flask, which was made up to volume with HPLC-grade deionised water and properly mixed.

3.3.2 Preparation of enzyme solution

A 3 mg/ml porcine pancreatic lipase stock solution was prepared by weighing 75 mg of porcine pancreatic lipase (Sigma Aldrich: L3126, St. Louis, USA) in a 25 ml volumetric flask. HPLC-grade deionised water was pre-heated in a heating block to 37 ºC and used to make the volumetric flask with the pancreatic lipase up to volume which was carefully mixed by turning the flask from top to bottom and back. The solution was the placed back onto the heating block to incubate at 37 ºC for 30 min and was mixed at regular intervals. The solution was then filtered through a 0.45 µm filter (Durapore, PVDF membrane) utilising a 20 ml syringe with Luer lock and the filtrate was immediately placed on ice. The pancreatic lipase stock solution was then diluted with HPLC-grade deionised water into a range covering lipase concentrations from 0.1 mg/mL to 3 mg/mL, to find an appropriate concentration for the assays to measure the activity. See section 3.3.5 for the activity determination.

3.3.3 Preparation of 4-methylumbelliferyl butyrate solution

A 4 mM (1 mg/ml) 4-methylumbelliferyl butyrate (MUB) (Sigma Aldrich: 19362, St. Louis, USA) solution was freshly prepared on the experimental day by weighing 15 mg MUB in a 15 ml amber vial after which a volume of 10125 µl dimethyl sulfoxide (DMSO) (Sigma Aldrich, St. Louis, USA) was added to produce a solution. After the powder was dissolved, a volume of 4875 µl of HPLC-grade deionised water was added to the amber vial, mixed and allowed to cool down. MUB, as a fluorometric substrate, makes it possible to determine lipase enzyme inhibitory activity of plant extracts by evading the possibility of colour interference that may occur when colorimetric substrates, like *para*-nitrophenyl butyrate, are used (Andlauer *et al*., 2009).

3.3.4 Preparation of orlistat control group solution

A stock solution of a known inhibitor of pancreatic lipase (i.e. orlistat, Sigma Aldrich, St. Louis, USA, IC_{50} = 25 µg/mL) was prepared by dissolving 10 mg orlistat in 5 ml DMSO. The solution was frozen at -20 ºC, which was defrosted when needed and a volume of 156 µl of the defrosted sample was added to a 2 ml boil proof reaction tube to which 844 µl HPLC-grade deionised water were added and vortexed to suspend the mixture. This mixture was used as stock concentration for the positive control at a concentration of 0.3125 mg/mL before addition

to the reaction volume. By using this concentration, a concentration of 25 µg/mL orlistat was achieved in the final reaction volume, which provided a positive control with approximately 50% inhibitory activity.

3.3.5 Determination of lipase activity

A volume of 65 µl of the various enzyme-dilutions, 80 µl of HPLC-grade deionised water and 65 µl of 75 mM potassium phosphate buffer were pipetted into 6 wells, in triplicate, of a black 96-well plate with a clear bottom (Greiner bio-one, Germany). The microplate was placed into the BioTek SunergyHT micro-plate reader (Biotek, Winooski, USA) to incubate at 37 °C for 15 minutes. After the incubation step was completed, the dispenser of the plate reader was thoroughly primed with 1500 µl of MUB and the assay initiated by dispensing 40 µl of MUB into each well of the assay plate. A 30 min incubation period commenced with fluorescence readings recorded with 2 min intervals. The enzyme concentration that yielded optimal activity was selected (e.g. the most suitable activity would yield fluorescence between 70000 and 80000 relative fluorescence units (RFUs) after a 20 min period). A working solution at a final volume of 20 ml was prepared with the concentration of enzyme selected to provide optimal activity to execute the assay.

3.3.6 Pre-incubation

A volume of 20 µl of the control (orlistat) and blank (deionised water) together with 125 µl of the 75 mM potassium phosphate buffer including 65 µl of lipase working solution were pipetted into allocated wells in triplicate on a black 96-well plate with a clear bottom. Samples were diluted with 75 mM potassium phosphate buffer after which 80 µL of sample dilutions, 65 µL potassium phosphate buffer and 65 µL of the lipase working solution was added. The plate was incubated in the micro-plate reader at 37 ºC for 15 min.

3.3.7 Assay incubation

After the 15 min pre-incubation period, the dispenser was again thoroughly primed with 1500 µL MUB and the assay was initiated by dispensing 40 µl of MUB into each well of the assay plate. The assay-mixture was incubated at 37 ºC for a period of 1 h while fluorescence of each well was measured at 2 min intervals. The data was obtained as fluorescence intensity at 460 nm.

Net fluorescence (NetFL) and percentage activity (% activity) was calculated using the following equations:

$$\text{NetFL}=\text{Fluorescence}_{30\ \text{min}}-\text{Fluorescence}_{0\ \text{min}}$$

$$\%\ \text{enzyme activity}=100\times\frac{\text{NetFL}_{\text{sample}}}{\text{NetFL}_{\text{blank}}} \qquad \textbf{[3.1]}$$

3.4 α-Glucosidase inhibition assay

3.4.1 Preparation of buffer

A 200 mm potassium phosphate buffer solution was prepared a day in advance of the enzyme inhibition experiment by weighing an amount of 13.6 g of KH_2PO_4 in a 250 ml glass beaker after which 150 ml HPLC-graded deionised water was added to dissolve the KH_2PO_4. The pH of the solution was adjusted to 6.8 with a 2 m KOH solution. Thereafter the solution was poured into a 500 ml volumetric flask, made up to volume and thoroughly mixed.

3.4.2 Extraction of rat intestinal acetone powders (RIAP)

A solution of rat α-glucosidase was prepared by weighing 350 mg Rat intestinal acetone powders (RIAP, Sigma Aldrich: I1630) in a 15 ml disposable screw cap centrifuge tube. A volume of 10 ml cold potassium phosphate buffer was added and carefully mixed by turning the tube from top to bottom and back, which was then placed on crushed ice.

Utilising an ultrasonic processor (Sonics and Materials, Connecticut, USA), the sample was placed under sonication using a sequence started of 12 x 30 s sonication steps (25 % amplitude) on ice with 1 min resting intervals. The tube with RIAP suspension was then centrifuged at 10 000 x g for 30 min in a Hettich Universal 320R (Sigma Aldrich, St. Louis, USA) at 4 ºC. The supernatant was filtered (Millex HV Durapore filter, 0.45 µm pore size, PVDF membrane) and kept on ice. All the waste was discarded for incineration at a later stage. The supernatant was diluted with cold HPLC-graded deionised water into a range of dilutions covering the expected activity required for the optimised assay and the activity determination performed as described in section 3.4.5.

3.4.3 Preparation of 4-methylumbelliferyl α-D-glucopyranoside solution

A 0.47 mm solution of 4-methylumbelliferyl α-D-glucopyranoside (MUG) (Sigma Aldrich: m9766, St. Louis, USA) substrate solution was freshly prepared on the experimental day by weighing 8 mg MUG in a 20 ml volumetric flask. The solution was dissolved with HPLC-grade deionised water and afterwards made up to volume and stored on ice. The MUG helps to

confirm the presence of any α-glucosidase activity as fluorescence at 460 nm will be observed upon the release of 4-methylumbelliferone from the substrate (Azuma *et al.,* 2011).

3.4.4 Preparation of acarbose control solution

A stock solution (2mg/ mL) of a known inhibitor of α-glucosidase (i.e. acarbose, Sigma Aldrich, St. Louis, USA, published IC_{50} = 42 µg/ml, 65 µM) was prepared as 10 mg acarbose/ 5 ml HPLC-grade deionised water. The acarbose solution was diluted to 525 µg/ mL with deionised water and used as positive control between the plates because it provided a concentration of 42 µg/mL acarbose in the final reaction volume and delivered 50% inhibitory activity.

3.4.5 Determination of α-glucosidase activity

Volumes of 65 µl of the various enzyme-dilutions, 20 µl of HPLC-grade deionised water and 125 µl of potassium phosphate buffer were pipetted into 6 triplicate wells of a black 96-well plate with a clear bottom and incubated in the micro-plate reader at 37 °C for 15 min. After incubation, the dispenser was primed thoroughly with 1500 µl of MUG. Thereafter, the assay was initiated by dispensing 40 µl of MUG into the wells allocated to the enzyme dilutions on the microplate before incubation for a 30 min period with fluorescence measured with 2 minute intervals. The enzyme concentration that yielded optimal activity was selected (e.g. the most suitable activity would yield fluorescence between 70000 and 80000 relative fluorescence units (RFUs) after a 20 min period). A working solution with a final volume of 20 ml was prepared with the correct enzyme dilution to provide optimal activity to conduct the assay.

3.4.6 Pre-incubation

A volume of 20 µl of the positive control (acarbose) and blank (deionised water) solutions together with 125 µl potassium phosphate buffer and 65 µl of the correct dilution α-glucosidase was pipetted into allocated wells on a black 96-well plate with a clear bottom. Samples were diluted with 200 mM potassium phosphate buffer after which 80 µL of sample dilutions, 65 µL potassium phosphate buffer and 65 µL of the lipase working solution was added to their allocated wells. The plate was incubated in the micro-plate reader at 37 ºC for 15 min.

3.4.7 Assay incubation

After the 15 min incubation period, the plate was pushed out of the micro-plate reader and placed to the side. The in-line dispenser was thoroughly primed 1500 µl MUG and the assay was started by dispensing 40 µl of MUG into each well of the assay plate. The microplate was

incubated inside the reader for 1 hour while measuring fluorescence at 2 min intervals. The data was given as fluorescence intensity at 460 nm. Net fluorescence (NetFL) and percentage activity (% activity) was calculated using the following equations:

$$\text{NetFL}=\text{Fluorescence}_{30\ \text{min}}-\text{Fluorescence}_{0\ \text{min}}$$

$$\%\ \text{enzyme activity}=100\times\frac{\text{NetFL}_{\text{sample}}}{\text{NetFL}_{\text{blank}}} \qquad \textbf{[3.2]}$$

3.5 DATA ANALYSIS

3.5.1 Calculation of IC_{50} values

The IC_{50} values were calculated using GraphPad Prism (V 5.04) and is an important parameter indicating the concentration of an inhibitor required to obtain 50% inhibition of a specific enzyme (Ogilvie *et al*., 2008). The IC_{50} values was calculated by a logarithmic regression analysis as discussed in Liu *et al*. (2013).

Confidence interval estimate (CI) is a variable parameter which indicates the statistical significant variation between the control group and the experimental group which are demonstrated as the mean ± 95% CI (Du Plessis and Hamman, 2013).

3.6 *IN VITRO* BI-DIRECTIONAL TRANSPORT STUDIES

3.6.1 Introduction

Different techniques are being applied to evaluate drug transport across the gastrointestinal epithelial membranes. In this study, the Sweetana Grass diffusion chamber apparatus was utilized to perform bi-directional experiments on excised pig intestinal tissues. This was done to evaluate the transport of marker molecules across the intestinal tissue after application of the different extracts of honeybush (*C. genistoides*).

3.6.2 Test solution preparation

Test solutions were prepared as previously reported (Huang *et al*., 2008; Tarirai *et al*., 2012). The crude extract solutions and the benzophenone/xanthone rich fractions, as shown in Table 3.3, were dissolved in Krebs-Ringer bicarbonate (KRB) buffer. To prepare the KRB buffer, the contents of an entire container of KRB mixture (Sigma Aldrich, Johannesburg, South Africa) was added to a 1 l volumetric flask and 1.26 g sodium bicarbonate (Sigma Aldrich, Johannesburg, South Africa) was added after which it was made up to volume with distilled

water and mixed on a magnetic stirrer for 5 min to dissolve completely. The pH was set at 7.4. The KRB buffer was then placed in the refrigerator until experiment commenced.

Table 3.3: Extract compounds utilised in transport experiments

Crude extracts	Enriched fractions
ARC188	ARC188 Benzophenone
	ARC188 Xanthone
ARC189	ARC189 IdH
	ARC189 Benzophenone
	ARC189 Xanthone

3.6.2.1 Tissue collection and preparation

Pig proximal jejunum tissue was collected at Potchefstroom abattoir directly after slaughtering of the pigs. An incision was made from the apex of the ascending loop of the duodenum to get a piece of the proximal jejunum (30-40 cm). The excised jejunal tissue was rinsed with and stored in ice cold KRB buffer during transportation to the laboratory. The clean piece of the dissected jejunum was pulled over a glass tube (Figure 3.1A). The glass tube was turned until the mesenteric border was visible (Figure 3.1B) to remove the serosa gently by blunt dissection (Figure 3.1D) while continuously keeping the segment moist with KRB buffer the whole time (Balimane *et al*., 2000; Legen *et al*., 2005). A cut was made alongside the mesenteric border of the jejunum (Figure 3.1E) after which it was gently washed off the glass tube onto a piece of filter paper (Figure 3.1F).

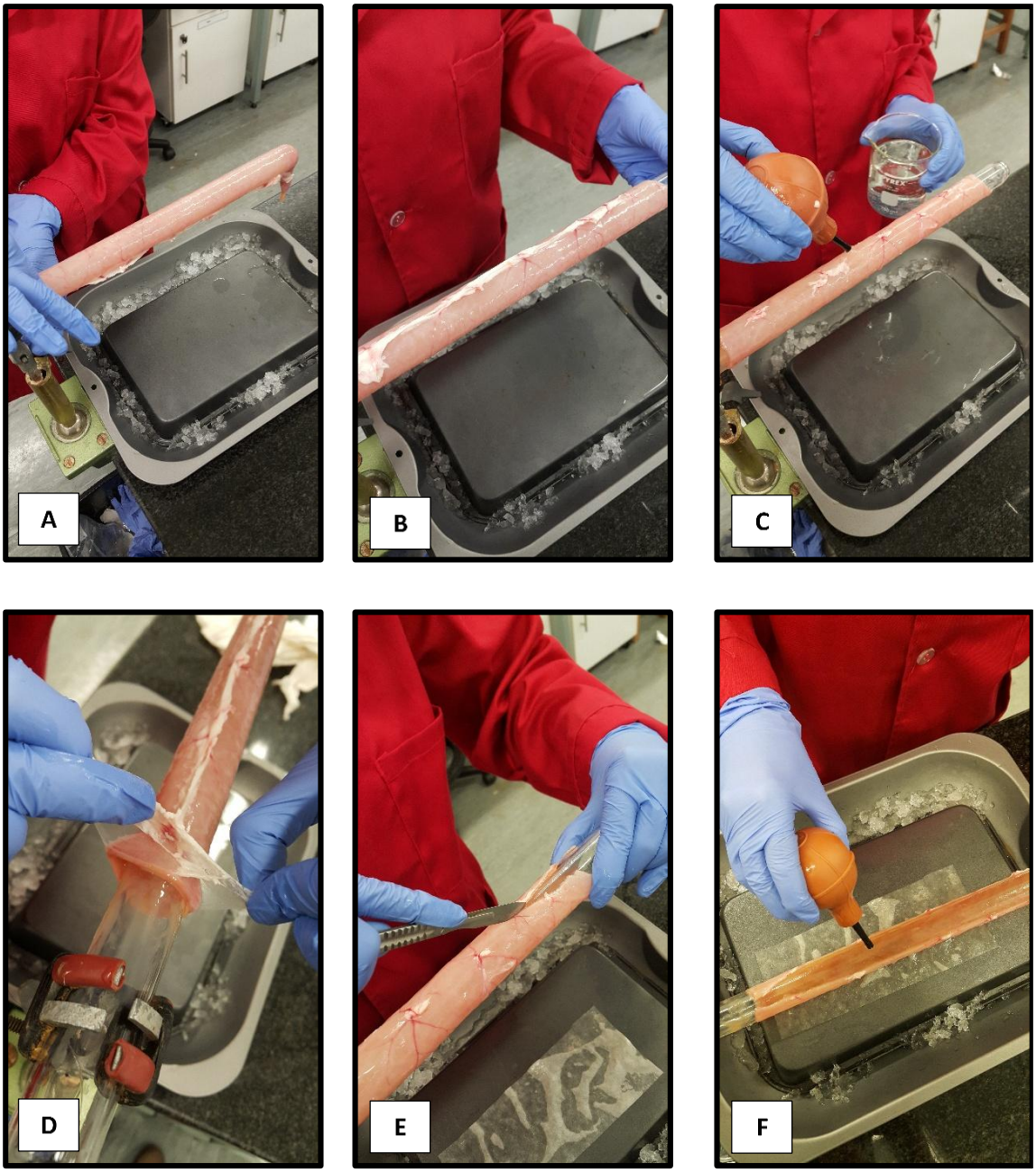

Figure 3.1: Photographs illustrating A) pulling of the proximal jejunum over the glass tube, B) adjusting the meseteric border to be on top, C) keeping the proximal jejunum moist, D) removing of the serosa, E) the cutting of the proximal jejunum alongside the mesenteric border and C) removing the jejunum of the glass test tube by rinsing it off with KRB onto the filter paper

Evenly sized jejunum pieces were cut (Figure 3.2G & H) and placed onto a Sweetana-Grass diffusion chamber half cell (Figure 3.2I).

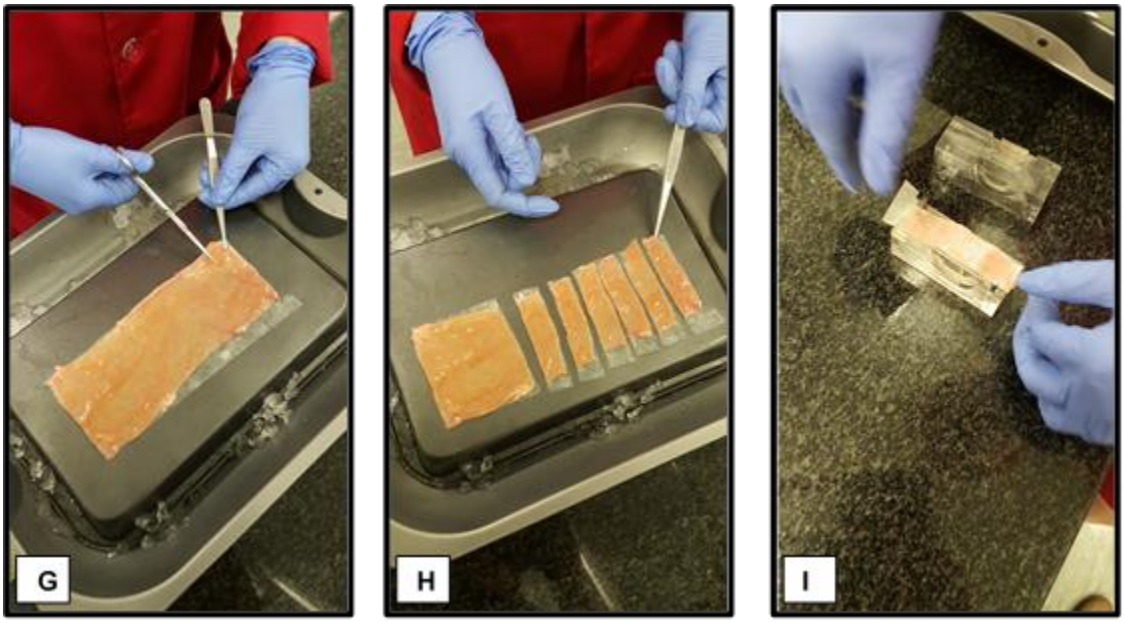

Figure 3.2: Photographs illustrating G) cutting of the proximal jejunum in evely 2 cm sized pieces, H) pieces to be mounted and i) mounting of jejunum pieces on the spikes of the half cells with the filter paper facing upwards

The side of the proximal jejunum facing downwards is the apical side. If any Payer's patches was observed on the jejunum segment, that specific part of the intestinum was removed and not used in the transport experiment. In each case before experiment commenced, the extracts were dissolved in KRB and made up to volume with the specific transport medium and placed in the 37 °C waterbath. After mounting of tissue pieces on all 6 half cells (Figure 3.3J & K), they were placed into the chamber system heating block (which can hold 6 diffusion cells at a temperature of 37 °C) connected with their gas supply (Figure 3.3L).

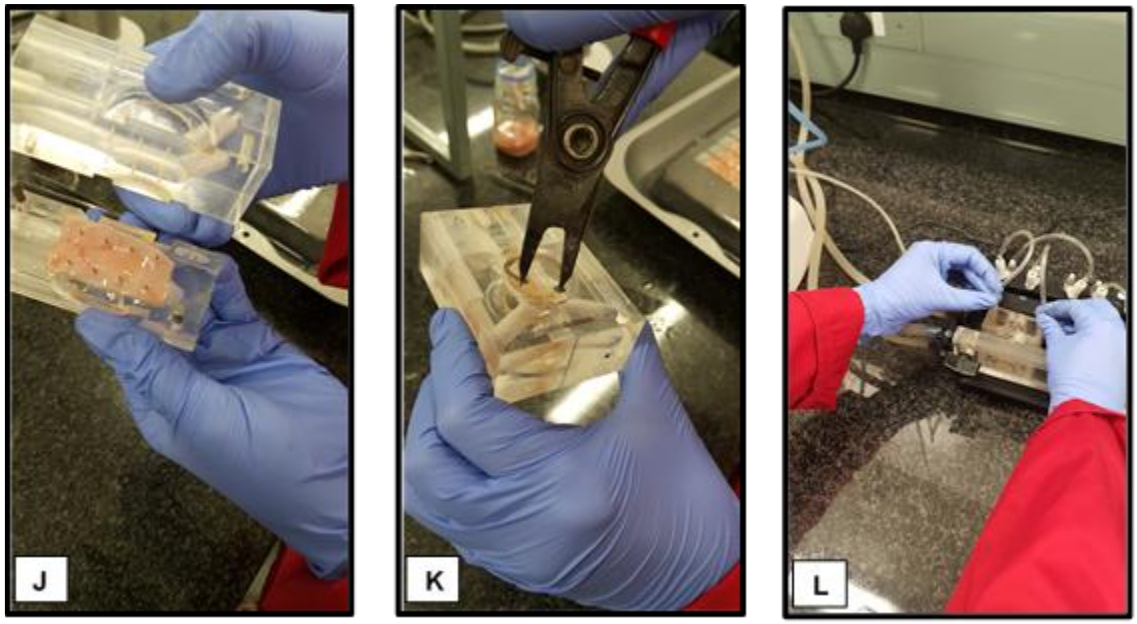

Figure 3.3: Photographs illustrating J) half cells being assembled together, K) adding sirclips to keep the half cells together and L) connection of O_2/CO_2 gas lines to the half cells.

A volume of 7 mL of the preheated KRB was placed into all of the half cell compartments (Figure 3.4M) where O_2(95%)/CO_2(5%) was allowed to pass through the buffer in both the apical and basolateral chambers for 15 min (Figure 3.4M) to ensure the jejunum tissue can adjust to the new environment they were placed in (Grass and Sweetana, 1988).

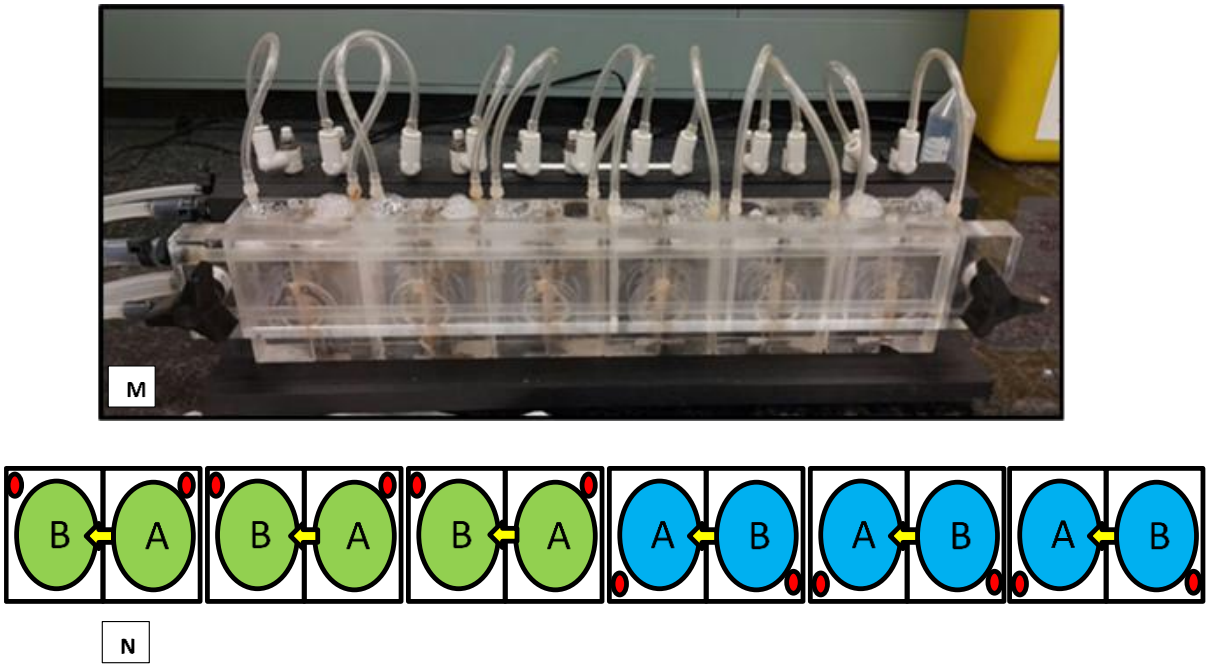

Figure 3.4: Photograph illustrating n) the KRB buffer placed into half cells with the O_2/CO_2 supply and N) transport direction from AP-BL direction (green circles) and BL-AP direction (blue circles)

After the 15 min have passed, the apical chambers (green circles) and basolateral chambers (blue circles) (Figure 3.4N) have been aspirated (Integra vacusafe aspirator, Labotec, South Africa) to remove the KRB buffer solution and to replaced it with the test solution.

3.6.3 Transport experiment

Bi-directional (apical-to-basolateral and basolateral-to-apical) transport experiments were performed after test solutions were added to the chambers as explained above. The excised pig intestinal tissue mounted in the Sweetana-Grass diffusion chambers was incubated for 2 h, during which samples of 400 µl were taken from the basolateral chambers (for AP-BL transport (green circles) and from the apical chambers (for BL-AP transport (blue circles)) (Figure 3.4N) at 20 min intervals and the volume was replaced with KRB buffer (Madgula *et al.,* 2008; Vermaak *et al.,* 2011b). By using dual channel voltage clamps, the transepithelial electrical resistance (TEER) was measured (Millipore corporations) at the beginning of the experiment after test compound was added and at the end of the 2 h experiment. The transport studies were done in triplicate for both the AP-BL direction and for the BL-AP direction.

The apparent permeability coefficient (P_{app}) (cm/s) values were calculated from the transport data according to the following equation (Hansen and Nilsen, 2009):

$$P_{app} = \left(\frac{dQ}{dt}\right) X \left(\frac{1}{(A)(C_0)(60)}\right) \quad \textbf{[3.3]}$$

P_{app} = Apparent permeability coefficient (cm/s),

dQ/dt = Rate of increase of the substrate in the receiver chamber (mg/min),

A = Surface area of the cell monolayer (cm^2),

C_0 = Initial concentration in the donor chamber.

Efflux ratio (ER) values will be calculated by the following equation (Hansen and Nilsen, 2009).

$$ER = \frac{P_{app}(BL\text{-}AP)}{P_{app}(AP\text{-}BL)} \quad \textbf{[3.4]}$$

P_{app}(BL-AP) and P_{app}(AP-BL) represent the apparent permeability coefficient values in the secretory and absorptive directions, respectively.

3.7 DEVELOPMENT OF A GASTRO-RETENTIVE DRUG DELIVERY SYSTEM

3.7.1 Introduction

Most oral dosage forms struggle to keep the released drug in the absorption window (i.e. region in the gastrointestinal tract where maximum absorption occurs) for long enough periods to optimise drug bioavailability. One approach to overcome this problem, is to develop a gastro-retentive delivery system that stays in the stomach and releases the drug at a slow rate over an extended period of time. This will allow drug to be released into the small intestine over relatively long periods. It therefore ensures that drug molecules are supplied to the site of absorption or site of action (e.g. when acting locally in the gastrointestinal tract) over an extended period of time. (Arora *et al*., 2005; Narang, 2010a; Sharma and Sharma, 2014; Streubel *et al*., 2006).

3.7.2 Formulation of beads with low density polymers

Two bead formulations were prepared by using low density polymeric excipients (polypropylene (PP) and polystyrene divinylbenzene copolymer (PDC), which will produce a non-effervescent floating gastro-retentive dosage form. Methods described by Krueger *et al*. (2013), Raval *et al*., (2011), Steckel and Mindermann-Nogly (2004) and Streubel *et al*., (2002) were adapted to prepare the beads from the selected low density polymers.

Different ratio combinations of the powder mixtures containing Pharmacel® 101 (MCC) (DFE Pharma, Germany) together with PP (Sigma Aldrich, Johannesburg, South Africa) or PDC

(SUPELCO, Sigma Aldrich, Johannesburg, South Africa) were evaluated (i.e. MCC:PP or MCC:PDC in ratios 10:90, 20:80, 30:70, 40:60, 50:50) to determine which combination will produce a suitable non-effervescent floating bead formulation. The best excipient and active combinations that were found to produce beads with acceptable buoyance are shown in Table 3.4.

Table 3.4: Bead formulation containing low density polymers to produce acceptable buoyancy

Formula number	Active ingredient	Polymer	Binding agent	Other excipients	Wetting agents
1	Honeybush crude extract (ARC 188) at 1.25% w/w (0.625 g)	Polypropylene (PP) at 50% w/w (25 g)	Pharmacel® 101 at 48.75% w/w (24.375 g)	Camphor at 2.5% w/w (1.25 g)	Distilled water (36 ml) and Ethanol (4 ml)
2	Honeybush crude extract (ARC 188) at 1.25% w/w (0.625 g)	Polystyrene divinylbenzene copolymer (PDC) 50% w/w (25 g)	Pharmacel® 101 48.75% w/w (24.375 g)	Camphor 2.5% w/w (1.25 g)	Distilled water (28 ml) and Ethanol (10 ml)

3.7.3 Extrusion spheronisation

After excipients were weighed and added together, each batch of powder was mixed for a period of 5 min in a Turbula mixer (Turbula T2C Heavy-Duty Shaker-Mixer, Champaign, Illinois) at 69 rpm to guarantee a homogenous mixture of ingredients. The evenly mixed dry powders were added to a mixing bowl and wetting agents (i.e. distilled water and ethanol) were added slowly. The powder mixture was stirred with a Kenwood hand mixer (Maraisburg, South Africa) during addition of the wetting agent to obtain an evenly wet mass. Extrusion was done utilising a Caleva Model 20 Extruder (North Brunswick, New Jersey) equipped with a 1.5 mm sieve at a constant rate of 35 rpm for 2-3 min to acquire an extrudate with spaghetti like cylinders (Figure 3.5).

A B

Figure 3.5: Photograph of the Caleva extruder apparatus with extrudate: A) front view, B) side view

Spheronisation followed where the extrudate was poured into the Multi-Bowl spheronizer (North Brunswick, New Jersey) for 5 min at 1500 rpm to ensure smooth spherical beads being formed from each extrudated rod (Figure 3.6).

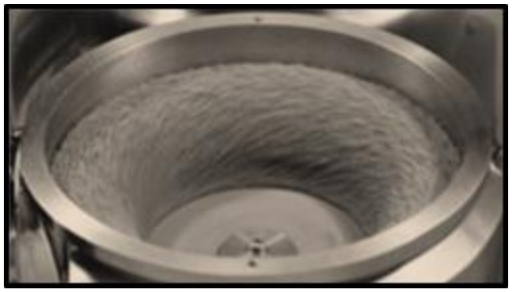

Figure 3.6: Photograph illustrating how the extrudate is being spheronised (Sachdeva *et al*., 2013)

Beads were collected after the completion of spheronisation process. Before the next batch could be extruded and spheronised, the equipment was cleaned to prevent contamination of the new batch. After collecting the beads, they were weighed and dried in a vacuum oven (Vismara Thermic Line's vacuum oven, Midrand, South Africa) at 35 °C at 200 mbar for a period of 7 days to ensure the camphor has been sublimated completely.

3.7.4 Preparation of a multi-unit pellet system tablet

The tabletting was done by using a single-punch tablet press (KORSCH XP 1 with the PharmaResearch® comprehensive analysis software, Berlin, Germany) having a standard convex lower and upper punch diameter of 10 mm. The filling depth max was set at 9 mm and the upper punch insertion depth was set at 10 mm. Each batch of beads was poured into the hopper shoe of the tablet press, followed by direct compression of low density MUPS tablets.

3.7.5 Bead characterisation

3.7.5.1 Angle of repose

To establish the flow properties of each batch of beads, the angle of repose (AOR) method was utilized. The funnel was closed before pouring the beads into the funnel to ensure the beads fall simultaneously through the funnel. The funnel was set at a fixed height of 4 cm above the platform surface of the fixed height cone apparatus (Potchefstroom, South Africa). After opening the shutter lever of the funnel, the beads flowed freely through the opening and formed a conical shape pile as shown in Figure 3.7 below. The test was performed in triplicate for each batch. AOR value of 25° represents exceptionally good flow properties, whereas values higher than 50° indicate unsatisfactory results in terms of flow properties (Stanifort and Aulton, 2007).

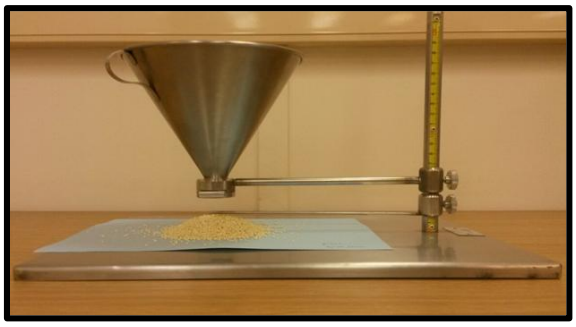

Figure 3.7: Photograph illustrating the angle of repose apparatus during use with one of the bead formulations

To calculate the AOR, the following equation has been applied (Monton *et al*., 2014):

$$\text{Angle of repose } (\theta) = \tan^{-1}\frac{h}{r} \qquad \textbf{[3.5]}$$

Where:

h = the cone height of the beads in cm,

r = the radius in cm of the cone which forms a round base on the platform surface

3.7.5.2 Flow rate

Another method for the determination of the flow properties of beads is the flow rate, which was determined with an ERWEKA GTL Powder and Granulate Flow Tester (Heusenstamm, Germany) (Figure 3.8). This apparatus is specifically designed for high-speed analysis on a small scale (Seppälä *et al*., 2010). The flow rate of each batch of beads was tested in triplicate. According to the British Pharmacopoeia (2016), flow rate values can be determined by mass per time flowing through a funnel which can be distinguish by continuous flow or discontinuous incremental flow patterns.

Figure 3.8: Photograph illustrating the Erweka flow rate apparatus

3.7.6 MUPS characterisation

3.7.6.1 Buoyancy

The buoyancy method was adapted from the method described by Hadi *et al*. (2013) and Kumaran *et al*. (2010). The buoyancy of each batch of MUPS tablets was tested by the placement of a tablet in a glass beaker containing 800 ml of 0.1 N HCl media (ACE, Southdale, Johannesburg) with a pH of 1.2 to mimic the gastrointestinal environment. The beakers were then placed on a magnetic stirrer with a magnet in the beaker and stirred while observing them for a period of 24 h or until the last tablet descended to the bottom of the beaker. The buoyance test of each batch of MUPS tablets was done in triplicate.

3.7.6.2 Disintegration

A disintegration test apparatus (ERWEKA, Heusenstamm, Germany) was used to test 6 tablets of each batch to determine whether the tablets disintegrate within a specified time frame (15 min) when inserted into the vessels and into the medium. A disintegration disk was

placed on top of the tablets to prevent the tablets from floating. The disintegration medium consisted of water, which was maintained at 37 °C. For the test to be successful all 6 tablets must disintegrate within 15 min and no fragments of the tablet must be visible on the sieve of the vessel (Alderborn, 2007; Schmid and Löbenberg, 2010).

3.7.6.3 Friability

A friability apparatus (ERWEKA TAR friability and abrasion apparatus, Heusenstamm, Germany) was utilized to evaluate the friability percentage of each batch of MUPS tablets. The friability was tested for 10 tablets of each batch. Each batch of MUPS tablets were dusted, weighed and placed in the friability drum at a rate of 25 rpm for 4 min. A tablet should have a friability value of <1 %. After the completion of the rotating cycle of the friability drum, the tablets were dusted again and weighed (Reddy *et al.,* (2016)):

$$\% \text{ Friability} = \frac{(W_0 - W)}{W_0} \times 100 \qquad \textbf{[3.6]}$$

Where:

W_0 = Tablets initial weight before the test commenced

W = Tablets weight after completion of the test

3.7.6.4 Hardness, thickness and diameter

The determination of the hardness, thickness and diameter of the MUPS tablets were done on a semi-automatic combination tester (ERWEKA TBH 425, Heusenstamm, Germany) measuring a quantity of 10 tablets from each batch.

3.7.6.5 Mass variation

To determine the mass variation of each batch of MUPS tablets, the average mass was calculated. A total of 10 tablets from each batch were weighed individually and the deviation of the average tablet's mass was determined and the mass variation limitations are shown in Table 3.5 (British Pharmacopoeia, 2016).

Table 3.5: Mass variation limitations (British Pharmacopoeia, 2016)

Pharmaceutical form	Average tablet mass	% deviation
Tablets (uncoated)	80 mg or less	10
	> 80 mg and < 250 mg	7.5
	≥ 250 mg	5

3.7.6.6 Assay for drug content evaluation

The assay which was performed is outlined in Annexure D. To determine the drug content in each formulation, three tablets from each batch were individually weighed and powdered in a pestle and mortar. The powdered mass was then rinsed out with a small volume of the 0.1 N HCl into a 100 ml volumetric flask. The volumetric flask was then placed on top of a magnetic stirrer and it was made up to volume and stirred for a period of 15 min. After the 15 min have passed, the volumetric flask was placed in an ultrasonic bath (Integral systems, Randburg, South Africa) for 10 min to ensure the extract was completely released. A sample was filtered through a 0.45 μm membrane and dried in a freeze dryer (VirTis BenchTop, Stone Ridge, New York) after which it was analysed by means of UHPLC for marker molecule content.

3.8 DISSOLUTION

A dissolution apparatus with automated sampler system Distek Model 2500, North Brunswick, New Jersey) was used to determine the release characteristics (or dissolution profile) for each of the MUPS formulations in 0.1 N HCl medium with a pH of 1.2 at 37 °C. The dissolution method was executed with the parameters as shown in Table 3.6.

Table 3.6: Dissolution parameters used in this study

Time interval (min)	Test rpm	Infinity rpm	Volume (ml)	Medium
15, 30, 60, 120, 180, 300 and 480	50	250 for 15 min	700	0.1 N HCl

When the waterbath reached a temperature of 37 °C, two tablets of each batch was placed in each of six dissolution vessels numbered from 1 – 6. The rotation speed of the paddle was set at a constant speed of 50 revolutions per minute (rpm) for the period of 480 min. At every time interval as shown in Table 3.6, samples were withdrawn utilising a 10 μm filter (QLA, 100% Porous polyethylene micron filter) to ensure that no suspended particulates are present when sample are analysed. Dissolution medium was replaced after every sample withdrawal. After the last sample was withdrawn at 480 min, the rotation speed was accelerated to 250 rpm to ensure complete drug release occurred from tablets where after another sample was withdrawn. There after the vessels were placed in an ultrasonic bath to ensure complete dissolution. Another sample was withdrawn and filtered through a 0.45 μm filter and placed on the freeze dryer. All the dissolution experiments were done in triplicate.

Various approaches can be utilized to compare the dissolution profiles of different formulations and they include (a) mean dissolution time (MDT) (Ritger and Peppas, 1987) and (b) fit factors (f_1=dissimilarity factor and f_2= similarity factor) (Moore and Flanner, 1996).

The mean dissolution time (MDT) is the intended time in a state of *in vitro* conditions for the drug to become incorporated into a solution. The MDT was calculated by comparing the cumulative mass dissolved against the time profile with the following equation (Ritger and Peppas, 1987):

$$MDT = \frac{\sum_{i=1}^{n} t_{mid}\Delta X_d}{\sum_{i=1}^{n} \Delta X_d} \quad \textbf{[3.7]}$$

Where: $\sum$ = Sum of the equation

n = total sample times

i = sample number

t_{mid} = time at midpoint between i and i-1

ΔX_d = additional mass of drug dissolved between i and i-1

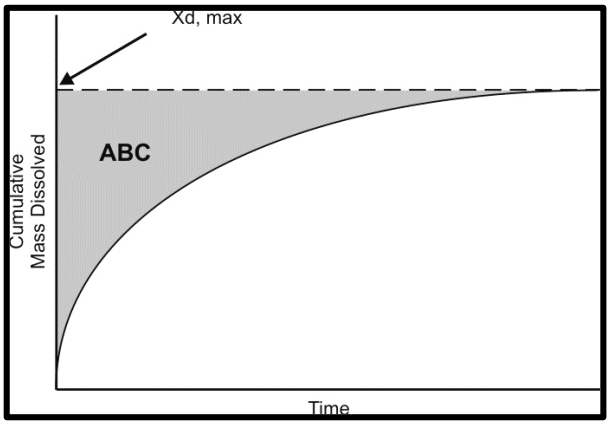

Figure 3.9: A diagrammatic illustration to interpret the parameters used for the determination of a specific MDT value (Ritger and Peppas, 1987).

To determine whether there's a variance between different dissolution profiles the dissimilarity (f_1) and the similarity factors (f_2) were calculated to illustrate the results by the following equations (Moore and Flanner, 1996):

$$f_1 = \left\{\frac{\sum_{t=1}^{n}|R_t - T_t|}{\sum_{t=1}^{n} R_t}\right\} \times 100 \quad \textbf{[3.8]}$$

Where: R_t = reference assay at time point t,

T_t = test assay at time point t,

n = number of samples withdrawn

$$f_2 = 50 \log \left\{ \left[1 + \frac{1}{n} \sum_{t=1}^{n} w_t (R_t - T_t)^2 \right]^{-0.5} \times 100 \right\} \quad \textbf{[3.9]}$$

Where: R_i = reference assay at time t

T_t = test assay at time t

n = number of pull pints

w_t = optional weight factor

As seen above, the equation for f_2 illustrates that it is a log value of the sum expressed as the sum of squared error to determine what the difference will be between the reference and test profiles at a point between 0-100. When the f_2 value reach hundred then the reference and the test samples can be seen as identical and as the dissimilarity increases the f_2 value will then approach zero (Moore and Flanner, 1996).

CHAPTER 4

RESULTS AND DISCUSSION

4.1 INTRODUCTION

This chapter presents all the results obtained for the different experiments conducted on honeybush crude extracts (i.e. ARC188 and ARC189), benzophenone (Benz) rich fractions (i.e. ARC188 Benz and ARC189 Benz) and xanthone (Xanth) rich fractions (i.e. ARC188 Xanth and ARC189 Xanth) from *Cyclopia genistoides*. Enzyme inhibitory effects of the selected extracts on lipase and α-glucosidase enzymes were evaluated to establish the possibility of these extracts to help prevent and/or treat "diabesity". Due to a lack of intestinal permeability data for honeybush extracts, it was important to establish the absorption potential of phytochemical marker molecules in an appropriate *in vitro* diffusion model. The buoyancy and dissolution profiles of non-effervescent gastro-retentive drug delivery systems containing honeybush crude extract were determined. The objective with the development of this formulation was to create a dosage form that can deliver the active components of honeybush extract into the small intestine over an extended period of time to inhibit the targeted enzymes in the lumen of the gastrointestinal tract.

4.2 CHEMICAL CHARACTERISATION OF HONEYBUSH EXTRACTS AND FRACTIONS

Representative chromatograms obtained from the high performance liquid chromatography diode-array (HPLC-DAD) of the marker molecules present in honeybush crude extracts and fractions are shown in Figures 4.1 - 4.7.

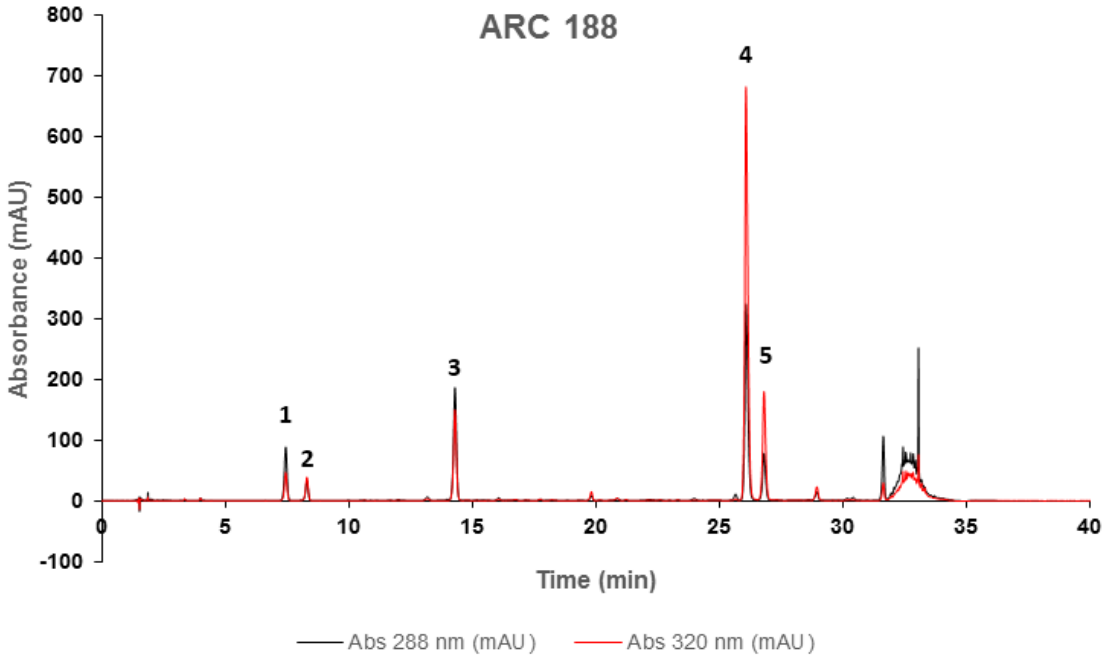

Figure 4.1: High performance liquid chromatogram of ARC188 crude extract with following marker molecules 1) IDG, 2) M3G, 3) I3G, 4) mangiferin and 5) isomangiferin

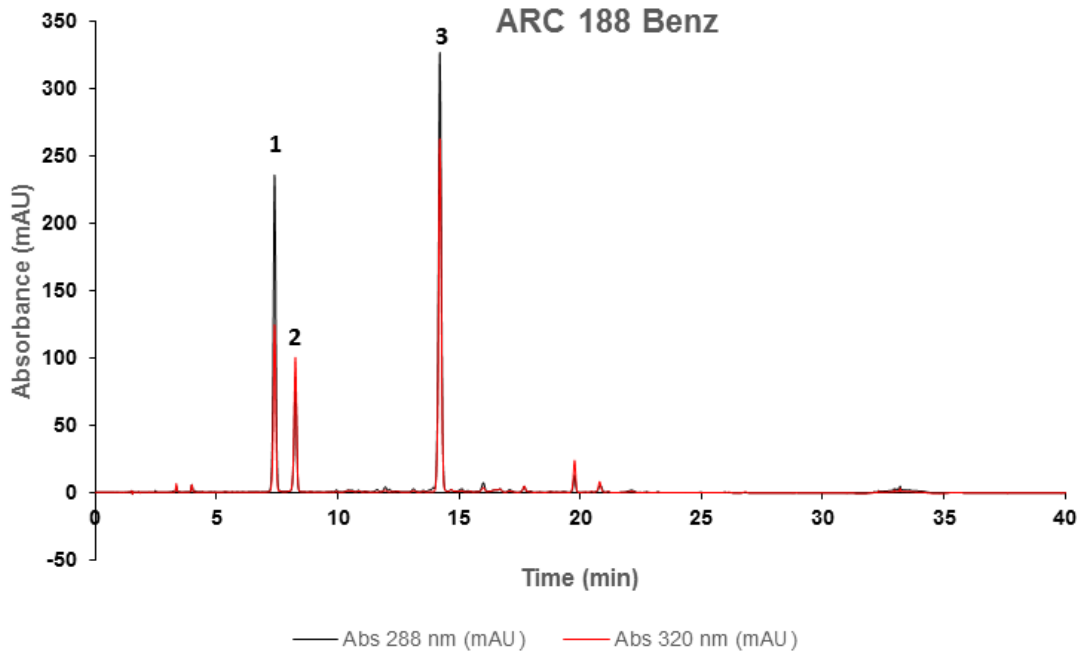

Figure 4.2: High performance liquid chromatogram of ARC188 Benz rich fraction with following marker molecules 1) IDG, 2) M3G, 3) I3G

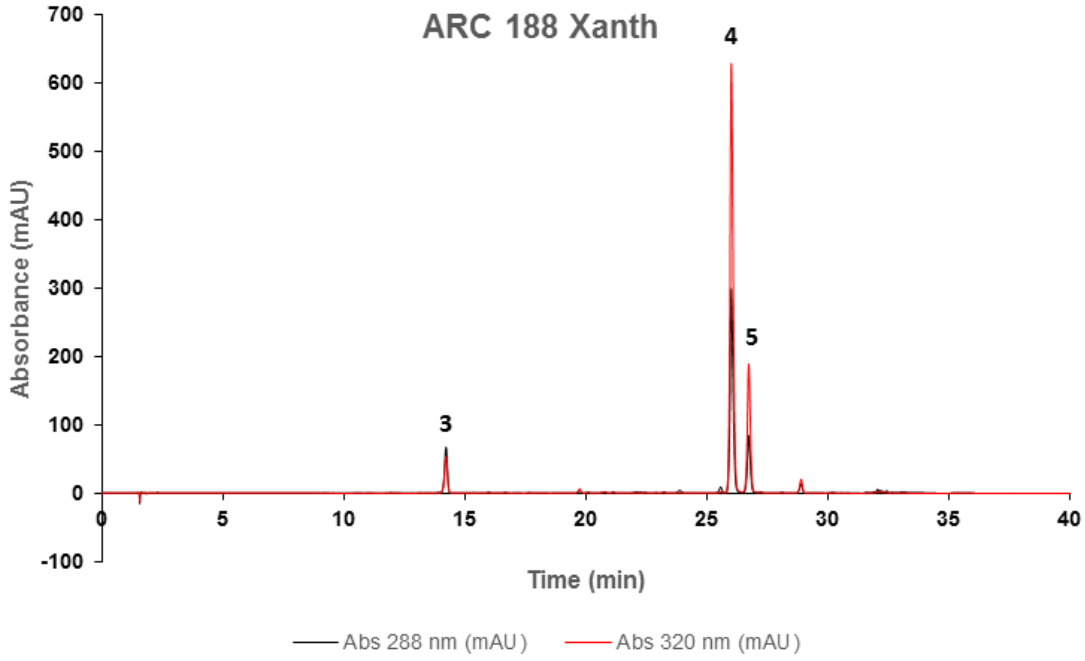

Figure 4.3: High performance liquid chromatogram of ARC188 Xanth rich fraction with following marker molecules 3) I3G, 4) mangiferin and 5) isomangiferin

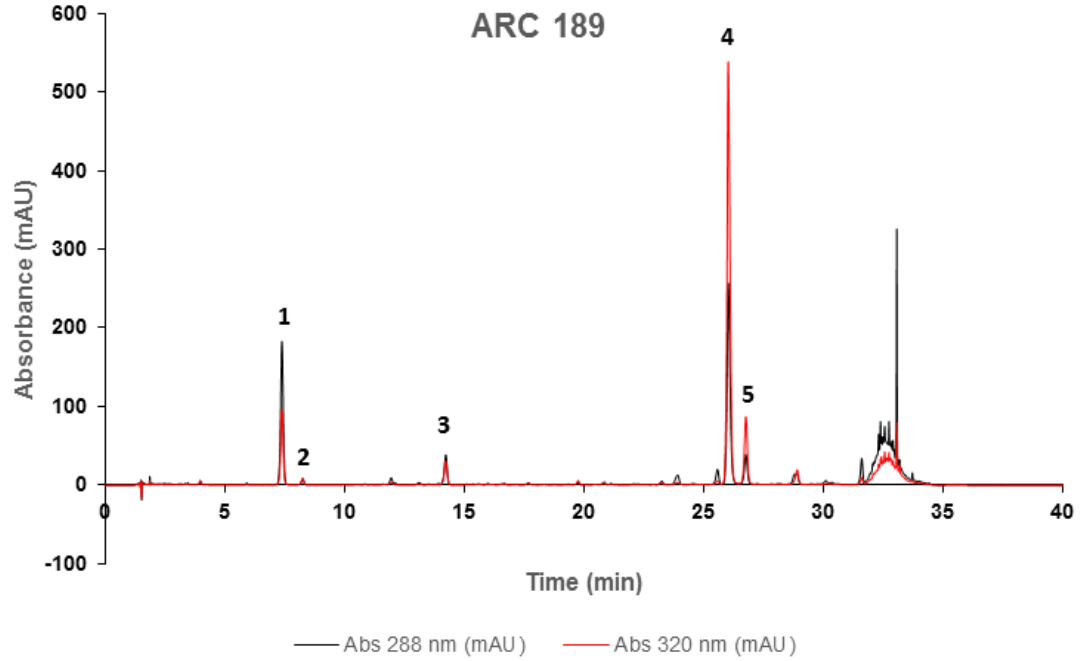

Figure 4.4: High performance liquid chromatogram of ARC189 crude extract with following marker molecules 1) IDG, 2) M3G, 3) I3G, 4) mangiferin and 5) isomangiferin

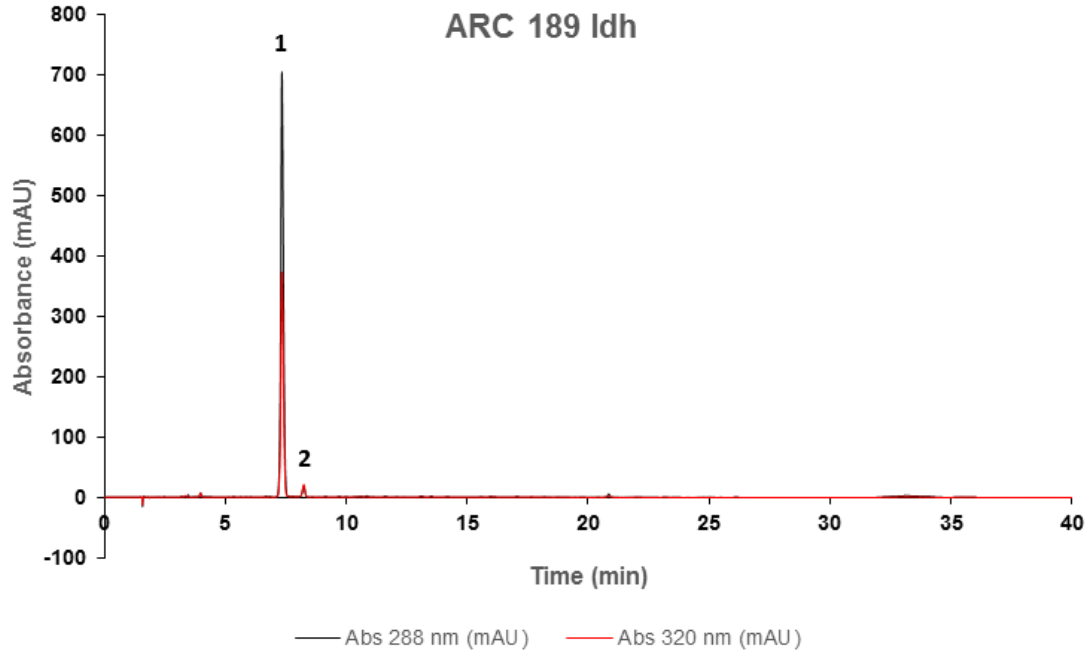

Figure 4.5: High performance liquid chromatogram of ARC18 IdH rich fraction with following marker molecules 1) IDG, 2) M3G

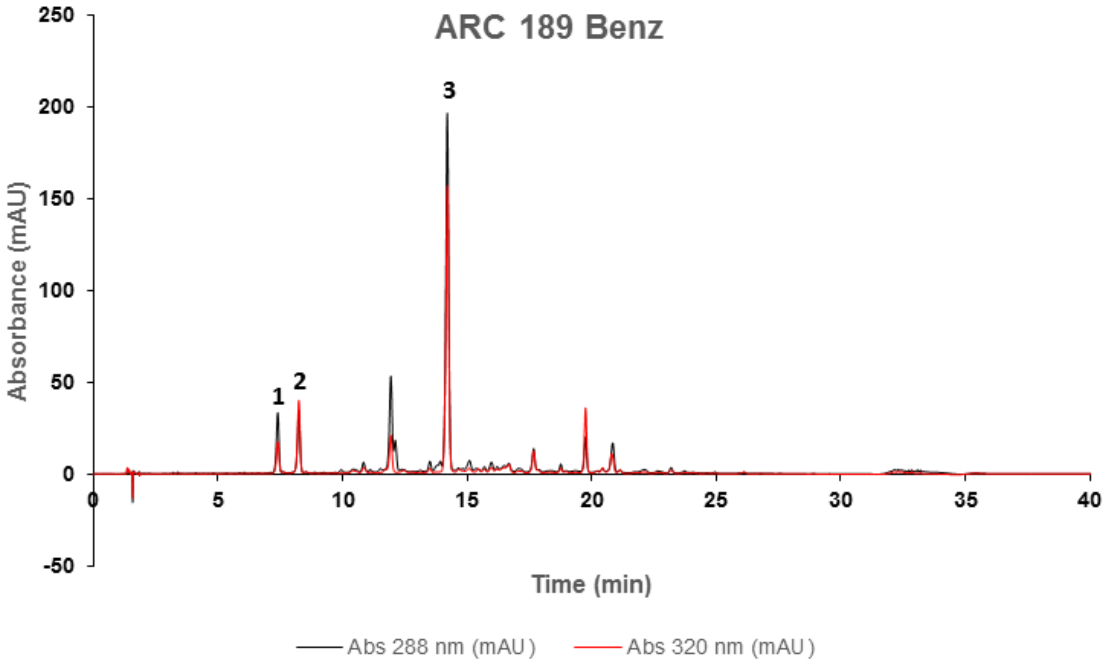

Figure 4.6: High performance liquid chromatogram of ARC189 Benz rich fraction with following marker molecules 1) IDG, 2) M3G, 3) I3G

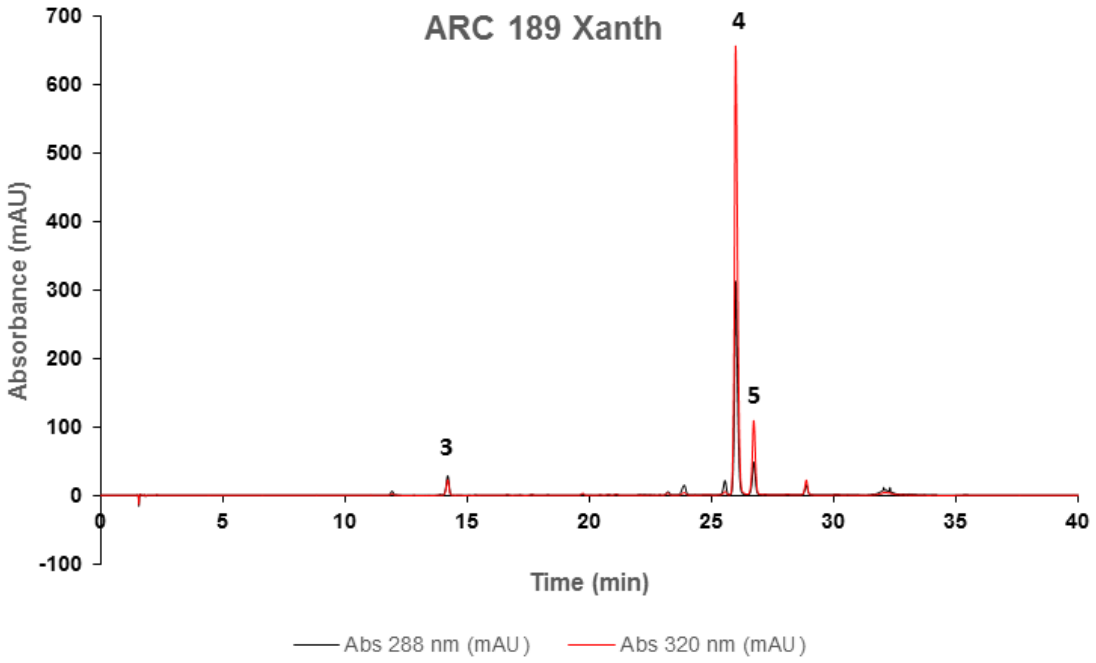

Figure 4.7: High performance liquid chromatogram of ARC189 Xanth rich fraction with following marker molecules 3) I3G, 4) mangiferin and 5) isomangiferin

The quantities of selected benzophenones and xanthones in the different crude extracts and fractions as measured by means of HPLC-DAD are shown in Table 4.1.

Table 4.1: The high performance liquid chromatography diode-array (HPLC-DAD) measured quantities of the different crude extracts and fractions containing benzophenones and xanthones

Crude extract and fractions	(g/100g powder)				
	Benzophenones			Xanthones	
	IDG	M3G	I3G	Mangiferin	Isomangiferin
ARC188	2.214	1.101	3.885	13.811	3.193
ARC188 Benz	23.267	11.384	28.272	0	0
ARC188 Xanth	0	0	5.804	54.016	14.352
ARC189	4.902	0.254	0.807	11.622	1.667
ARC189 IdH	74.966	2.389	0	0	0
ARC189 Benz	3.048	4.400	16.602	0	0
ARC189 Xanth	0	0	2.233	53.792	7.869

4.3 ENZYME INHIBITION

4.3.1 Pancreatic lipase inhibition

An important enzyme group regulating the metabolism of fats from dietary preferences are known as the lipases (e.g. pancreatic lipases etc.) (Birari and Bhutani, 2007). To evaluate the potential of the phytoconstituents present in honeybush for inhibitory properties against lipases in the intestine, it is important to benchmark it against a known enzyme inhibitor such as orlistat (a synthetic pancreatic lipase inhibitor), which was utilized as the positive control in the current study. The porcine pancreatic lipase (PPL) inhibitory effects of honeybush extracts and fractions were analysed and the results obtained are illustrated in Figure 4.8 and Figure 4.9.

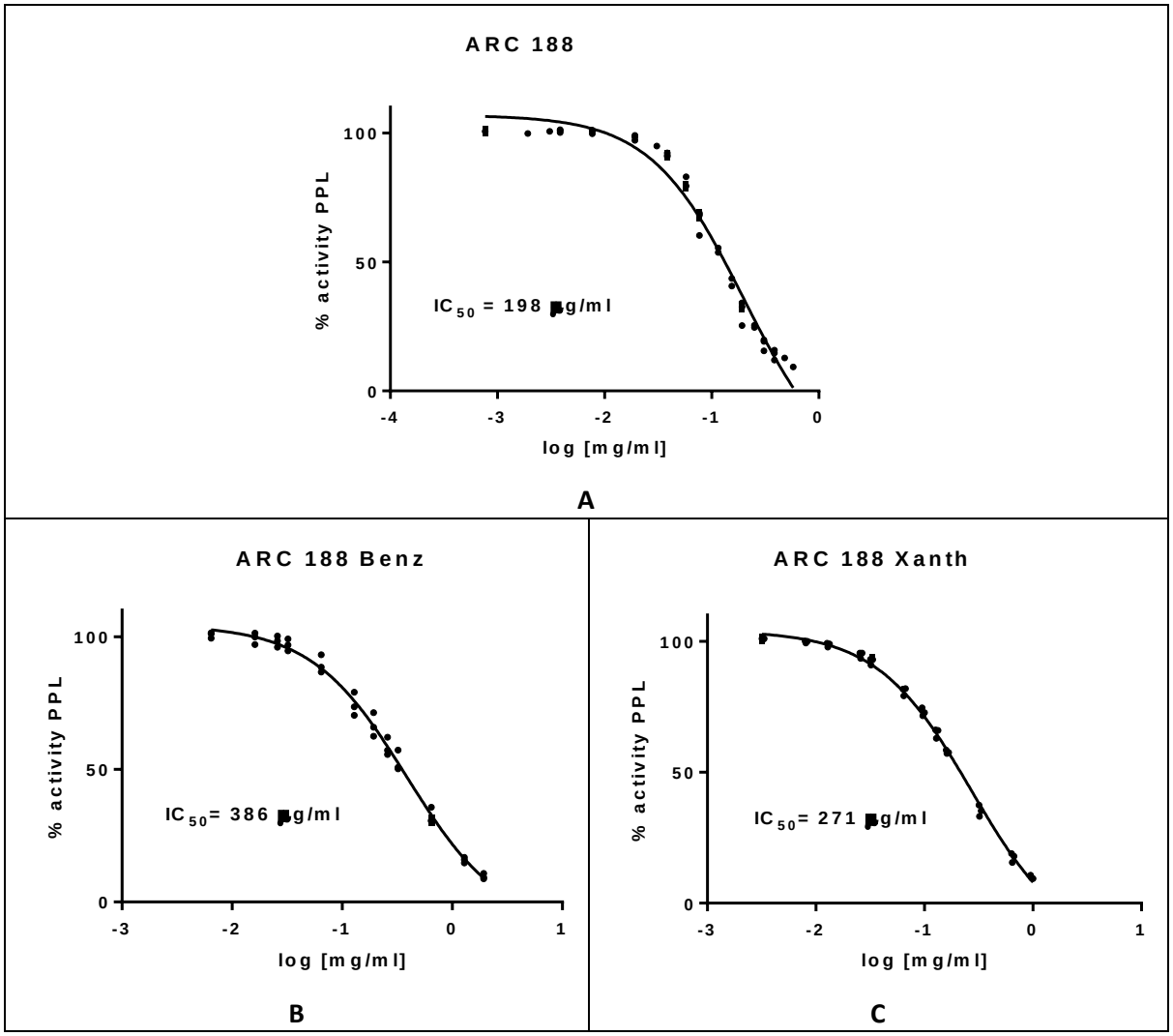

Figure 4.8: Semi-logarithmic plot of the percentage porcine pancreatic lipase (PPL) activity as a function of concentration for A) ARC188 honeybush crude extract, B) ARC188 Benz rich fraction and C) ARC188 Xanth rich fraction (n = 3)

From Figure 4.8A, higher inhibitory effects against the porcine pancreatic lipase enzyme are observed for the ARC188 crude extract (IC_{50} = 198 µg/ml) than for the ARC188 Xanth (IC_{50} = 271 µg/ml) rich fraction and the ARC188 Benz (IC_{50} = 386 µg/ml) rich fraction. It is noted that the ARC188 Xanth rich fraction (containing mangiferin and isomangiferin) showed a higher inhibitory action against porcine pancreatic lipase than the ARC188 Benz rich fraction (containing IDG, M3G and I3G). The reason why the ARC188 crude extract may have shown better lipase inhibitory activity could be that the extract contains xanthone marker molecules in addition to the benzophenone marker molecules, which may have worked additively or synergistically (Table 4.1). Results from Zhang *et al*. (2011) have shown that mangiferin, isolated from their plant material, showed the highest inhibitory activity. Zhang *et al*. (2011)

have also found that accumulation of free fatty acids can be profoundly suppressed by the benzophenone compounds they have isolated (i.e. I3G and M3G) which corresponds with our findings that they exhibit lipase inhibitory action.

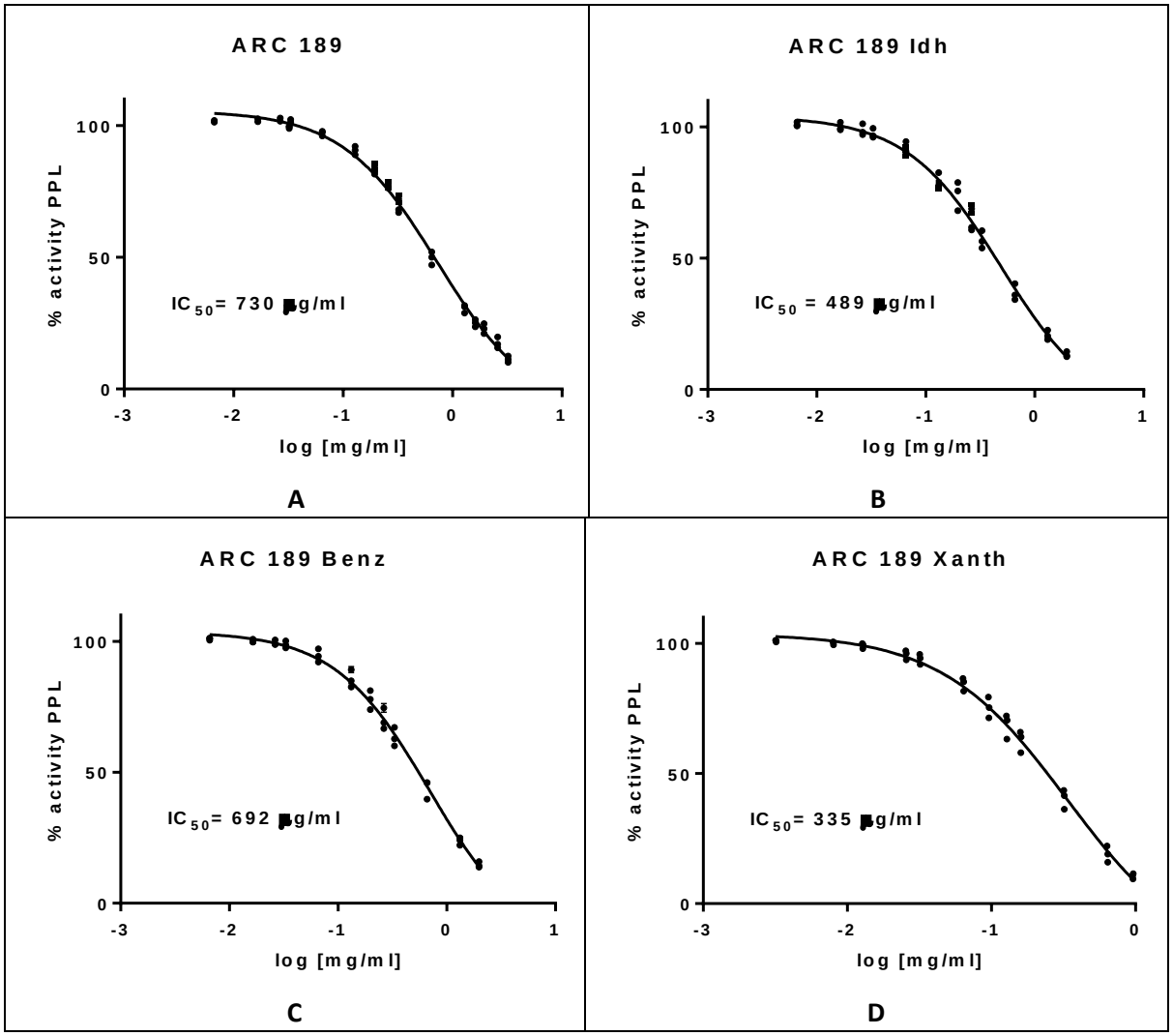

Figure 4.9: Semi-logarithmic plot of the percentage porcine pancreatic lipase (PPL) inhibitory activity of A) ARC189 crude extract, B) ARC189 IdH rich fraction C) ARC189 Benz rich fraction and D) ARC189 Xanth rich fraction (n = 3)

In accordance with the enzyme inhibition results obtained for ARC188 Xanth rich fraction (Figure 4.8C), the ARC189 Xanth rich fraction (Figure 4.9D) also demonstrated the highest inhibitory action against the porcine pancreatic lipase of all the ARC189 related fractions. When looking at Table 4.1, mangiferin presented with the highest concentration in both the ARC188 Xanth and ARC189 Xanth rich fractions. It is possible that mangiferin may be responsible for increasing the lipase inhibition effect when considering the results of Zhang *et al*. (2011) which determined that mangiferin have strong inhibitory activity against lipase.

It is clear from Figure 4.9A that the ARC189 crude extract presented the lowest inhibitory activity relative to the ARC189 related fractions as well as to ARC188 crude extract and related fractions with an IC_{50} of 730 µg/ml. The ARC189 IdH (Figure 4.9B) showed moderate inhibition activity against the porcine pancreatic lipase, which may be due to the fact that a relatively high concentration of the benzophenone, IDG, is present in this fraction (Table 4.1). Of the three enriched fractions from ARC189, the ARC189 Benz fraction showed the lowest inhibitory activity (IC_{50} = 692 µg/ml) against porcine pancreatic lipase compared to the ARC189 IdH (IC_{50} = 489 µg/ml) and the ARC189 Xanth (IC_{50} = 335 µg/ml) fractions as shown in Table 4.2.

When the lipase inhibition results of the ARC188 and ARC189 crude extracts and fractions are compared to that of orlistat (positive control with IC_{50} = 50 µM or 25µg/ml), it indicates that the honeybush crude extracts and fractions have a much lower inhibitory effect on lipase. This much milder inhibition effect by honeybush extracts, when compared to orlistat, may be well suited to the use of a gastro-retentive drug delivery system in patients as it may cause less side-effects while the delivery system will provide a prolonged period of mild inhibitory activity.

Table 4.2: IC_{50} values (µg/ml) and CI95% of porcine pancreatic lipase inhibitory activity for honeybush crude extracts and fractions (n = 3)

IC_{50} (µg/ml)						
ARC 188	**ARC 188 Benz**	**ARC 188 Xanth**	**ARC 189**	**ARC 189 Benz**	**ARC 189 IdH**	**ARC 189 Xanth**
198	386	271	730	692	489	335
95% CI ranges (µg/ml)						
ARC 188	**ARC 188 Benz**	**ARC 188 Xanth**	**ARC 189**	**ARC 189 Benz**	**ARC 189 IdH**	**ARC 189 Xanth**
171-230	359-416	256-286	689-775	637-752	449-532	309-363

*IC_{50} = concentration where 50% inhibition occurs, 95%CI = 95% confidence interval

From Table 4.2, it is clear that ARC189 Benz had the widest confidence interval range, suggesting higher variability in the enzyme inhibition results obtained for this fraction.

4.3.2 α-Glucosidase inhibition

The α-glucosidase inhibitory effects of ARC188 honeybush crude extract, ARC188 Benz rich fraction and ARC188 Xanth rich fraction are depicted in Figure 4.10.

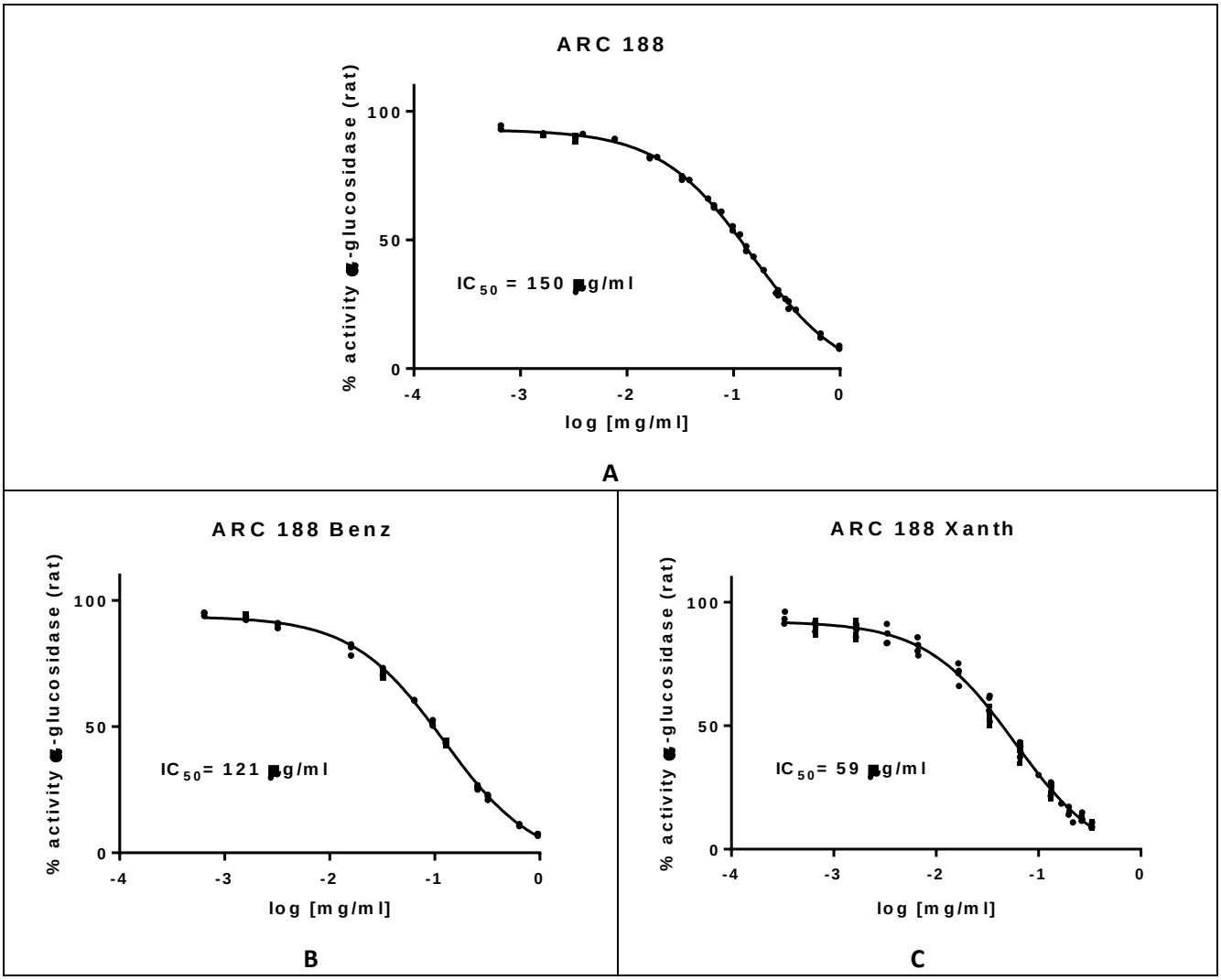

Figure 4.10: Semi-logarithmic plot of the percentage α-glucosidase inhibitory activity as a function of concentration for A) ARC188 crude extract, B) ARC188 Benz rich fraction and C) ARC188 Xanth rich fraction (n = 3)

From Figure 4.10 it is clear that the ARC188 Xanth rich fraction (IC_{50} = 59 µg/ml) exhibited a better α-glucosidase inhibitory activity than the ARC188 Benz rich fraction (IC_{50} = 121 µg/ml) as well as the ARC 188 honeybush crude extract (IC_{50} = 150 µg/ml). This indicates that xanthone molecules such as mangiferin and isomangiferin have a higher α-glucosidase enzyme inhibition effect than benzophenone molecules such as I3G in the honeybush extracts. This is in accordance with the findings of Feng *et al*. (2011), whom suggested that mangiferin is a strong α-glucosidase inhibitor.

The enzyme inhibitory activity of ARC189 honeybush crude extract, ARC189 IdH, ARC189 Benz and ARC189 Xanth fractions against α-glucosidase are shown in Figure 4.11. Similar

to the findings with the ARC188 extract and fractions (Figure 4.10), the ARC189 Xanth rich fraction exhibited the highest α-glucosidase inhibitory activity. This may be explained by a higher concentration of xanthones (i.e. mangiferin and isomangiferin) in the ARC189 Xanth rich fraction than in the ARC189 honeybush crude extract as shown in Table 4.1. The same trend of superior enzyme inhibition effect is therefore observed for the ARC189 Xanth rich fraction and the ARC188 Xanth rich fraction when compared to the crude extracts.

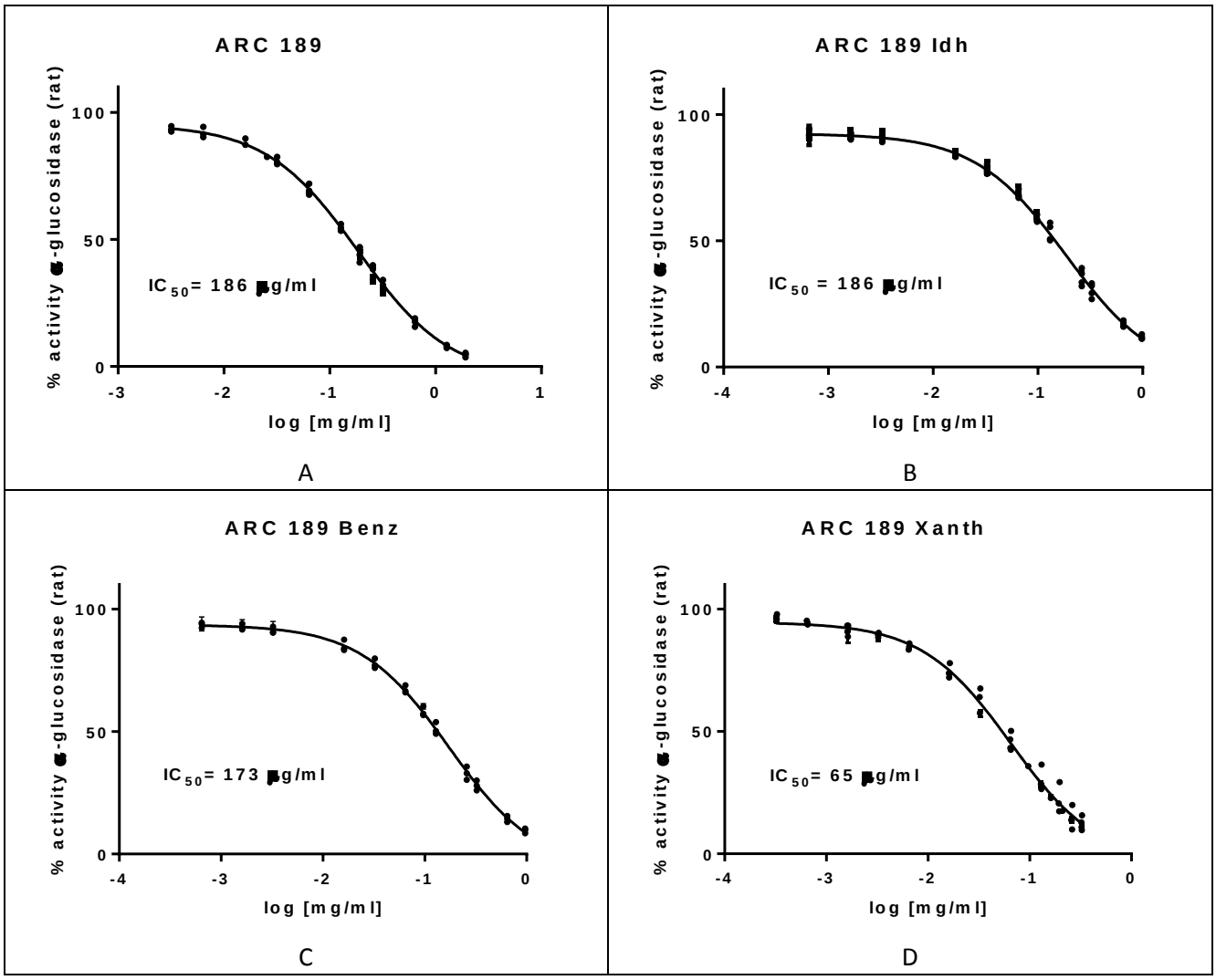

Figure 4.11: Semi-logarithmic plot of the percentage of α-glucosidase inhibitory activity of A) ARC189 crude extract, B) ARC189 IdH rich fraction, C) ARC189 Benz rich fraction and D) ARC189 Xanth rich fraction (n = 3)

When comparing the results to acarbose (positive control with IC_{50} = 65 µM or 0.64561 µg/ml) all the ARC 188 and ARC 189 crude extracts and fractions showed lower enzyme inhibitory effects than acarbose, but when considering acarbose side-effects it may be beneficial for patients to use a milder enzyme inhibitor with less side-effects.

From Table 4.3, it is clear that ARC189 Benz has the widest confidence interval range suggesting larger variation between the replicates, whereas ARC188 Benz and ARC188 Xanth has the narrowest confidence interval.

Table 4.3: IC_{50} values (µg/ml) and CI95% of α-glucosidase inhibitory activity for different honeybush crude extracts and fractions (n = 3)

IC_{50} (µg/ml)						
ARC188	**ARC188 Benz**	**ARC188 Xanth**	**ARC189**	**ARC189 Benz**	**ARC189 IdH**	**ARC189 Xanth**
150	121	59	186	173	186	65
95%CI ranges (µg/ml)						
ARC188	**ARC188 Benz**	**ARC188 Xanth**	**ARC189**	**ARC189 Benz**	**ARC189 IdH**	**ARC189 Xanth**
144-156	116-126	54-64	180-192	163-183	176-198	59-71

*IC_{50} = concentration where 50% inhibition occurs, 95%CI = confidence interval

4.3.3 Conclusion

The variations in terms of enzyme inhibition obtained for the two honeybush crude extracts and fractions may be explained by the difference in their phytochemical composition. Overall, the ARC188 crude extract has shown to be more effective in terms of lipase inhibition activity. Furthermore, ARC188 crude extract was more effective in terms of α-glucosidase inhibition than the ARC189 crude extract. The xanthone rich fractions have shown the highest *in vitro* inhibition of α-glucosidase. Based on this result, the decision was made to incorporate the ARC188 crude extract into a gastro-retentive dosage form as it had the highest lipase inhibitory activity while also showing considerable inhibitory activity against α-glucosidase.

4.4 *IN VITRO* BI-DIRECTIONAL TRANSPORT STUDIES

Aqueous solubility and membrane permeability are the most important parameters that will determine the bioavailability of a compound and therefore the Biopharmaceutics Classification System has been based on these two parameters (Amidon *et al*., 1995; Dahan *et al*., 2009). Furthermore, in order to permeate biological membranes, compounds need to possess certain critical physio-chemical properties. Criteria for physio-chemical properties that will provide acceptable membrane permeability (i.e. passive diffusion) were established by Lipinski and co-workers (i.e. the rule of five). For the rule of five, the following limits have been set for four physico-chemical properties of compounds in order to display acceptable membrane permeation: molecular weight (MW < 500 g/mol), hydrogen bond acceptors (HBA < 10), hydrogen bond donors (HBD < 5) and LogP (< 5). Recently, limits for other physico-chemical

properties have been added to the rule of five, namely the number of rotatable bonds (RB < 10) and polar surface area (PSA < 140 $Å^2$) (Clark and Pickett, 2000; Lipinski *et al*., 2001; Veber *et al*., 2002; Bergström *et al*., 2014).

The values of selected physico-chemical properties for three of the marker molecules present in honeybush extract are shown in Table 4.4. The data in this table will be used in the discussions of the results obtained from the *in vitro* transport studies.

Table 4.4: Physico-chemical properties for some of the marker molecules in honeybush extract

	MW (g/mol)	**HBA**	**HBD**	**ClogP**	**RB**	**PSA ($Å^2$)**
I3G	408	10	8	1.915	12	188.4
Mangiferin	422	11	8	0.582	10	197.4
Isomangiferin	422	11	8	0.223	10	197.4

4.4.1 *In vitro* transport of marker molecules from honeybush crude extracts (ARC188 and ARC189)

Da Silva *et al*. (2015) mentioned that a TEER value of more than 30 $Ω/cm^2$ can be seen as acceptable for intact excised intestinal tissue. The TEER values at the beginning and end of the transport study (Annexure C) indicated values above 30 $Ω/cm^2$ and a relatively low decrease in TEER was observed over the entire period of the transport study. The application of the test solution could have contributed to the decrease in TEER values over the transport study, because the excised tissue need to adjust to the test solution.

The percentage transport of the marker molecules in the apical (AP) to basolateral (BL) direction obtained after application of the ARC188 crude extract plotted as a function of time, is shown in Figure 4.12. From this figure, it is evident that relatively low percentage transport occurred for all four marker molecules and that a lag phase was present over the first 20 min. The relatively low transport of the four marker molecules across the intestinal tissue in the AP-BL direction may be due to their physico-chemical properties (Table 4.4, especially as indicated by high HBD and PSA). The relatively low permeability also indicate that the

phytochemicals will probably stay longer in the lumen of the gastrointestinal tract, which may be beneficial to the patient as this is the site of enzyme inhibition.

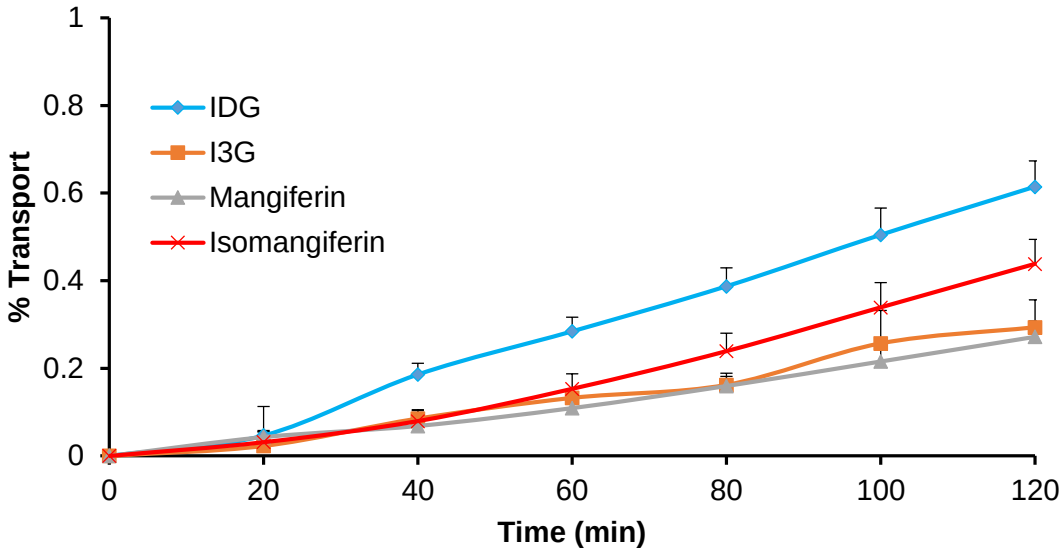

Figure 4.12: Percentage transport of marker molecules from the ARC188 honeybush crude extract in the apical to basolateral (AP-BL) direction plotted as a function of time (n = 3) (The error bars represent SD)

The percentage transport of the marker molecules in the basolateral (BL) to apical (AP) direction after application of the ARC188 crude extract as a function of time, is shown in Figure 4.13.

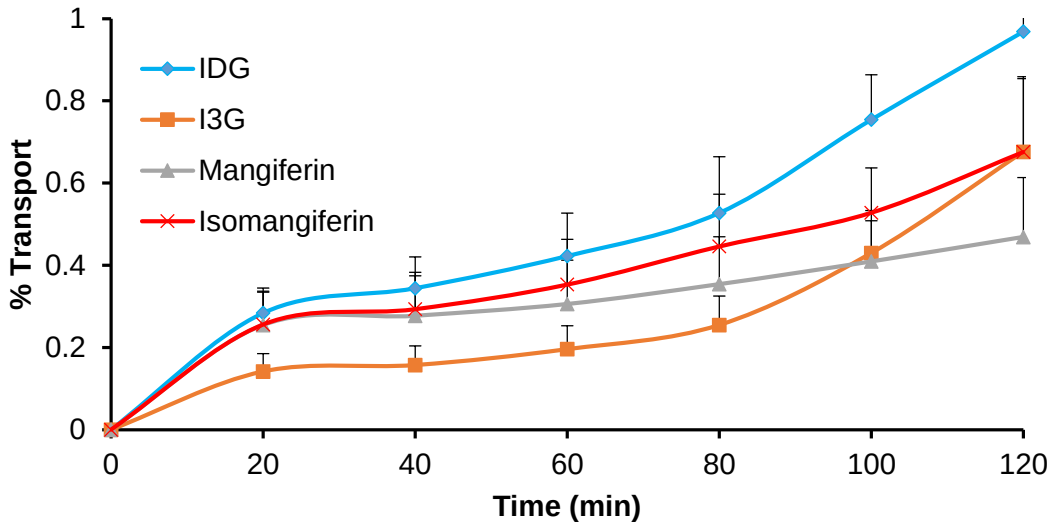

Figure 4.13: Percentage transport of marker molecules from the ARC188 honeybush crude extract in the basolateral to apical (BL-AP) direction plotted as a function of time (n = 3) (The error bars represent SD)

The apparent permeability coefficient (P_{app}) values as well as efflux ratio (ER) values of the marker molecules from ARC188 honeybush crude extract are shown in Figure 4.14. When looking at Figures 4.13 and 4.14, it is evident that the marker molecules were transported to a higher extent in the BL-AP direction than in the AP-BL direction. The reason for this higher transport in the BL-AP direction may be explained by active efflux transport. It has been previously shown that many phytochemicals present in plants are capable to modulate P-gp expression and that mangiferin (a xanthone) inhibits P-gp via mRNA expression and in this study the results confirmed it is also a substrate for P-gp due to the efflux ratio being higher than unity (ER > 1) (Chieli *et al*., 2010).

Seelig (1998) noticed for a compound to be a suitable substrate for P-gp, certain recognition elements need to be considered such as the electron donor groups (> 2 electron donor groups) and fixed spatial separation of the compounds. In Table 4.4 the three marker molecules with their number of donor and acceptor groups are indicated. It is clear that all three marker molecules contain more than two donor groups (HBD > 5).

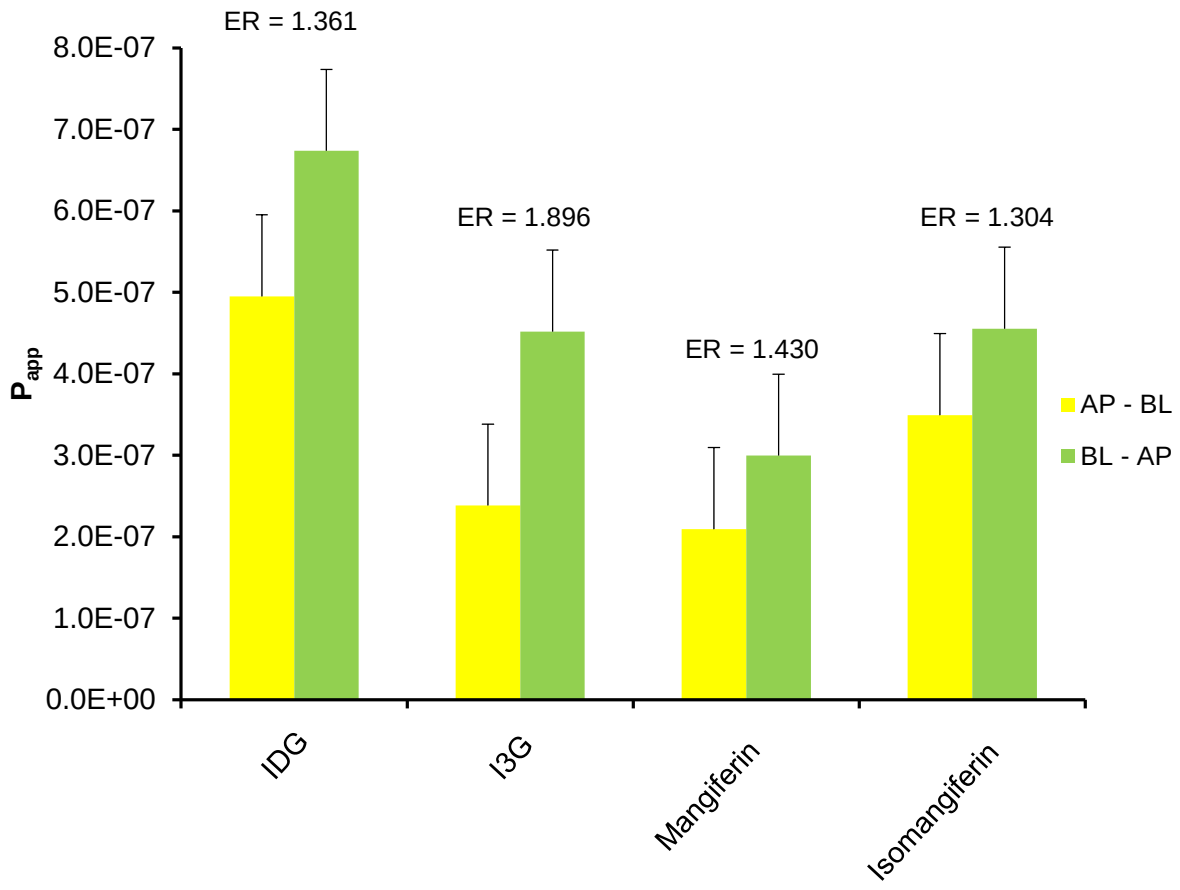

Figure 4.14: Apparent permeability coefficient (P_{app}) values for the bi-directional transport of marker molecules from the crude extract ARC188 with efflux ratio (ER) values indicated above the bar graphs (n=3) (SD represented by error bars)

The percentage transport of the marker molecules in the apical (AP) to basolateral (BL) direction after application of the ARC189 crude extract as a function of time, is shown in Figure 4.15, while the percentage transport in the basolateral (BL) to apical (AP) direction is shown in Figure 4.16.

The AP-BL transport of the isomangiferin marker molecules was notably lower after application of ARC189 crude extract (Figures 4.15 and 4.17) when compared to that of ARC188 crude extract (Figure 4.14), which can be explained by the concentration differences of these phytoconstituents in these crude extracts. Isomangiferin are present in much higher concentrations in ARC188 crude extract than in ARC189 crude extract (refer to Table 4.1).

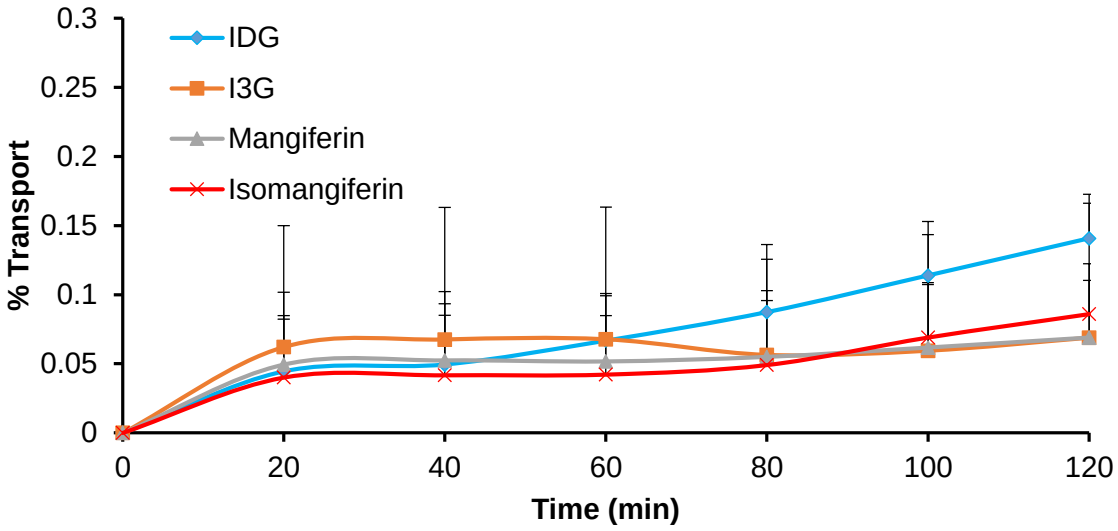

Figure 4.15: Percentage transport of marker molecules from the ARC189 honeybush crude extract in the AP-BL direction plotted as a function of time (n = 3) (The error bars represent SD)

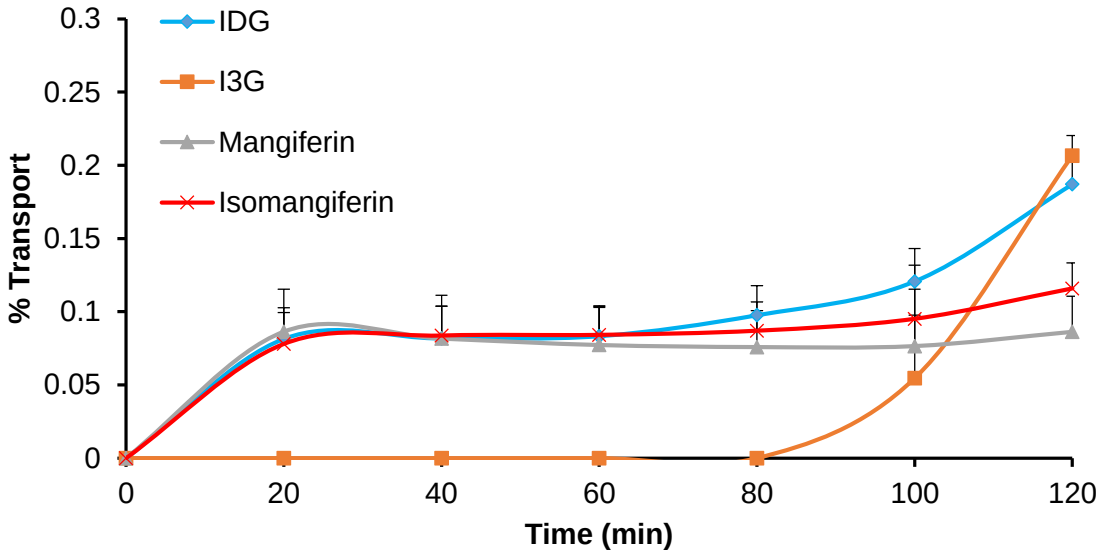

Figure 4.16: Percentage transport of marker molecules from the ARC189 honeybush crude extract in the BL-AP direction plotted as a function of time (n = 3) (The error bars represent SD)

In Figure 4.16 it is noted that the transport of I3G in the BL-AP direction only occurred after 80 when applied as ARC189 crude extract, which was not observed in the AP-BL direction or for ARC188. This may also be the reason for the low ER value shown in Figure 4.17.

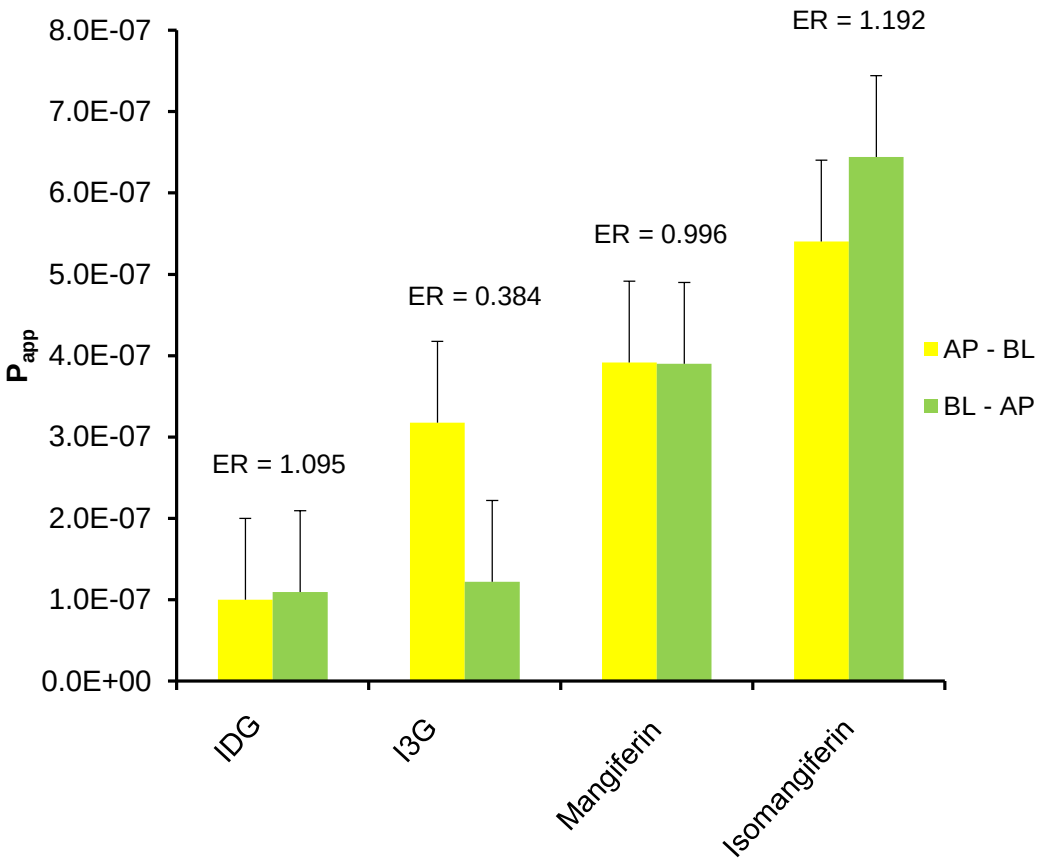

Figure 4.17: Apparent permeability coefficient (P_{app}) values for the bi-directional transport of marker molecules from the crude extract ARC189 with efflux ratio (ER) values indicated above the bar graphs (n=3) (SD represented by error bars)

4.4.2 *In vitro* transport of marker molecules from fractions (ARC189 IdH and ARC189 Xanth)

The transport of the ARC189 IdH fraction was used as representative of the benzophenone rich fractions.

In Figure 4.18, a lag phase (40 min) for IDG transport in the AP-BL direction was noted. According to Atlabachew *et al*. (2016), susceptibility to efflux and/or slow diffusion through the mucous layer of excised tissue may be factors that cause a lag phase in transport. In Figure 4.18, it is also clear that a higher percentage transport occurred in the BL-AP direction probably due to efflux of the marker molecule. In Figure 4.19, the ER value is shown, which is > 1 (ER = 1.512) confirming efflux did occur.

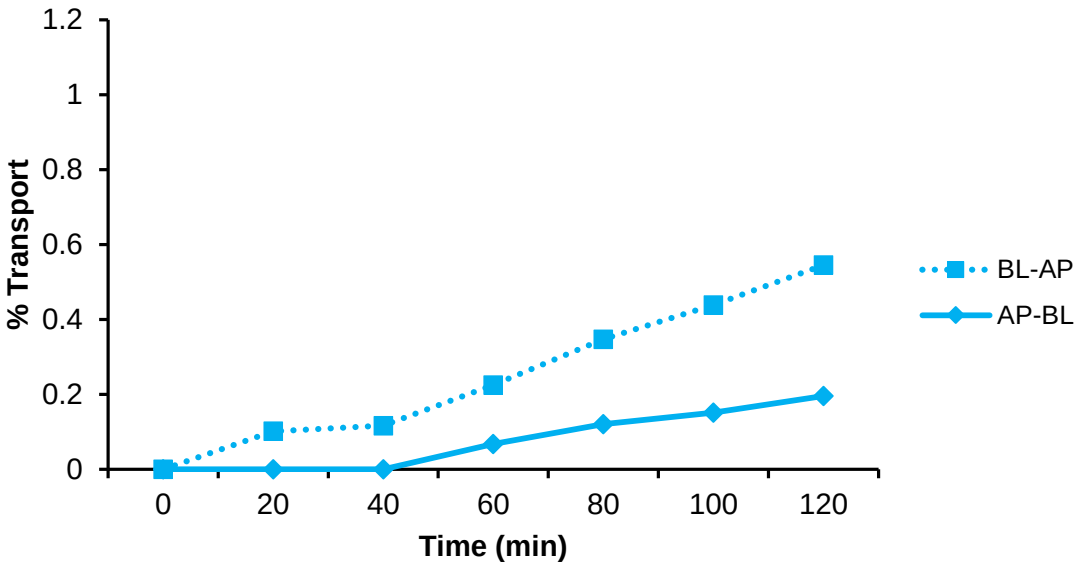

Figure 4.18: Percentage transport of a marker molecule (IDG) from ARC189 IdH rich fraction in the AP-BL and BL-AP directions plotted as a function of time (n = 3) (The error bars represent SD)

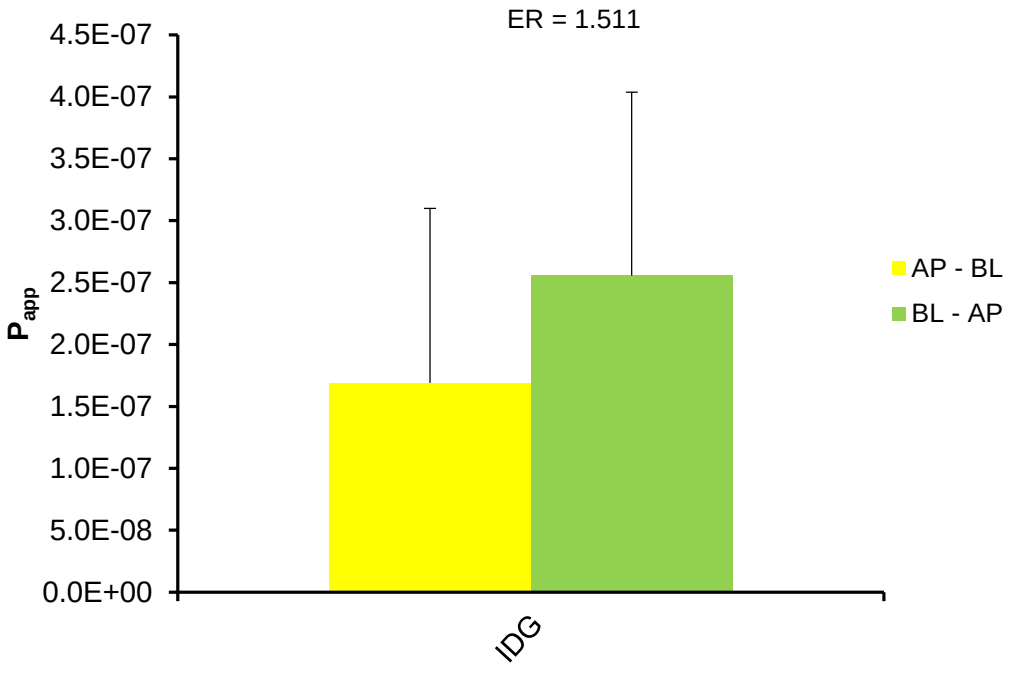

Figure 4.19: Apparent permeability coefficient (P_{app}) values for the bi-directional transport of marker molecule (IDG) from the ARC189 IdH rich fraction with efflux ratio (ER) values indicated above the bar graphs (n=3) (SD represented by error bars)

The transport of the marker molecules present in ARC188 Xanth fraction (i.e. mangiferin and isomangiferin) are shown in Figures 4.20 for AP-BL direction and in Figure 4.21 for the BL-AP direction. A relatively low transport is visible for these marker molecules, which may be explained by their physico-chemical properties (both the marker molecules have HBA >10; HBD > 5; RB > 10 and PSA > 140). The slightly higher transport of mangiferin compared to that of isomangiferin can possibly be explained by the concentration differences (Table 4.1). Previous studies done by Chieli *et al*. (2009) on HK-2 cells and Louisa *et al*. (2014) on Doxorubicin-treated MCF-7 cells have shown that mangiferin inhibited P-gp activity. The results from the current transport study illustrated that both mangiferin and isomangiferin are substrates for P-gp due to the ER value considerably higher than unity (i.e. ER of isomangiferin = 1.739 and ER of mangiferin 1.659) when looking at Figure 4.22.

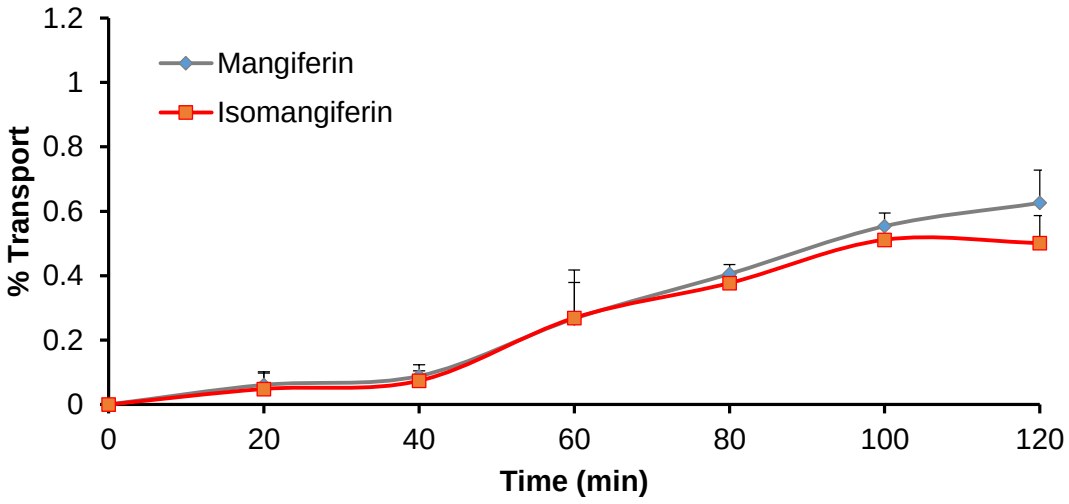

Figure 4.20: Percentage transport of marker molecules from the ARC188 Xanth rich fraction in the AP-BL direction plotted as a function of time (n = 3) (The error bars represent SD)

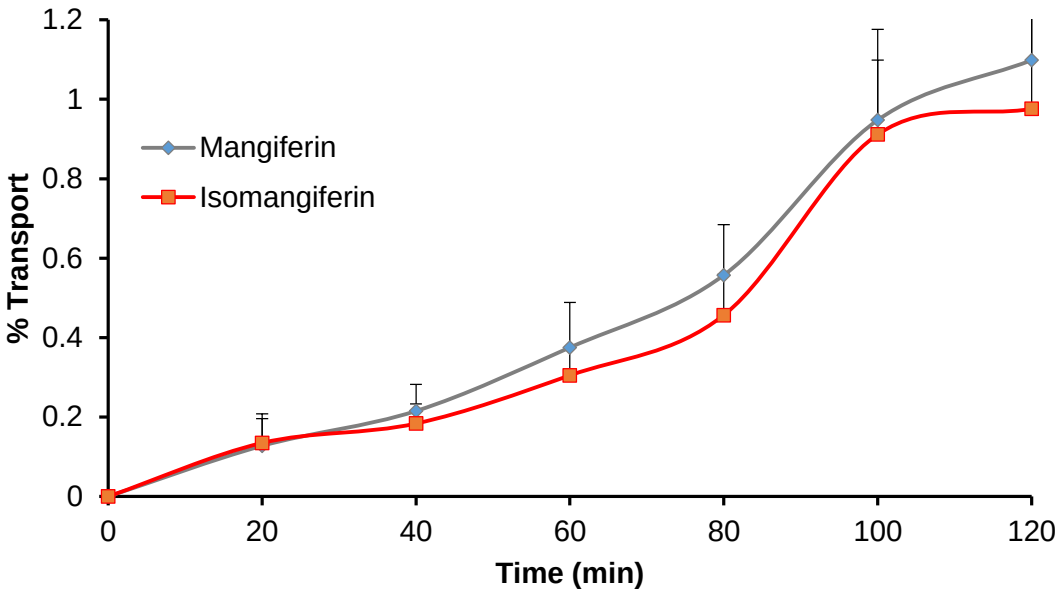

Figure 4.21: Percentage transport of marker molecules from ARC188 Xanth rich fraction in the BL-AP direction plotted as a function of time (n = 3) (The error bars represent SD)

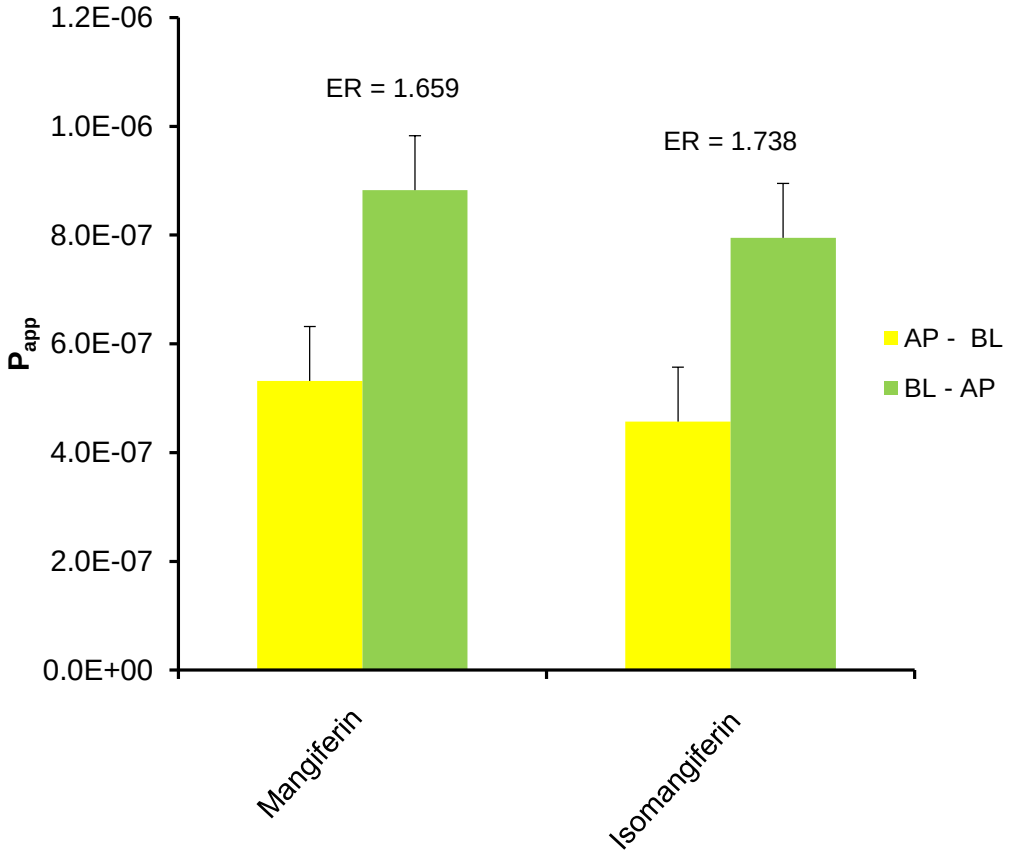

Figure 4.22: Apparent permeability coefficient (P_{app}) values for the bi-directional transport of marker molecules from the ARC188 Xanth fraction with efflux ratio (ER) values indicated above the bar graphs (n=3) (SD represented by error bars)

When comparing the transport results of the xanthone marker molecules from ARC189 Xanth rich fraction, the same trend was followed as observed for ARC188 Xanth fraction. From Figure 4.25, it is clear that both marker molecules presents with ER values > 1, which confirmed that these marker molecules are susceptible to P-gp related efflux. Mangiferin has an ER of 1.252 and isomangiferin has an ER of 1.214 both very close to each other, which may be due to their similar structures.

Although it is noted that mangiferin may present as a better P-gp substrate it is transported in a lower extend in comparison with isomangiferin when looking at Figure 4.23 and 4.24.

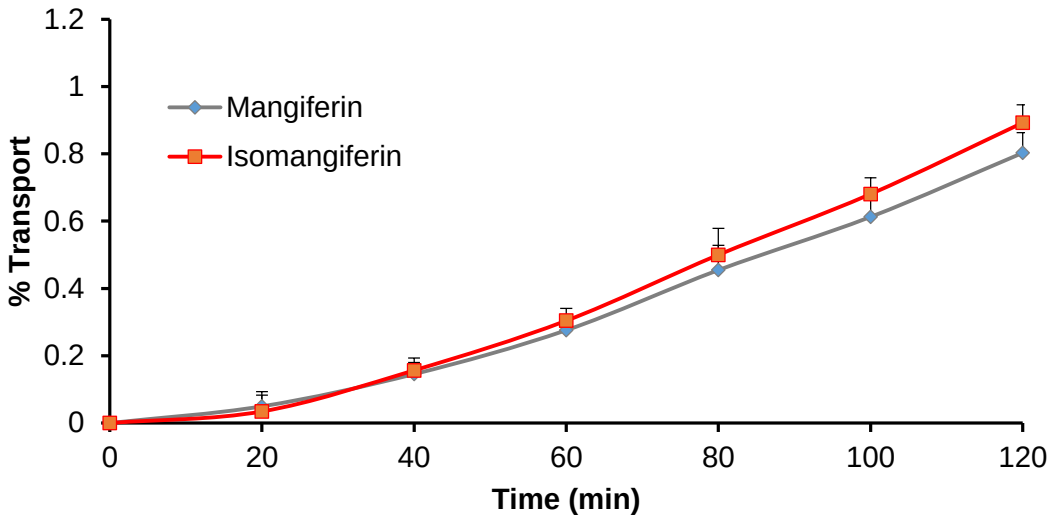

Figure 4.23: Percentage transport of marker molecules from ARC189 Xanth rich fraction in the AP-BL direction plotted as a function of time (n = 3) (The error bars represent SD)

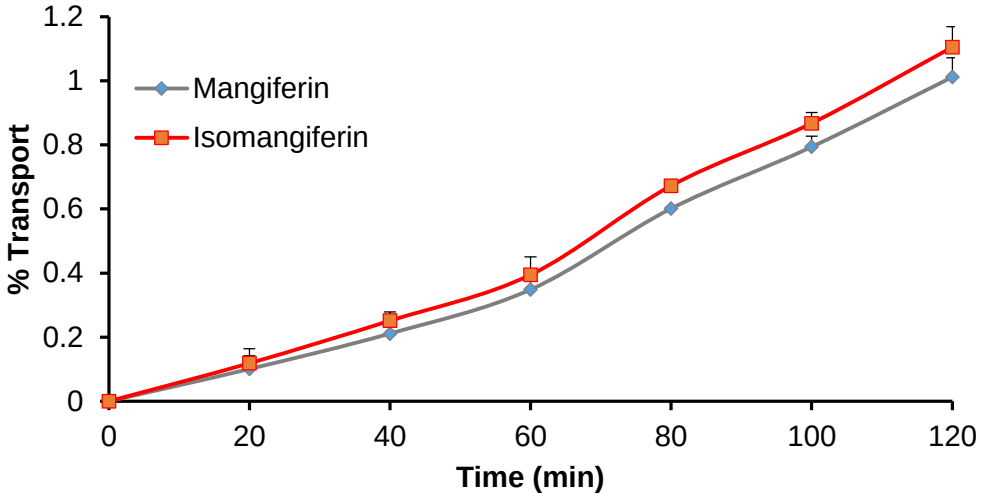

Figure 4.24: Percentage transport of marker molecules from ARC189 Xanth rich fraction in the BL-AP direction plotted as a function of time (n = 3) (The error bars represent SD)

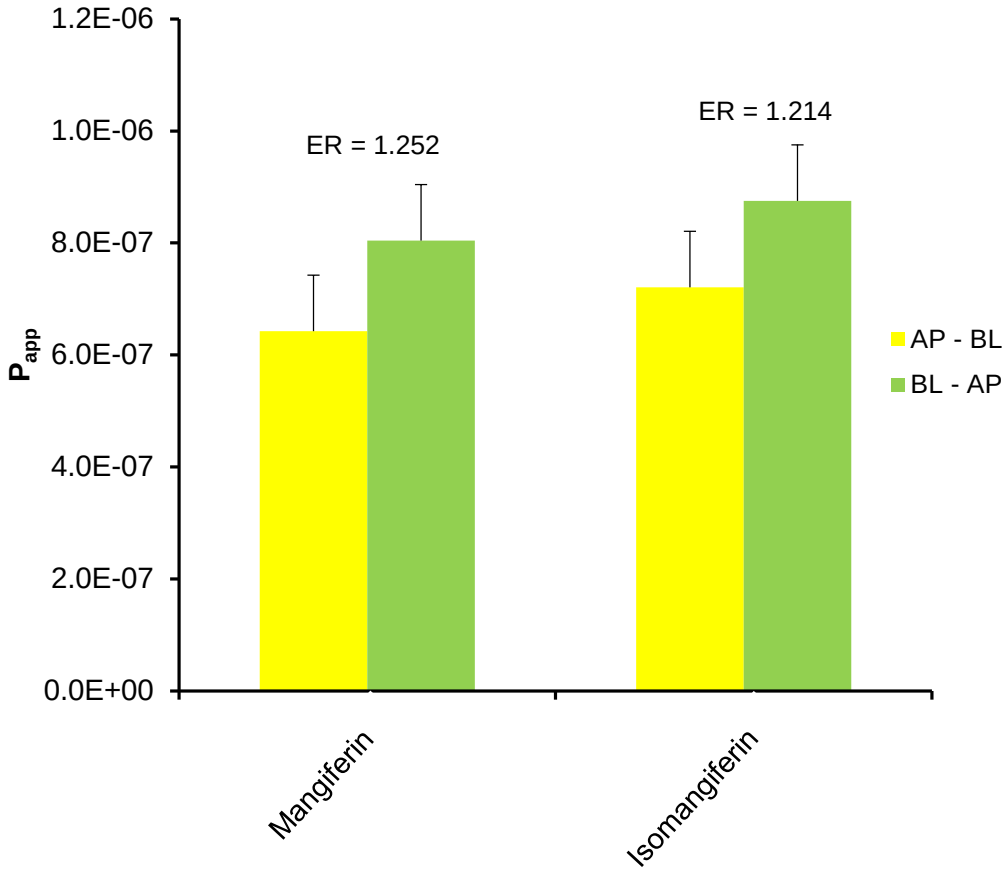

Figure 4.25: Apparent permeability coefficient (P_{app}) values for the bi-directional transport of marker molecules from the ARC189 Xanth rich fraction with efflux ratio (ER) values indicated above the bar graphs (n=3) (SD represented by error bars)

4.4.3 Conclusion

From the results it is clear that for all the crude and enriched fractions, relatively low permeability results was observed for marker molecules across the excised tissue of the pig. The fact that most of the fractions showed susceptibility towards P-gp efflux may be the reason for the variations observed in transport of the marker molecules between the crude and enriched fractions, but matrix effects, due to other compounds in the extracts, may also play a role. Due to the fact that the target for “diabesity” is in the gastrointestinal lumen, where targeted enzymes are located, efflux of the marker molecules contributes to the active molecules being transported back into the lumen and will help to keep the active compounds in the region where enzyme inhibition can occur. The ARC188 crude extract showed more favourable potential to be utilized in the gastro-retentive dosage form due to the higher efflux ratios and relatively low permeability of the compounds from the ARC188 crude extract in comparison with the ARC189 crude extract.

4.5 GASTRO-RETENTIVE DRUG DELIVERY SYSTEM CHARACTERISATION

Figure 4.26 illustrates various approaches that can be implemented to develop a gastro-retentive drug delivery system to ensure the release of the drug can be regulated. In the current study, a non-effervescent gastro-retentive floating dosage form has been developed containing the ARC188 crude extract of honeybush incorporated into the dosage form (Kankal *et al*., 2013).

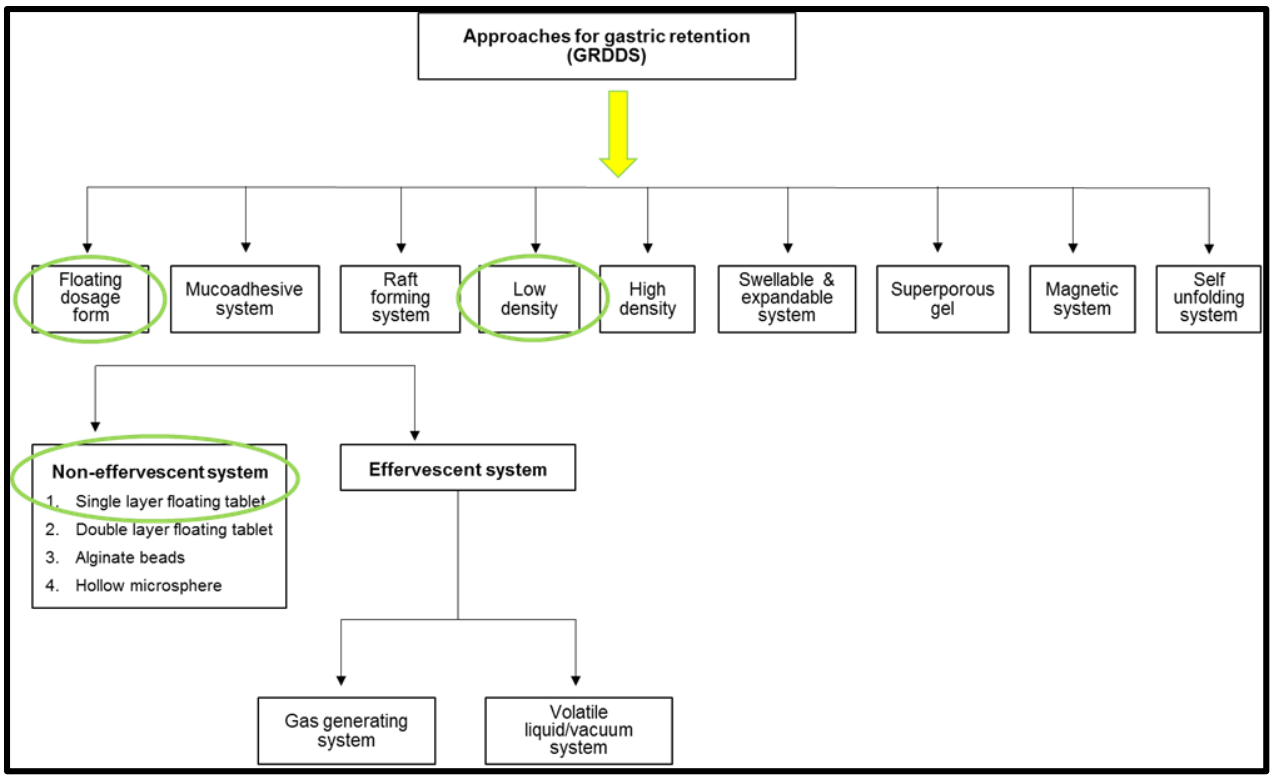

Figure 4.26: Types of gastro-retentive drug delivery systems (GRDDS) to ensure gastric-retention (adapted from Kankal *et al*., 2013)

4.5.1 Flow properties of spherical bead formulations

Torrado and Augsburger (2008) mentioned that electrostatic charges from the surfaces of beads can affect the flow properties negatively. The size difference between excipient components and can also have an effect on the flow properties and that spherical particles can separate more easily from each other than non-spherical particles. The flow properties of uncoated beads prepared in this study were evaluated by means of angle of repose and flow rate parameters. The British Pharmacopoeia (2016) has an universal accepted flowability scale to determine the perfect flow properties by utilizing the angle of repose as shown in Table 4.5.

Table 4.5: Illustrative flowability scale (British Pharmacopeia, 2016)

Flowability characteristics	Angle of repose (°)
Excellent	25-30
Good	31-35
Fair	36-40
Passable	41-45
Poor	46-55
Very poor	56-65
Extremely poor	> 66

The flow properties in terms of angle of repose and flow rate of the two polymer bead formulations are depicted in Table 4.6. According to the results obtained from a study conducted by Singh *et al*. (2010), polypropylene foam powder exhibited excellent flow properties, whereas Kojima and Elliott (2013) showed that polystyrene divinylbenzene polymer resulted in lower flowability due to its high cohesive properties.

For both the polypropylene (PP) and polystyrene divinylbenzene copolymer (PDC) bead formulations, acceptable flow properties were obtained. The results are expressed in terms of the angle of repose (~37° for PP and ~38° for PDC), which adhere to the British Pharmacopoeia (2016) criteria for fair flow (between 36-40°). This may be due to the fact that some beads are more spherical in shape than others. This may indicate that the beads need to be spheronized for a longer time period, so that all the beads possess a more uniform shape to be able to flow better, because according to Torrado and Augsburger (2008) beads possess acceptable flow characteristics due to their round shape and relatively large size. Both PP and PDC beads showed similar flow properties in terms of angle of repose and flow rate.

Table 4.6: Flow properties of the bead formulations

	Polypropylene (PP)	**Polystyrene divinylbenzene copolymer (PDC)**
Angle of repose (°)	36.905 ± 1.241	38.164 ± 1.582
Flow rate ($g.s^{-1}$)	18.183	18.186

4.5.2 Buoyancy of multiple unit pellet systems (MUPS)

To ensure acceptable buoyancy properties were obtained in the MUPS, two different low density polymers were incorporated into the MUPS dosage forms as described in section 3.7.2. The buoyancy was evaluated to establish which polymer formulation was the most suitable to reach floatation for the longest period of time. Streubel *et al*. (2002) establish that the PP foam powder utilized in their gastro-retentive bead formulation was very porous which contributed to the floatability of the beads and more than 80% of the beads continued to float for up to 8 h. The air which was entrapped within the pore structure of the beads was released at a slow rate, which caused the floating time to last for a longer period. The floating matrix tablets formulated by Streubel *et al*. (2003), which also contained PP foam powder, presented with the same results. The tablets also appeared to float at immediate contact with the dissolution medium and demonstrated a floating time for up to 8 h. They also formulated tablets containing both PP foam powder and hydroxypropyl methylcellulose (HPMC), which did not float immediately upon contact with dissolution medium. These tablets presented with lag times between 9 and 33 min and when they replaced 8% of the HPMC in the formulation with PP foam powder, the tablets lag time decreased to approximately 2 min. Another experiment utilizing PP foam powder was done by Treesinchai *et al*. (2016) who formulated a sustained release tablet. The results demonstrated that the tablet containing PP foam powder floated instantaneously not showing any lag time when it came in contact with the dissolution medium. So they concluded that when a dosage form contains more than 10% w/w of a low density polymer (e.g. PP foam powder), it will float upon contact with a dissolution medium.

Raval *et al*. (2009) investigated the impact of the utilization of PDC, which is known as a low density polymer with excellent porosity, to contribute to a better floating behaviour in the formulation. They established that this polymer doesn't have favourable buoyancy behaviour when the formulation consisted of a 50% w/w PDC polymer, which resulted in a submerged position at the bottom of the container. Trivedi *et al.* (2011) also conducted a study on PDC polymer and found that a 17% w/w concentration was sufficient to achieve a floating behaviour, whereas tablets containing less than 12% w/w did not float at all.

The results obtained from the buoyancy test (Figure 4.27) showed that when both the MUPS tablets came into contact with the 0.1 N HCl dissolution medium, the formulation containing the PP polymer floated for a period of 24 h, which corresponds with previous results (Streubel *et al*. 2002, Streubel *et al*. 2003 and Treesinchai *et al*. (2016). On the other hand, the formulation containing PDC polymer submerged to the bottom of the flask directly upon contact with the dissolution medium. The PDC MUPS tablet contained 50% w/w polymer and the results are similar to the findings of Raval *et al*. (2009).

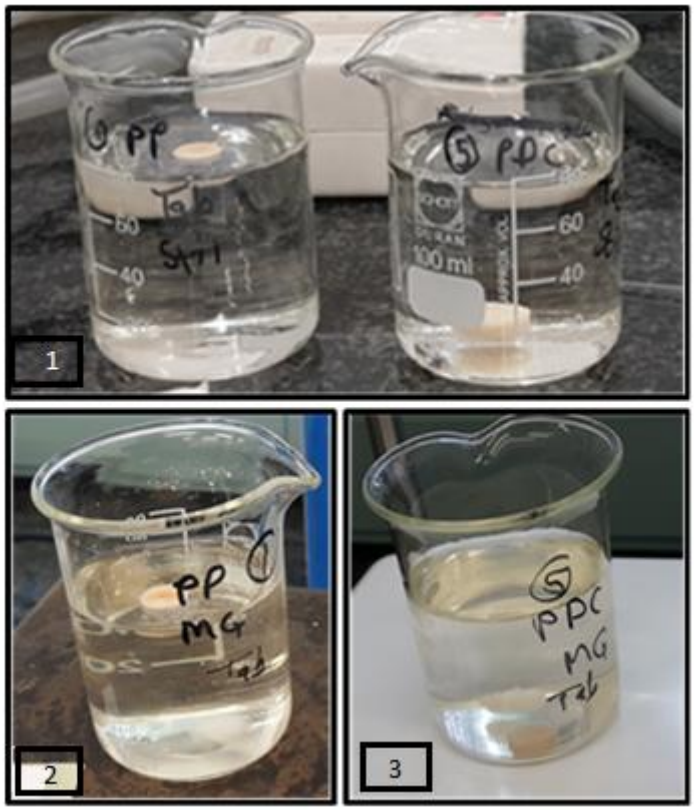

Figure 4.27: MUPS tablet floating properties (1) stationary MUPS tablet containing PP (left side) and PDC (right side) (2) MUPS tablet containing PP on magnetic stirrer and (3) MUPS tablet containing PDC on magnetic stirrer all taken after 24 hours

Thus, the buoyancy results provided evidence that the MUPS tablet containing the PP polymer is capable of floating, while the MUPS containing PDC polymer is not capable of floating.

4.5.2.1 Disintegration and friability

Disintegration properties of dosage forms are mainly examined to determine that the solid dosage forms breaks up into small pieces to ensure that the correct amount of drug is released within a specific time frame. Friability helps to determine the mechanical strength of a solid dosage form to establish whether a dosage form will be viable for formulation purposes (Moreton, 2008).

No disintegrants were added to the formulation of this study, but various tablet components can contribute to disintegration and the effect of the compaction pressure can also influence the disintegration ability of a dosage form (Heng and Liew, 2008).

The MUPS tablet containing PP disintegrated faster (lower disintegration time of 3.30 min) than the MUPS tablet containing PDC (6.23 min). This may be due to the fact that the PP

may be slightly less hydrophobic than PDC and because the PDC has stronger van der Waals interparticulate forces than the PP. According to Kojima and Elliott (2013), PDC contains more cohesive properties and thereby producing a tighter structure in the tablet which leads to a longer time to disintegrate.

Both the MUPS formulations adhere to the British Pharmacopeia (2016) criteria for friability where the mass loss is below 1%. The MUPS tablet containing PP exhibited an average friability value of 0.532% and the MUPS tablet containing PDC had an average friability value of 0.262%.

Table 4.7: Disintegration and friability of the two MUPS tablets

	Polypropylene (PP)	**Polystyrene divinylbenzene copolymer (PDC)**
Disintegration (min)	3.300	6.230
Friability (%)	0.532	0.262

4.5.2.2 Hardness, thickness, diameter and mass variation

It can be seen in Table 4.8 that the MUPS tablet containing PP has a relatively low hardness value (22.70 N ± 2.11) compared to that of the MUPS tablet containing PDC (30.30 N ± 6.96). A conventional immediate release tablet hardness should be in the region of ± 90 N. However, both the PP and PDC containing MUPS tablets are gastro-retentive systems made of low density polymers to which camphor was added and sublimated to create pores inside the MUPS tablet to achieve a more floatable system. These pores contributed to decrease the hardness as Bashaiwoldua *et al*. (2011) explained that larger pore sizes in tablets may affect the tensile strength.

The normal range for uncoated tablets with an average mass of more than 250 mg, the mass variation should not be more than 5% according to the British Pharmacopoeia (2016). As seen in Table 4.8, the average tablet mass is 374 mg for PP and 380 mg for PDC MUPS and both deviate more than 5% which can be due to the beads incorporated into the MUPS and because the dosage form are not formed of powder excipients compressed into a tablet, but beads compressed into a tablet.

Table 4.8: Physical test results for the MUPS tablets containing polypropylene and polystyrene divinylbenzene copolymer

	Polypropylene (PP)	Polystyrene divinylbenzene copolymer (PDC)
Average tablet mass (mg)*	374.000 ± 9.661	380.000 ± 10.541
Hardness (Newton (N))*	22.700 ± 2.111	30.300 ± 6.961
Thickness (mm)*	5.798 ± 0.072	5.121 ± 0.289
Diameter (mm)*	10.117 ± 0.033	10.139 ± 0.075

*n = 10

4.5.2.3 Assay for drug content evaluation

An assay is an analytical way to keep record and to ensure if the correct amount of active ingredient is incorporated within a specific dosage form. The MUPS tablets were formulated to contain 4.75 mg active ingredient (ARC188 crude extract) per PP tablet and 4.79 mg (ARC188 crude extract) per PDC tablet. The quantities of each marker molecule that were found to be present in one MUPS tablet (PP and PDC, respectively) by means of the assay that was performed, are outlined in Table 4.9.

Table 4.9: Honeybush extract marker molecule content (µg) of MUPS tablets (polypropylene and polystyrene divinylbenzene, respectively as low density polymer) (n = 3)

	µg per Tablet	
	Polypropylene (PP)	**Polystyrene divinylbenzene copolymer (PDC)**
IDG	78.300	80.000
I3G	66.900	86.100
Mangiferin	113.500	50.700
Isomangiferin	36.900	21.300

4.6 DISSOLUTION

For modified release dosage forms, the first dissolution sample taken is used to ensure that no dose dumping occurred and the last dissolution sample is used to determine whether complete release of the drug took place. By taking the sampling method and the replacement

of dissolution medium into account, the concentration of the samples selected for the dissolution study can then be converted to the drug amount released after a certain time period. The time points at which the sample was taken in between the first and the last sample indicate whether sustained release of the drug occurred (Long and Chen, 2009).

The dissolution results of the two MUPS formulation were processed in terms of the mean dissolution time (MDT) (Ritger and Peppas, 1987) and fit factors (f_1 = dissimilarity factor and f_2 = similarity factor) (Moore and Flanner, 1996), which were utilized to compare the dissolution profiles of different formulations.

The dissolution profiles of each honeybush extract marker molecules from the MUPS tablets containing PP and PDC polymers, respectively, are shown in Figures 4.28 and 4.29.

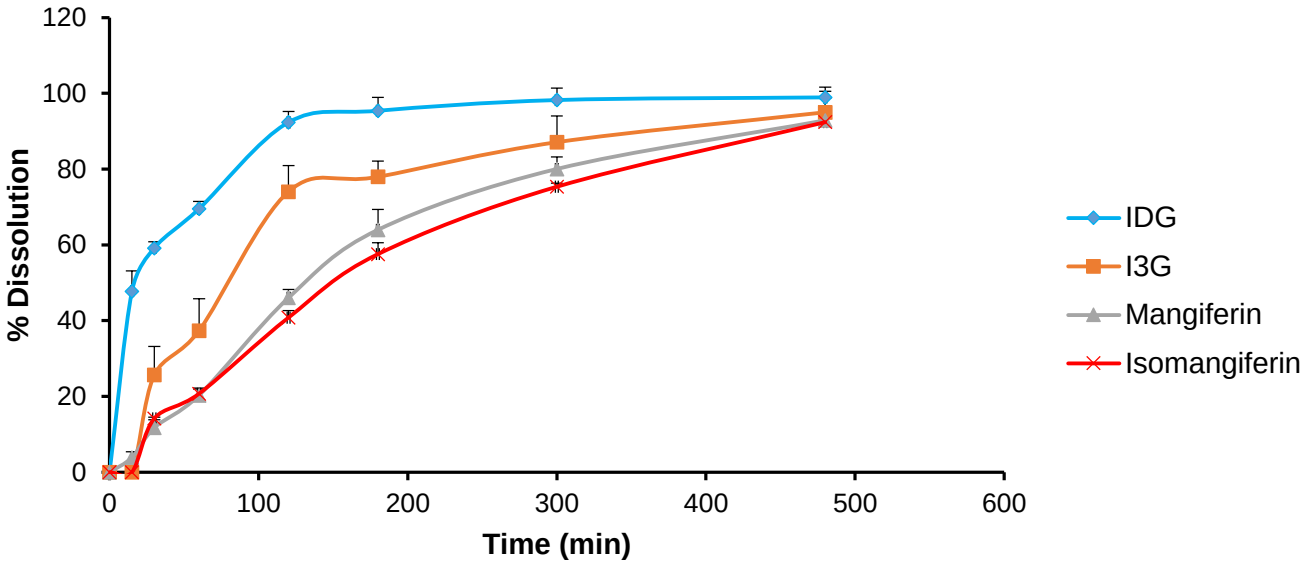

Figure 4.28: Percentage marker molecules released from MUPS tablets containing 50% w/w polypropylene low density polymer in 0.1 N HCl plotted as a function of time (Error bars represent SD and n = 3)

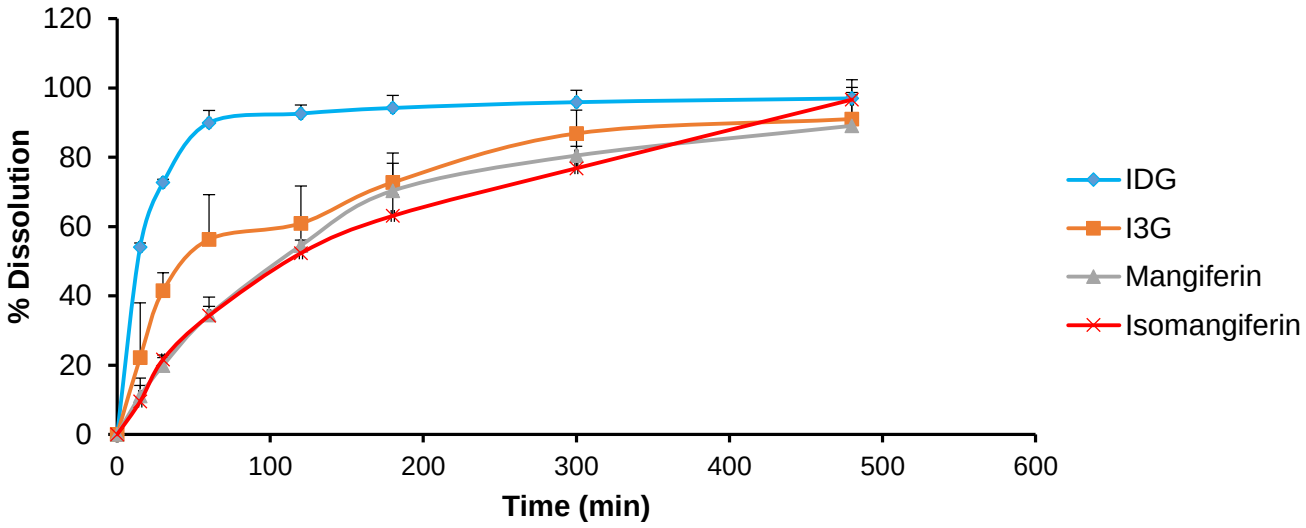

Figure 4.29: Percentage marker molecules released from MUPS tablets containing 50% w/w PDC polymer in 0.1 N HCl dissolution medium as a function of time (Error bars represent SD and n = 3)

It is clear from Figures 4.28 and 4.29 that the four honeybush extract marker molecules have been released at different rates and to different extents from each of the MUPS tablets. IDG exhibited a steep ascending curve from both MUPS tablets, which indicates immediate and relatively fast release. Mangiferin and isomangiferin were released at a slower rate, which were similar and relatively close to each other. Their dissolution curves are also close to straight lines (therefore their release rates approached zero order kinetics).

Streubel *et al*. (2002) have noted that the PP polymer amount present in the formulation (i.e. approximately 60%) is important to prevent a burst release effect due to the fact that the polymer may form a protective layer around the active ingredient particles. They concluded that the formulation containing this polymer presented with acceptable sustained release of the drug over a certain time period.

Table 4.10: The mean dissolution time (MDT) values for both PP and PDC containing MUPS tablets

	PP containing MUPS tablet				**PDC containing MUPS tablet**			
	IDG	**I3G**	**Mangiferin**	**Isomangiferin**	**IDG**	**I3G**	**Mangiferin**	**Isomangiferin**
***MDT (min)**	16.255	29.801	39.169	42.318	11.660	24.313	31.460	39.622

*MDT= Mean dissolution time

The MDT values in Table 4.10 confirmed that the four marker molecules of honeybush extract were released at different rates from the MUPS tablets. The following order in dissolution rates was obtained from our assays on the two MUPS tablets for the four marker molecules: IDG **>** I3G **>** Mangiferin **>** Isomangiferin. The order of release has remained the same for both polymers, but when comparing the honeybush extract marker molecule dissolution for the different MUPS, the PDC containing MUPS has exhibited slightly higher dissolution rates than the PP containing MUPS.

When comparing divergent dissolution profiles it is important to make use of certain parameters like the dissimilarity (f_1) and the similarity (f_2) fit factors of Moore and Flanner (1996). The dissolution profiles of the marker molecules released from the two MUPS formulas containing PP and PDC polymer were compared with each other. The fit factors calculated from the dissolution profiles of the honeybush extract marker molecules from each of the MUPS tablets are shown in Table 4.11.

Table 4.11: The fit factors (f_1 and f_2) for the comparison between PP and PDC MUPS tablets

	Fit factors comparison between PP and PDC MUPS tablets			
	IDG	**I3G**	**Mangiferin**	**Isomangiferin**
***f_1**	10.417	27.187	21.928	26.243
***f_2**	50.586	43.029	54.695	53.203

*f_1 = Dissimilarity factor; f_2 = Similarity factor.

The criteria for both fit factors are as follows: $f_1 \leq 15$ indicating the dissolution profile are quite similar and when f_1 value increases then the dissimilarity will start to increase. When $f_2 \geq 50$ then the dissolution profiles being compared are similar and as dissimilarity increases the f_2 value will approach zero (Anderson *et al*., 1998; Moore and Flanner, 1996). When considering the results shown in Table 4.10, it is clear that for the marker molecule IDG dissolution profile for the comparison between the MUPS PP and PDC formulations are similar to each other which can also be seen in Figure 4.28 and Figure 4.29. For the rest of the marker molecules, a dissimilarity of the dissolution profiles between PP and PDC MUPS tablets were obtained. Various factors may cause these dissimilarity which can either be the camphor added for sublimation purposes or the fact that the polymers have different characteristics.

4.6.1 Conclusion

The results obtained from the evaluation of the MUPS tablets indicated that the PP polymer produced more favourable properties in terms of physical properties, buoyancy and dissolution profiles for the manufacture of a gastro-retentive system containing honeybush crude extract.

CHAPTER 5

FINAL CONCLUSIONS AND FUTURE RECOMMENDATIONS

5.1 FINAL CONCLUSIONS

In this study, crude extracts as well as benzophenone and xanthone rich fractions showed the potential to inhibit intestinal enzymes in the gastrointestinal tract (i.e. lipase and alpha-glucosidase). The honeybush crude extracts showed differences in their enzyme inhibition activities, where the ARC188 crude extract shown better α-glucosidase and lipase inhibition activities than the ARC189 crude extract, which can be explained by differences in their phytochemical compositions. In general, the benzophenone and xanthone rich fractions showed higher enzyme inhibition activities than the crude extracts. Furthermore, the xanthone rich fractions have shown higher enzyme inhibitory activity than the benzophenone rich fractions. Enzyme inhibition in the gastrointestinal tract can be considered as one of the mechanisms by which honeybush extracts contribute to the management and prevention of "diabesity".

The results from the *in vitro* transport studies indicated that the relative low transport was obtained for the marker molecules from both the honeybush crude extracts and the benzophenone and xanthone rich fractions across excised pig intestinal tissue. This can potentially be explained by the unfavourable physico-chemical properties of these molecules for membrane permeation based on Lipinski's rule of five. It was shown that most of the marker molecules were susceptible to active efflux transport, which may have further contributed to the low transport in the uptake direction. Furthermore, the relatively low uptake of active marker molecules from the crude extracts as well as the fractions may be beneficial in the treatment and prevention of "diabesity" due to the local enzyme inhibition action of these honeybush phytochemicals in the gastrointestinal tract.

A successful non-effervescent multiple-unit pellet system (MUPS) gastro-retentive dosage form containing ARC188 crude extract was developed. The sustained release of some of the phytoconstituents of the honeybush crude extract from the gastro-retentive system indicated that these components can be delivered over an extended period of time to the small intestine, which is the region of the gastrointestinal tract where enzyme inhibition is achieved. The polypropylene polymer seemed to be the most suitable candidate to achieve the buoyancy effect required from a floatable gastro-retentive drug delivery system. The camphor seemed to have sublimated and thereby left pores filled with air that contributed to the MUPS tablet's

ability to float (i.e. buoyancy effect). This MUPS dosage form prepared from the polypropylene polymer therefore showed potential to deliver honeybush phytoconstituents for the treatment and prevention of “diabesity”.

5.2 FUTURE RECOMMENDATIONS

The following recommendations for future research are made to assist in the exploration of honeybush (*C. genistoides*) extracts to obtain further insights on the medicinal value of this plant:

Determine whether the *C*-monoglucosides (i.e. I3G and mangiferin) have better enzyme inhibitory activity than their aglycones for the inhibition of lipase as postulated by Beelders *et al*. (2014a) to be the reason for better α-glucosidase inhibitory action.

Further investigation can be performed to calculate the kinetic parameters, e.g. K_i values for the benzophenones as well as the xanthones in honeybush, involved in their inhibitory effect on lipase and α-glucosidase. It would be beneficial to ascertain the type of inhibition (i.e. competitive, non-competitive and uncompetitive) exerted by each of the marker compounds.

Transport studies on different regional segments of the gastro-intestinal tract should be conducted and *in vivo* bioavailability studies should be carried out to confirm the relatively low transport of the marker molecules present in the crude and enriched fractions of honeybush.

More studies can be performed utilising extracts from other honeybush plant species than *C. genistoides*.

Determine whether efflux of honeybush extract marker molecules can be inhibited by other P-gp mediated transport substrates/inhibitors, which can enhance the uptake of the marker molecules present in honeybush. Furthermore, to determine the effect that this enhanced uptake may have on enzyme inhibition in the lumen of gastrointestinal tract. The marker molecules of the crude extract and rich fractions of honeybush (*C. genistoides*) can be screened for pharmacokinetic interaction with other drugs that might be taken concomitantly.

Determine toxicity of the crude extracts and enriched fractions of honeybush to confirm that the phytoconstituents are not harmful to the human body.

Optimise the gastro-retentive dosage form to perform zero-order release of the honeybush extract marker molecules over an extended period of time and confirm gastro-retention in an appropriate animal model (e.g. pig).

BIBLIOGRAPHY

Alderborn, G. 2007. Tablets and compaction. (*In* Aulton, M.E., *ed*. Pharmaceutics: the design and manufacture of medicines. 3rd ed. New York: Churchill Livingstone. p. 441-482).

Alqahtani, S., Mohamed, L.A. & Kaddoumi, A. 2013. Experimental models for predicting drug absorption and metabolism. *Expert Opinion on Drug Metabolism & Toxicology*, 9:1-14.

Anderson, N.H., Bauer, M., Boussac, N., Khan-Malek, R., Munden, P. & Sardaro, M. 1998. An evaluation of fit factors and dissolution efficiency for the comparison of in vitro dissolution profiles. *Journal of Pharmaceutical and Biomedical Analysis*, 17:811-822.

Andlauer, W., Prunier, P. & Prim, D. 2009. Fluorometric method to assess lipase inhibition activity. *CHIMIA International Journal for Chemistry*, 63:695-697.

Anon. 2014. Report: honey bush tea. p. 1-32 http://www.elsenburg.com/economics/downloads/honeybush.pdf Date of access: 5 Mrt. 2015.

Arora, S., Ali, J., Ahuja, A., Khar, R.K. & Baboota, S. 2005. Floating drug delivery systems: a review. *Journal of American Association of Pharmaceutical Scientists*, 6:E372-E390.

Artursson, P. & Karlsson, J. 1991. Correlation between oral drug absorption in humans and apparent drug permeability coefficients in human intestinal epithelial (Caco-2) cells. *Biochemical and Biophysical Research Communications*, 175: 880-885.

Ashford, M. 2007. Assessment of biopharmaceutical properties. (*In* Aulton, M.E., *ed*. Pharmaceutics: the design and manufacture of medicines. 3rd ed. New York: Churchill Livingstone. p. 304-323).

Astrup, A. & Finer, N. 2000. Redefining type 2 diabetes: 'Diabesity' or 'Obesity dependent diabetes mellitus'. *Obesity Reviews*, 1:57-59.

Atkins, P. & De Paula, J. 2011. Physical chemistry for the life sciences. New York: W. H. Freeman and Company. p. 272-303.

Atlabachew, M., Combrinck, S., Viljoen, A.M., Hamman, J.H. & Gouws, C. 2016. Isolation and in vitro permeation of phenylpropylamino alkaloids from Khat (*Catha edulis*) across oral and intestinal mucosal. *Journal of Ethnopharmacology*, 1:1-30.

Awortwe, C., Fasinu P.S. & Rosenkranz, B. 2014. Application of Caco-2 cell line in herb-drug interaction studies: current approaches and challenges. *Journal of Pharmaceutical Sciences*, 17:1–19.

Azuma, T., Kayano, S., Matsumura, Y., Konishi, Y., Tanaka, Y. & Kikuzaki, H. 2011. Antimutagenic and α-glucosidase inhibitory effects of constituents from *Kaempferia parviflora*. *Food chemistry*, 125:471-475.

Baggett, S., Mazzola, E.P. & Kennelly, E.J. 2005. The benzophenones: Isolation, structural elucidation and biological activities. *Studies in Natural Products Chemistry*, 32:721-771.

Bahadur, B., Reddy, K.J., & Rao, M.L.N. 2007. Medicinal plants: an overview. (*In* Reddy, K.J., *ed*. Advances in medicinal plants. India, IN: Universities Press. p. 1-50).

Baleta, A. & Mitchell, F. 2014. Country in focus: diabetes and obesity in South Africa. *The Lancet Diabetes & Endocrinology*, 2:687-688.

Balimane, P.V., Chong, S. & Morrison, R.A. 2000. Current methodologies used for evaluation of intestinal permeability and absorption. *Journal of Pharmacological and Toxicological Methods*, 44:301-312.

Bardonnet, P.L., Faivre, V., Pugh, W.J., Piffaretti, J.C. & Falson, F. 2006. Gastroretentive dosage forms: overview and special case of *Helicobacter pylori*. *Journal of Controlled Release,* 111:1-18.

Barry, B.W. 2007. Transdermal drug delivery. (*In* Aulton, M.E., *ed*. Pharmaceutics: the design and manufacture of medicines. 3rd ed. New York: Churchill Livingstone. p. 565-597).

Bashaiwoldua, A.B., Podczeckb, F. & Newtona, J.M. 2011. Compaction of and drug release from coated pellets of different mechanical properties. *Advanced Powder Technology*, 22:340-353.

Beaupoil-Abadie, B., Raffalli, M., Cozzone, P. & Marchis-Mouren, G. 1973. Determination of the carbohydrate content of porcine pancreatic amylase. *Biochimica et Biophysica Acta (BBA) - General Subjects*, 297:436-440.

Beelders, T., Brand, D.J., De Beer, D., Malherbe, C.J., Mazibuko, S.E., Muller, C.J.F. & Joubert, E. 2014a. Benzophenone *C*- and *O*-glycosides from *Cyclopia genistoides* (honeybush) inhibit mammalian α-glycosidase. *Journal of Natural Products*, 77:2694-2699.

Beelders, T., De Beer, D., Stander, M.A. & Joubert, E. 2014b. Comprehensive phenolic profiling of *Cyclopia genistoides (L.) Vent*. by LC-DAD-MS and -MS/MS reveals novel xanthone and benzophenone constituents. *Molecules*, 19:11760-11790.

Beelders, T. 2015. Xanthones and benzophenones from *Cyclopia genistoides* (honeybush): chemical characterisation and assessment of thermal stability. Stellenbosch University. (Thesis – PhD)

Bellamakondi, P.K., Godavarthi, A. & Ibrahim, M. 2014. Anti-hyperglycaemic activity of *Caralluma umbellata* Haw. *BioImpacts*, 4:113-116.

Berg, J.M, Tymoczko, J.L. & Stryer, L. 2002. Biochemistry. 5th ed. New York: Freeman and Sumanas, Inc. p. 304-357.

Bergh, E.W. & Compton, J.S. 2015. A one-year post-fire record of macronutrient cycling in a mountain sandstone fynbos ecosystem, South Africa. *South African Journal of Botany*, 97:48-58.

Berggren, S. 2006. Drug transport and metabolism in rat and human intestine. Digital comprehensive summaries of Uppsala dissertations from the faculty of pharmacy 41. Uppsala: Sweden. p. 1-54. http://www.diva-portal.org/smash/record.jsf?pid=diva2%3A169157&dswid=2393 Date of access: 9 Mrt. 2015.

Bergström, C.A.S., Holm, R., Jørgensen, S.A., Andersso, S.B.E., Artursson, P., Beato, S., Borde, A., Box, K., Brewster, M., Dressman, J., Feng, K., Halbert, G., Kostewicz, E., McAllister, M., Muenster, U., Thinnes, J., Taylor, R. & Mullertz, A. 2014. Early pharmaceutical profiling to predict oral drug absorption: Current status and unmet needs. *European Journal of Pharmaceutical Sciences*, 57:173-199.

Bhaskaran, S. & Lakshmi, P.K. 2010. Extrusion spheronization: a review. *International Journal of Pharmtech Research*, 2:2429-2433.

Birari, R.B. & Bhutani, K.K. 2007. Pancreatic lipase inhibitors from natural sources: unexplored potential. *Drug Discovery Today*, 12:879-889.

Bischoff, H. 1994. Pharmacology of alpha-glucosidase inhibition. *European Journal of Clinical Investigation*, 24:3-10.

Boath, A.S., Grussu, D., Stewart, D. & McDougall, G.J. 2012. Berry polyphenols inhibit digestive enzymes: a source of potential health benefits? *Journal of Food Digestion*, 3:1-7.

British Pharmacopoeia. 2016. https://www-pharmacopoeia-com.nwulib.nwu.ac.za/bp-2016/appendices/appendix-17/appendix-xvii-n--powder-flow1.html?date=2016-07-01&text=flow+property Date of access: 28 Jul. 2016.

Bressler, R. 2005. Herb-drug interactions: interactions between Kava and prescription medications. *Geriatrics*, 60:24-25.

Carai, M.A.M., Fantini, N., Loi, B., Colombo, G., Riva, A. & Morazzoni, P. 2009. Potential efficacy of preparations derived from *Phaseolus vulgaris* in the control of appetite, energy intake, and carbohydrate metabolism. *Diabetes, Metabolic Syndrome and Obesity: Targets and Therapy*, 2:145-153.

Chae, S.W., Woo, S., Park, J.H., Kwon, Y., Na, Y. & Lee, H.J. 2015. Xanthone analogues as potent modulators of intestinal P-glycoprotein. *European Journal of Medicinal Chemistry*, 26:237-245.

Chiba, S. 1988. Handbook of amylases and related enzymes: their sources, isolation methods, properties and applications. 1st ed. Oxford: Pergamon press. https://books.google.co.za/books?id=2lKeBQAAQBAJ&printsec=frontcover#v=onepage&q=glucosidae&f=false Date of access: 3 Feb. 2016.

Chieli, E., Romiti, N., Rodeiro, I. & Garrido, G. 2009. In vitro effects of *Mangifera indica* and polyphenols derived on ABCB1/P-glycoprotein activity. *Food and Chemical Toxicology*, 47:2703-2710.

Chieli, E., Romiti, N., Rodeiro, I. & Garrido, G. 2010. *In vitro* modulation of ABCB1/P-glycoprotein expression by polyphenols from *Mangifera indica*. *Chemico-Biological Interactions*, 186:287-294.

Clark, D.E. & Pickett, S.D. 2000. Computational methods for the prediction of 'drug-likeness'. Research focus, 5:49-58.

Collett, J.H. & Moreton, R.C. 2007. Modified-release peroral dosage forms. (*In* Aulton, M.E., *ed.* Pharmaceutics: the design and manufacture of medicines. 3rd ed. New York: Churchill Livingstone. p. 4-14).

Cooper, G.M. 2000. The central role of enzymes as biological catalysts. Sunderland: Sinauer Associates. http://www.ncbi.nlm.nih.gov/books/NBK9921/ Date of access: 26 Jan. 2016.

Corelli, R.L. 2009. Basic and clinical pharmacology: therapeutic & toxic potential of over-the-counter agents. 11th ed. Singapore: McGraw-Hill Companies. p. 1110.

Cragg, G.M. & Newman, D.J. 2013. Natural products: A continuing source of novel drug leads. *BBA - General Subjects*, 1830:3670-3695.

Da Silva, L.D., Da Silva, T.L., Antunes, A.H. & Rezende, K.R. 2015. A sensitive medium-throughput method to predict intestinal absorption in humans using rat intestinal tissue segments. *Journal of Pharmaceutical Sciences*, 104:2807-2812.

Dash, V., Behera, S.K., Agarwal, R. & Sinha, N. 2012. Pelletization technique in drug delivery system. *Journal of Chemical and Pharmaceutical Research*, 9:19-25.

Dave, B.S., Amin, A.F. & Patel, M.M. 2004. Gastroretentive drug delivery system of ranitidine hydrochloride: formulation and in vitro evaluation. *AAPS PharmSciTech*, 5:77-82.

De Beer, D., Schulze, A.E., Joubert, E., De Villiers, A. & Malherbe, C.J & Stander, M.A. 2012. Food ingredient extracts of Cyclopia subternata (honeybush): variation in phenolic composition and antioxidant capacity. *Journal of Molecules*, 17:14602-14624.

Demeester, J. 1997. Biopharmaceutical aspects of enzyme absorption. (*In* Lauwers, A., *ed*. Pharmaceutical enzymes. New York: Marcel Dekker. p. 1-20).

Dhital, S., Gidley, M.J. & Warren, F.J. 2015. Inhibition of α-amylase activity by cellulose: kinetic analysis and nutritional implications. *Carbohydrate Polymers*, 123:305-312.

Diderot, N.T., Silvere, N. & Etienne, T. 2006. Xanthones as therapeutic agents: chemistry and pharmacology. *Advances in Phytomedicine*, 2:273-298.

Du Plessis, L.H. & Hamman, J.H. 2013. *In vitro* evaluation of the cytotoxic and apoptogenic properties of aloe whole leaf and gel materials. *Drug and Chemical Toxicology*, 37:169-77.

Du Toit, J. & Joubert, E. 1998. The effect of pretreatment on the fermentation of honeybush tea (*Cyclopia maculata*). *Journal of the Science of food and agriculture*, 76(4):537-545.

Du Toit, J., Joubert, E. & Britz, T.J. 1998. Honeybush tea - a rediscovered indigenous South African herbal tea. *Journal of Sustainable Agriculture*, 12:67-84.

Dwibhashyam, V.S.N. M. & Ratna, J.V. 2008. Key Formulation Variables in Tableting of Coated Pellets. *Indian Journal of Pharmaceutical Sciences*, 70:555-564.

Dudhia, Z., Louw, J., Muller, C., Joubert, E., De Beer, D., Kinnear, C. & Pheiffer, C. 2013. *Cyclopia maculata* and *Cyclopia subternata* (honeybush tea) inhibits adipogenesis in 3T3-L1 pre-adipocytes. *Phytomedicine*, 20:401-408.

Dukić-Ott, A., Thommes, M., Remon, J.P., Kleinebudde, P. & Vervaet, C. 2009. Production of pellets via extrusion-spheronisation without the incorporation of microcrystalline cellulose: a critical review. *European Journal of Pharmaceutics and Biopharmaceutics*, 71:38-46.

El-Seedi, H.R., El-Barbary, M.A., El-Ghorab, D.M.H., Bohlin, L. & Borg-Karlson, A. 2010. Recent insights into the biosynthesis and biological activities of natural xanthones. *Current Medicinal Chemistry*, 17:854-901.

Ferreira, D., Kamara, B.I., Brandt, E.V. & Joubert, E. 1998. Phenolic compounds from *cyclopia intermedia* (honeybush tea). *Journal of Agricultural and Food Chemistry*, 46:3406-3410.

Filippatos, T.D., Derdemezis, C.S., Gazi, I.F., Nakou, E.S., Mikhailidis, D.P. & Elisaf, M.S. 2008. Orlistat-associated adverse effects and drug interactions. *Drug Safety*, 31:53-65.

Franco, M., Lopedota, A., Trapani, A., Cutrignelli, A., Meleleo, D., Micelli, S. & Giuseppe Trapani, G. 2008. Frog intestinal sac as an in vitro method for the assessment of intestinal permeability in humans: Application to carrier transported drugs. *International Journal of Pharmaceutics*, 352: 182-188.

Fromm, H.J. & Hargrove, M.S. 2012. Essentials of biochemistry. New York: Springer. p. 53-121.

Galia, M., Svec, F. & Frechet, J.M.J. 1994. Monodisperse polymer beads as packing material for high-performance liquid chromatography: Effect of divinylbenzene content on the porous and chromatographic properties of poly(styrene-co-divinylbenzene) beads prepared in presence of linear polystyrene as a porogen. *Journal of Polymer Science Part A: Polymer Chemistry*, 32: 2169–2175.

Gandhi, R., Kaul, C.L. & Panchagnula, R. 1999. Extrusion and spheronization in the development of oral controlled-release dosage forms. *Pharmaceutical Science & Technology Today (PSTT)*, 2(4):160-170.

Gautam, M.K. & Deva, V. 2012. Floating drug delivery of ranitidine hydrochloride. *International Journal of Life Sciences Biotechnology and Pharma Research (IJLBPR)*, 1:142-150.

Gilham, D. & Lehner, R. 2005. Techniques to measure lipase and esterase activity in vitro. *Journal of Molecular and Cell Biology of Lipids*, 36:139–147.

Grass, G.M. & Sweetana, S.A. 1988. *In vitro* measurement of gastrointestinal tissue permeability using a new diffusion cell. *Journal of Pharmaceutical Research*, 5:372-376.

Guyton, A.C. & Hall, J.E. 2011. Guyton and Hall textbook of medical physiology. 12th ed. Philadelphia: Saunders Elsevier. p. 11-790.

Hadi, M.A., Rao, A.S., Martha, S., Sirisha, Y. & Chandrika, P.U. 2013. Development of a floating multiple unit controlled-release beads of zidovudine for the treatment of AIDS. *Journal of Pharmacy Research*, 6:78-83.

Hamden, K., Mnafgui, K., Amri, Z., Aloulou, A. & Elfeki, A. 2012. Inhibition of key digestive enzymes related to diabetes and hyperlipidaemia and protection of liver-kidney functions by trigonelline in diabetic rats. *Scientia Pharmaceutica*, 81:233-246.

Hansen, T.S. & Nilsen, O.G. 2009. Echinacea purpurea and P-glycoprotein drug transport in caco-2 cells. *Journal of Phytotherapy Research*, 23:86-91.

Harvey, W.H. 1868. The genera of South African plants. 2nd ed. London: Green reader and dyer. p.70. http://www.biodiversitylibrary.org/item/60398#page/7/mode/1up Date of access: 30 Sept. 2015.

Harvey, R., Ferrier, D., Fried, S.K. & Horenstein, R.B. 2011. Lippincott's illustrated reviews: Biochemistry. 5th ed. Philadelphia: Williams & Wilkins. p. 53-68.

Herbst, M.C. 2014. Cancer Association of South Africa (CANSA): fact sheet on honeybush tea. http://www.cansa.org.za/files/2014/06/Fact-Sheet-Honeybush-Tea-June-2014.pdf Date of access: 5 Mrt. 2015.

Highley, T.L. 1997. Carbohydrolase Assays*. Methods in plant biochemistry and molecular biology. Boca Raton, FL: CRC Press. p. 309-321.

Hoag, S.W. & Lim, H. 2008. Particle and powder bed properties. (*In* Augsburger, L.L., *ed*. Pharmaceutical dosage forms: tablets. 3rd ed. New York: Informa Healthcare. p. 17-73).

Huang, M., Du Plessis, J., Du Preez, J., Hamman, J. & Viljoen, A. 2008. Transport of aspalathin, a Rooibos tea flavonoid, across the skin and intestinal epithelium. *Phytotherapy Research*, 22:699-704.

Iwu, M.M. 2014. Handbook of African medicinal plants. 2nd ed. Rosewood Drive, Danvers: Taylor & Francis Group, LLC. p. 199-201.

Jaimini, M., Ranga, S., Kumar, A., Sharma, S.K. & Chauhan, B.S. 2013. A review on immediate release drug delivery system by using design of experiment. *Journal of Drug Discovery and Therapeutics*, 1:21-27.

Jämstorp, E., Yarra, T., Cai, B., Engqvist, H., Bredenberg, S. & Strømme, M. 2012. Polymer excipients enable sustained drug release in low pH from mechanically strong in organic geopolymers. *Results in Pharma Sciences*, 2:23-28.

Jigar, V., Tulsi, U., Harsh, V., Pankit, D. & Nirali, T. 2013. Development and evaluation of bilayered gastro-retentive tablet containing metforminHCl SR and pioglitazoneHCl IR. *Journal of Drug Delivery & Therapeutics*, 3:58-61.

Jo, Y.H., Kim, S.B., Ahn, J.H., Liu, Q., Hwang, B.Y. & Lee, M.K. 2013. Inhibitory activity of benzophenones from *Anemarrhena asphodeloides* on pancreatic lipase. *Natural Product Communications*, 8:481-483.

Johnson, V.A. 2015. Introduction to Drug Metabolism. http://webcache.googleusercontent.com/search?q=cache:BG3rN5DB-bcJ:www.healthsci.jmu.edu/common/knitter/powerpoint/Drug%2520Metabolism.ppt+&cd=1&hl=en&ct=clnk&gl=za Date of access: 26 Jan. 2016.

Joubert, E. & De Beer, D. 2011. Rooibos (*Aspalathus linearis*) beyond the farm gate: from herbal tea to potential phytopharmaceutical. *South African Journal of Botany*, 77:869-886.

Joubert, E., Gelderblom, W.C.A., Louw, A. & De Beer, D. 2008a. South African herbal teas: *Aspalathus linearis*, *Cyclopia* spp. and *Athrixia phylicoides*—A review. *Journal of Ethnopharmacology*, 119:376-412.

Joubert, E., Joubert, M.E., Bester, C., de Beer, D. & De Lange, J.H. 2011. Review: Honeybush (Cyclopia spp.): from local cottage industry to global markets: the catalytic and supporting role of research. *South African journal of Botany*, 77(4):887-907.

Joubert, E., Richards, E.S., Van Der Merwe, J.D., De Beer, D., Manley, M. & Gelderblom, W.C.A. 2008b. Effect of species variation and processing on phenolic composition and *in vitro* antioxidant activity of aqueous extracts of *Cyclopia spp*. (honeybush tea). *Journal of Agricultural and Food Chemistry*, 56:954-963.

Joubert, M.E., Botma, P.S., Kotzé, W.A.G. & Wooldridge, J. 2007. Honeybush (*Cyclopia* spp.) response to phosphorus fertilisation and mulching. *South African Journal of Plant and Soil*, 24:176-177.

Jyothi, J.B. & Doniparthi, J. 2014. Multiparticulate drug delivery systems using natural polymers as release retardant materials. *International Journal of Pharmacy and Pharmaceutical Sciences*, 6:61-65.

Kalra, S. & Bhutani, J. 2014. Alpha-glucosidase inhibitors. *Journal of Pakistan medical association (JPMA)*, 1:55-65.

Kamara, B.I., Brand, D.J., Brandt, E.V. & Joubert, E. 2004. Phenolic metabolites from honeybush tea (cyclopia subternata). *Journal of Agricultural and Food Chemistry*, 52:5391-5395

Kamara, B.I., Brandt, E.V., Ferreira, D. & Joubert, E. 2003. Polyphenols from honeybush tea (*Cyclopia intermedia*). *Journal of Agricultural and Food Chemistry*, 51:3874-3879.

Kandra, L. 2003. α-Amylases of medical and industrial importance. *Journal of Molecular Structure (Theochem)*, 666:487-498.

Kandukuri, J.M., Allenki, V., Eaga, C.M., Keshetty, V. & Jannu, K.K. 2009. Pelletization techniques for oral drug delivery. *International Journal of Pharmaceutical Sciences and Drug Research*, 1:63-70.

Kankal, G., Mahale, N.B., Salunkhe K.S. & Chaudhari S.R. 2013. Review on- gastroretentive drug delivery system. *International Journal of Pharma and Bio Sciences*, 3:410-422.

Kies, P. 1951. Revision of the genus Cyclopia and notes on some other sources of bush tea. *Bothalia*, 6:161-176.

Kitanov, G.M. & Nedialkov, P.T. 2001. Benzophenone *O*-glucoside, a biogenic precursor of 1,3,7-trioxygenated xanthones in *Hypericum annulatum*. *Phytochemistry*, 57:1237-1243.

Klausner, E.A., Lavy, E., Friedman, M. & Hoffman, A. 2003. Expandable gastroretentive dosage forms. *Journal of Controlled Release*, 90:143-162.

Klazema, A. 2014. Lock and Key Hypothesis: Understanding Enzymes. https://blog.udemy.com/lock-and-key-hypothesis/ Date of access: 22 Jan. 2016.

Kojima, T. & Elliott, J.A. 2013. Effect of silica nanoparticles on the bulk flow properties of fine cohesive powders. *Chemical Engineering Science*, 101:315-328.

Kokotkiewicz, A. & Luczkiewicz, M. 2009. Honeybush (*Cyclopia* sp.): a rich source of compounds with high antimutagenic properties. *Fitoterapia*, 80:3-11.

Kokotkiewicz, A., Bucinski, A. & Luczkiewicz, M. 2015. Xanthone, benzophenone and bioflavonoid accumulation in *Cyclopia genistoides* (L.) vent. (honeybush) shoot cultures grown on membrane rafts and in a temporary immersion system. *Journal of Plant Cell, Tissue and Organ Culture*, 120:373-378.

Kokotkiewicz, A., Luczkiewicz, M., Kowalski, W., Badura, A., Piekus, N. & Bucinski, A. 2013. Isoflavone production in *Cyclopia subternata vogel* (honeybush) suspension cultures grown in shake flasks and stirred-tank bioreactor. *Journal of Applied Microbiology and Biotechnology*, 97:8467-8477.

Krueger, C., Thommes, M. & Kleinebudde, R. 2013. Spheronisation mechanism of MCC II-based pellets. *Powder Technology*, 238:176-187.

Ku, M.J., Kim, J.H., Lee, J., Cho, J.Y., Chun, T. & Lee, S.Y. 2015. Maclurin suppresses migration and invasion of human non-small-cell lung cancer cells via anti-oxidative activity and inhibition of the Src/FAK-ERK-β-catenin pathway. *Molecular and Cellular Biochemistry*, 402:243-252.

Kumar, A., Verma, A., Sharma, G., Saini, R., Sharma, S., Singh, S., Jain, U.K. & Sharma, M. 2013. Formulation and characterization of effervescent floating matrix tablets of famotidine hydrochloride. *Asian Journal of Biomedical and Pharmaceutical Sciences*, 3:43-47.

Kumar, S., Narwal, S., Kumar, V. & Prakash, O. 2011. α-Glucosidase inhibitors from plants: A natural approach to treat diabetes. *Pharmacognosy Reviews*, 5:19-29.

Kumaran, K.S., Manjunath, S.Y. & Wamorka, V.V. 2010. Development of a floating multiple unit controlled-release system for mosapride. *Asian Journal of Pharmaceutics*, 4:163-167.

Kumari, M.H., Samatha, K., Balaji, A. & Uma-Shankar, M.S. 2013. Recent novel advancements in pellet formulation: a review. *International Journal of Pharmaceutical Sciences Review and Research*, 4:3803-3822.

Le Ferrec, E., Chesne, C., Artusson, P., Brayden, D., Fabre, G., Gires, P., Guillou, F., Rousset, M., Rubas, W. & Scarino, M. 2001. *In vitro* models of the intestinal barrier: the report and

recommendations of ECVAM workshop 46. European centre for the validation of alternative methods. *Alternatives to Laboratory Animals*, 29:649-668.

Le Roux, M., Cronje, J.C., Burger, B.V. & Joubert, E. 2012. Characterization of volatiles and aroma-active compounds in honeybush (*Cyclopia subternata*) by GC-MS and GC-O analysis. *Journal of Agricultural and Food Chemistry*, 60:2657-2664.

Le Roux, M., Cronje, J.C., Joubert, E. & Burger, B.V. 2008. Chemical characterization of the constituents of the aroma of honeybush, *Cyclopia genistoides*. *South African Journal of Botany*, 74:139-143.

Legen, I., Salobir, M. & Kerč, J. 2005. Comparison of different intestinal epithelia as models for absorption enhancement studies. *International Journal of Pharmaceutics*, 291:183-188.

Li, X., Gao, Y., Li, F., Liang, A., Xu, Z., Bai, Y., Mai, W., Han, L. & Chen, D. 2014. Maclurin protects against hydroxyl radical-induced damages to mesenchymal stem cells: antioxidant evaluation and mechanistic insight. *Chemico-Biological Interactions*, 5:221-228.

Lipinski, C.A., Lombardo, F., Dominy, B.W. & Feeney, P.J. 2001. Experimental and computational approaches to estimate solubility and permeability in drug discovery and development settings. *Advanced Drug Delivery Reviews*, 46:3–26.

Liu, S., Li, D., Huang, B., Chen, Y., Lu, X. & Wang, Y. 2013. Inhibition of pancreatic lipase, α-glucosidase, α-amylase and hypolipidemic effects of the total flavonoids from *Nelumbo nucifera* leaves. *Journal of Ethnopharmacology*, 149:263-269.

Lo Piparo, E., Scheib, H., Frei, N., Williamson, G., Grigorov, M. & Chou, C.J. 2008. Flavonoids for controlling starch digestion: structural requirements for inhibiting human α-amylase. *Journal of Medicinal Chemistry*, 51:3555-3561.

Long, M. & Chen, Y. 2009. Dissolution testing of solid products. (*In* Qiu, Y., *eds*. Developing solid oral dosage forms: pharmaceutical theory and practice. London: Academic Press. p. 319-340).

Luczkiewicz, P., Kokotkiewicz, A., Dampc, A. & Luczkiewicz, M. 2014. Mangiferin: a promising therapeutic agent for rheumatoid arthritis treatment. *Medical Hypotheses*, 83:570-574.

Madgula, V.L., Avula, B., Pawar, R.S., Shukla, Y.J., Khan, I.A., Walker, L.A. & Khan, S.I. 2008. *In vitro* metabolic stability and intestinal transport of P57AS3 (P57) from *Hoodia gordonii* and its interaction with drug metabolizing enzymes. *Planta Medica*, 74:1269-1275.

Malherbe, C.J., Willenburg, E., de Beer, D., Bonnet, S.L., van der Westhuizen, J.,H. & Joubert, E. 2014. Iriflophenone-3-*C*-glucoside from *cyclopia genistoides*: isolation and quantitative comparison of antioxidant capacity with mangiferin and isomangiferin using on-line HPLC antioxidant assays. *Journal of Chromatography B*, 951-952:164-171.

Mansbach, C.M., Tso, P. & Kuksis, A. 2001. Intestinal lipid metabolism. New York: Springer science business media. p. 37-48.

Marnewick, J.L. 2009. Rooibos and honeybush: recent advances in chemistry, biological activity and pharmacognosy. Washington, DC: American Chemical Society. p. 277-294. http://port-trading.com/wp-content/uploads/2010/08/newsletter1.pdf Date of access: 30 Jan. 2015.

Marnewick, J.L., Joubert, E., Swart, P., Van Der Westhuizen, F. & Gelderblom, W.C.A. 2003. Modulation of hepatic drug metabolizing enzymes and oxidative status of green and black (*Camellia sinensis*), rooibos (*Aspalathus linearis*) and honeybush (*Cyclopia intermedia*) teas in rats. *Journal of Agriculture and Food Chemistry*, 51:8113-8119.

Matkowski, A., Kuś, P., Góralska, E. & Woźniak, D. 2013. Mangiferin - a bioactive xanthonoid, not only from mango and not just antioxidant. *Mini-Reviews in Medicinal Chemistry*, 13:439-455.

Matsumoto, K., Takayama, K., Abesundara, K.J.M. & Matsui, T. 2003. Assay of α-glucosidase inhibitory activity using flow-biosensor system. *Analytica Chimica Acta*, 479:135-141.

McKay, D.L. & Blumberg, J.B. 2007. A review of the bioactivity of South African herbal teas: rooibos (Aspalathus linearis) and honeybush (Cyclopia intermedia). *Phytotherapy Research*, 21:1-16.

Mehta, P., Shah, R., Lohidasan, S. & Mahadik, K.R. 2015. Pharmacokinetic profile of phytoconstituent(s) isolated from medicinal plants—A comprehensive review. *Journal of Traditional and Complementary Medicine*, 5:207-227.

Misra, P. 2008. AMP activated protein kinase: a next generation target for total metabolic control oncologic, endocrine & metabolic. *Expert Opinion on Therapeutic Targets*, 12:91-100.

Monton, C., Saingam, W., Suksaeree, J., Sakunpak, A. & Kraisintu, K. 2014. Preformulation and physical properties study of fast disintegrating tablets from Thai traditional formula. *International Journal of Pharmacy & Pharmaceutical Sciences*, 6:431-434.

Moore, J.W. & Flanner, H.H. 1996. Mathematical comparison of curves with an emphasis on in vitro dissolution profiles. *Pharmaceutical Technology*, 20:64-74.

Mukherjee, M. 2003. Human digestive and metabolic lipases—a brief review. *Journal of Molecular Catalysis B: Enzymatic*, 22:369-376.

Muller, C.J.F., Joubert, E., Gabuza, K., De Beer, D., Fey, S.J. & Louw, J. 2011. Assessment of the antidiabetic potential of an aqueous extract of honeybush (*Cyclopia intermedia*) in streptozotocin and obese insulin resistant Wistar rats. (*In* Rasooli, I., *ed*. Phytochemicals - bioactivities and impact on health. China, CN: InTech p. 313-332).

Narang, N. 2011b. An updated review on: floating drug delivery system (FDDS). *International Journal of Applied Pharmaceutics*, 3:1-7.

Narang, N., Mastnath, S.B. & Bohar, A. 2010a. An updated review on: floating drug delivery system (FDDS). *International Journal of Applied Pharmaceutics*, 3:1-7.

Nejdfors, P., Ekelund, M., Jeppsson, B. & Weström, B.R. 2000. Mucosal in vitro permeability in the intestinal tract of the pig, the rat and man: species- and region-related differences. *Scandinavian Journal of Gastroenterology*, 35:501-507.

Nelson, D.L. & Cox, M.M. 2005. Lehninger principles of biochemistry. 4th ed. New York: W.H. Freeman and Company. p. 16-1031.

Newton, J.M. 2008. The preparation of pellets by extrusion/spheronisation. (*In* Augsburger, L.L., *ed*. Pharmaceutical dosage forms: tablets. 3rd ed. New York: Informa Healthcare. p. 337-371).

Nolte, M.S. 2009. Pancreatic hormones & antidiabetic drugs. (*In* Katzung, B.G., *ed*. Basic and clinical pharmacology. 11th ed. New York, NY: McGraw-Hill. p. 727-751).

Odaci, D., Telefoncu, A. & Timur, S. 2010. Maltose biosensing based on co-immobilization of α-glucosidase and pyranose oxidase. *Bioelectrochemistry*, 79:108-113.

Ogilvie, B.W., Usuki, E., Yerino, P. & Parkinson, A. 2008. *In vitro* approaches for studying the inhibition of drug-metabolising enzymes and identifying the drug-metabolizing of drugs

(reaction phenotyping) with emphasis on cytochrome P450. (*In* Rodrigues, A.D., *ed*. Drug-drug interactions. 2nd ed. New York: informa healthcare. p. 231-254).

Oh, T., Kim, J., Ha, J., Chi, S., Rhee, Y., Park, C. & Park, E. 2013. Preparation of highly porous gastroretentive metformin tablets using a sublimation method. *European Journal of Pharmaceutics and Biopharmaceutics*, 83:460-467.

Oxford dictionaries. 2016. http://www.oxforddictionaries.com/definition/english/cyclize Date of access: 25 Feb. 2016.

Ozeki, K., Kato, M., Sakurai, Y., Ishigai, M., Kudo, T. & Ito, K. 2015. Evaluation of the appropriate time range for estimating the apparent permeability coefficient (P_{app}) in a transcellular transport study. *International Journal of Pharmaceutics*, 495:963-971.

Palmer, T. & Bonner, P.L. 2007. Enzymes: Biochemistry, Biotechnology and Clinical chemistry. 2nd ed. England: Horwood. p. 1-393.

Peng, X., Zhang, G., Liao, Y. & Gong, D. 2016. Inhibitory kinetics and mechanism of kaempferol on α-glucosidase. *Food Chemistry*, 190:207-215.

Peng, Y., Yadava, P., Heikkinen, A.T., Parrott, N. & Railkar, A. 2014. Applications of a 7-day Caco-2 cell model in drug discovery and development. *European Journal of Pharmaceutical Sciences*, 56:120-130.

Pinto, E., Williamson, J., Usher, C., Porter, S. & Dürig, T. 2013. Controlled release multi-unit pellet system (MUPS) tablets: effect of coating composition. http://www.ashland.com/pages/aaps Date of access: 2 Mar. 2016.

Powers, A.C. & D´Alessio, D. 2011. Endocrine pancreas and pharmacotherapy of diabetes mellitus and hypoglycaemia. (*In* Brunton, L.L., *ed*. Goodman & Gilman's: The pharmacological basis of therapeutics. 12th ed. New York: McGraw-Hill. p. 1237-1273).

Quiroga, A.D. & Lehner, R. 2011. Acylglycerol lipases (neutral lipid hydrolysis). http://lipidlibrary.aocs.org/Biochemistry/content.cfm?ItemNumber=39188 Date of access: 5 Nov. 2015.

Rabasa-Lhoret, R. & Chiasson, J. 2004. α-Glucosidase inhibitors. International textbook of diabetes mellitus. Canada: John Wiley & Sons. p. 901-914.

Ragoonanan, N. 2013. Tag archives: pH and enzyme relationship. https://biochemist01.wordpress.com/tag/ph-and-enzyme-relationship/ Date of access: 24 Jan. 2016.

Rao, G.U. & Pavan, M. 2012. Buoyant sustained release drug delivery systems current potentials advancements and role of polymers: a review. *International Journal of Comprehensive Pharmacy*, 2:1-5.

Rathod, V.G., Kadam, V., Jadhav, S.B., Zamiruddin, M., Bharkad, V.B. & Biradar, S.P. 2014. Immediate release drug delivery system: a review. *World Journal of Pharmacy and Pharmaceutical Sciences*, 3:545-558.

Raval, J.A., Patel, J.K. & Li, N. 2011. Formulation of floating mixed matrix tablets using low density copolymer. *International Research Journal of Pharmaceuticals*, 1:1-7.

Raval, J.A., Patel, M.M., Li, N-H. & Patel, J.K. 2009. Formulation and evaluation of famotidine floating matrix tablets. *Pharmaceutical Technology*, 33:60-70.

Reddy, G.L.N., Rajnarayana, K. & Jayaveera, K.N. 2016. Development and *in vitro-in vivo* evaluation of extended-release multiple-unit pellet system tablets of metoprolol succinate. *Asian Journal of Pharmaceutics*, 10:S339-S42.

Ritger, P.L. & Peppas, N.A. 1987. A simple equation for description of solute release II. Fickian and anomalous release from swellable devices. *Journal of Controlled Release*, 5:37-42.

Roy, P. & Shahiwala, A. 2009. Multiparticulate formulation approach to pulsatile drug delivery: current perspectives. *Journal of Controlled Release*, 134:74-80.

Ryu, H.W., Cho, J.K., Curtis-Long, M.J., Yuk, H.J., Kim, Y.S., Jung, S., Kim, Y.S., Lee, B.W. & Park, K.H. 2011. α-Glucosidase inhibition and antihyperglycemic activity of prenylated xanthones from *Garcinia mangostana*. *Phytochemistry*, 72:2148-2154.

SAHTA (South African Honeybush Tea Association). 2016a. The honeybush plant. http://www.sahoneybush.co.za/honeybush.html?layout=blog Date of access: 21 Feb. 2016.

SAHTA (South African Honeybush Tea Association). 2016b. Species: *Cyclopia* genistoides. http://www.sahta.co.za/photos/species-cyclopia-genistoides/category/4.html Date of access: 25 May 2016.

SAMF (South African medicines formulary). 2012. Antiobesity preparations. 10th ed. Cape Town: FA Print. p. 69-70.

Sancheti, S., Sancheti, S., Bafna, M., Lee, S. & Seo, S. 2011. Persimmon leaf (*Diospyros kaki*), a potent α-glucosidase inhibitor and antioxidant: alleviation of postprandial hyperglycemia in normal and diabetic rats. *Journal of Medicinal Plants Research*, 5:1652-1658.

Sarojini, S. & Manavalan, R. 2012. An overview on various approaches to Gastroretentive dosage forms. *International Journal of Drug Development and Research*, 4:1-13.

Scanlon, V.C. & Sanders, T. 2011. Essentials of anatomy and physiology. 6th ed. Philadelphia: F.A. Davis Company. p. 34-418.

Scharpé, S., Uyttenbroeck, W. & Samyn, N. 1997. Pancreatic enzyme replacement. (*In* Lauwers, A., *ed*. Pharmaceutical enzymes. New York: Marcel Dekker. p. 187-221).

Schmid, K. & Löbenberg, R. 2010. Influence of the changed USP specifications on disintegration test performance. *Dissolution Technologies*, 17:6-10.

Schmidt, J.S., Nyberg, N.T. & Staerk, D. 2014. Assessment of constituents in allium by multivariate data analysis, high-resolution α-glucosidase inhibition assay and HPLC-SPE-NMR. *Food Chemistry*, 161:192-198.

Schulze, A.E., Beer, D., Villiers, A., Manley, M. & Joubert, E. 2014. Chemometric analysis of chromatographic fingerprints shows potential of Cyclopia maculata (Andrews) kies for production of standardized extracts with high xanthone content. *Journal of Agricultural and Food Chemistry*, 62:10542-10551.

Schulze, A.E., Beelders, T., Koch, I.S., Erasmus, L.M., De Beer, D. & Joubert, E. 2015. Honeybush herbal teas (*Cyclopia* spp.) contribute to high levels of dietary exposure to xanthones, benzophenones, dihydrochalcones and other bioactive phenolics. *Journal of Food Composition and Analysis*, 44:139-148.

Schutte, A.L. 1997. Systematics of the genus *Cyclopia* Vent. (Fabaceae, Podalyrieae). *Edinburgh Journal of Botany*, 54(2):125-170.

Schutte, A.L. 2012. Plants of the greater cape floristic region: Fabaceae. 1st ed. Pretoria, RSA: SANBI. p. 518-550.

Seppälä, K., Heinämäki, J., Hatara, J., Seppälä, L. & Yliruusi, J. 2010. Development of a new method to get a reliable powder flow characteristics using only 1 to 2 g of powder. *American Association of Pharmaceutical Scientists*, 11:402-408.

Sfetcu, N. 2014. Health & drugs: disease, prescription & medication. https://books.google.co.za/books?id=8jF-AwAAQBAJ&printsec=frontcover#v=onepage&q&f=false Date of access: 6 Feb. 2016.

Sharma, D. & Sharma, A. 2014. Gastroretentive drug delivery system - a mini review. *Asian Pacific Journal of Health Sciences*, 1:80-89.

Sharma, N., Agarwal, D., Gupta, M.K. & Khinchi, M.P. 2011. A comprehensive review on floating drug delivery system. *International Journal of Research in Pharmaceutical and Biomedical Sciences*, 2:1-14.

Singh, A., Pathak, D. & Pathak, K. 2010. Use of microporous accurel MP 1000 for duodenal delivery of secnidazole: a high dose, gastric pH unstable drug. *International Journal of Drug Delivery Technology*, 2:26-34.

Singh, B.N. & Kim, K.H. 2000. Floating drug delivery systems: an approach to oral controlled drug delivery via gastric retention. *Journal of Controlled Release*, 63:235-259.

Singhal, A.K., Jarald, E.E., Showkat, A. & Daud, A. 2012. *In vitro* evaluation of *Moringa oleifera* gum for colon-specific drug delivery. *International Journal of Pharmaceutical Investigation*, 2: 48-51.

Slanc, P., Doljak, B., Kreft, S., Lunder, M., Janes, D. & Strukelj, B. 2009. Screening of selected food and medicinal plant extracts for pancreatic lipase inhibition. *Phytotherapy Research*, 23:874-877.

Soumyanath, A. 2006. Traditional medicines for modern times: antidiabetic plants. Boca Raton: Taylor & Francis Group. p. 99-104.

Steckel, H. & Mindermann-Nogly, F. 2004. Production of chitosan pellets by extrusion/spheronization. *European Journal of Pharmaceutics and Biopharmaceutics*, 57:107-114.

Streubel, A., Siepmann, J. & Bodmeier, R. 2002. Floating microparticles based on low density foam powder. *International Journal of Pharmaceutics*, 241:279-292.

Streubel, A., Siepmann, J. & Bodmeier, R. 2003. Floating matrix tablets based on low density foam powder: effects of formulation and processing parameters on drug release. *European Journal of Pharmaceutical Sciences*, 18:37-45.

Streubel, A., Siepmann, J. & Bodmeier. 2006. Gastroretentive drug delivery systems. *Expert Opinion Drug Delivery, 3:217-233.*

Surya, S., Salam, A.D., Tomy, D.V., Carla, B., Kumar, R.A. & Sunil, C. 2014. Diabetes mellitus and medicinal plants-a review. *Asian Pacific Journal of Tropical Disease*, 4:337-347.

Tadera, K., Minami, Y., Takamatsu, K. & Matsuoka, T. 2006. Inhibition of α-glucosidase and α-amylase by flavonoids. *Journal of Nutritional Science and Vitaminology*, 52:149-153.

Takano, M., Yumoto, R. & Murakami, T. 2006. Expression and function of efflux drug transporters in the intestine. *Pharmacology & Therapeutics*, 109:137-161.

Tarirai, C., Viljoen, A.M. & Hamman, J.H. 2012. Effects of dietary fruits, vegetables and a herbal tea on the in vitro transport of cimetidine: comparing the Caco-2 model with porcine jejunum tissue. *Journal of Pharmaceutical Biology*, 50:254-263.

Taylor, P.M. 2007. Packs and packaging. (*In* Aulton, M.E., *ed*. Pharmaceutics: the design and manufacture of medicines. 3rd ed. New York: Churchill Livingstone. p. 626-639).

Telleen, S. 2015. Organic compounds essential to human functioning. http://cnx.org/contents/0458d04c-f759-4726-8486-db16f98d9de0@3/Organic-Compounds-Essential-to Date of access: 29 Oct. 2015.

The InterAct Consortium. 2012. Tea consumption and incidence of type 2 diabetes in Europe: the EPIC-InterAct case-cohort study. *PLoS ONE*, 7:e36910.

The International Diabetes Federation. 2015. Diabetes: A global emergency. http://www.idf.org/about-diabetes/facts-figures Date of access: 20 Jan 2017.

Thoorensa, G., Kriera, F., Leclercqb, B., Carlinc, B. & Evrarda, B. 2014. Microcrystalline cellulose, a direct compression binder in a quality by design environment—A review. *International Journal of Pharmaceutics*, 1-2:64-72.

Torrado, J.J. & Augsburger, L.L. 2008. Tableting of multiparticulate modified release systems. (*In* Augsburger, L.L., *eds*. Pharmaceutical dosage forms: tablets. 3rd ed. New York: Informa Healthcare, Inc. p. 509-532).

Treesinchai, S., Puttipipatkhachorn, S., Pitaksuteepong, T. & Sungthongjeen, S. 2016. Development of curcumin floating tablets based on low density foam powder. *Asian Journal of Pharmaceutical Sciences*, 2:130-131.

Van de Laar, F.A., Lucassen, P.L., Akkermans, R.P., Van de Lisdonk, E.H., Rutten, G.E. & Van Weel, C. 2005. α-Glucosidase inhibitors for patients with type 2 diabetes. *Diabetes Care*, 28:154-163.

Van Wyk, B. 2008. A broad review of commercially important southern african medicinal plants. *Journal of Ethnopharmacology*, 119:342-355.

Van Wyk, B. & Wink, M. 2009. Medicinal plants of the world. 4th ed. South Africa: Briza publication. p. 118-119.

Veber, D.F., Johnson, S.R., Cheng, H.Y., Smith, B.R., Ward, K.W. & Kopple, K.D. 2002. Molecular properties that influence the oral bioavailability of drug candidates. *Journal of Medicinal Chemistry*, 45:2615-2623.

Vela-Soria, F., Jiménez-Díaz, I., Rodríguez-Gómez, R., Zafra-Gómez, A., Ballesteros, O., Navalón, A., Vílchez, J.L., Fernández, M.F. & Olea, N. 2011. Determination of benzophenones in human placental tissue samples by liquid chromatography–tandem mass spectrometry. *Journal of Talanta*, 85:1848-1855.

Vermaak, I., Viljoen, A.M. & Hamman, J.H. 2011a. Natural products in anti-obesity therapy. *Natural Product Reports*, 28:1493-1533.

Vermaak, I., Viljoen, A.M., Chen, W. & Hamman, J.H. 2011b. In vitro transport of the steroidal glycoside P57 from Hoodia gordonii across excised porcine intestinal and buccal tissue. *Phytomedicine*, 18:783-787.

Volpe, D.A. 2010. Application of method suitability for drug permeability classification. *American Association of Pharmaceutical Scientists*, 12:670-678.

WHO. 2010. Pharmaceutical excipients – an overview including considerations for paediatric. http://apps.who.int/prequal/trainingresources/pq_pres/workshop_China2010/english/22/002-Excipients.pdf. Date of access: 30 Jun. 2016.

WHO. 2016. Ending childhood obesity. http://apps.who.int/iris/bitstream/10665/204176/1/9789241510066_eng.pdf?ua=1 Date of access: 24 Jan. 2017.

York, P. 2007. Design and dosage forms. (*In* Aulton, M.E., *ed*. Pharmaceutics: the design and manufacture of medicines. 3rd ed. New York: Churchill Livingstone. p. 4-14).

Zhang, Y., Han, L., Ge, D., Liu, X., Liu, E., Wu, C., Gao, X. & Wang, T. 2013. Isolation, structural elucidation, MS profiling, and evaluation of triglyceride accumulation inhibitory effects of benzophenone C-glucosides from leaves of Mangifera indica L. *Journal of Agricultural and Food Chemistry*, 61:1884-1895.

Zhang, Y., Qian, Q., Ge, D., Li, Y., Wang, X., Chen, Q., Gao, X. & Wang, T. 2011. Identification of benzophenone C-glucosides from mango tree leaves and their inhibitory effect on triglyceride accumulation in 3T3-L1 adipocytes. *Journal of Agricultural and Food Chemistry*, 59:11526-11533.

Annexure A

CONGRESS POSTER & CERTIFICATES

In vitro evaluation of the enzyme inhibition and membrane permeation properties of benzophenones extracted from honeybush

Madelaine Raaths[1], Lissinda H. du Plessis[1], Christiaan J. Malherbe[2], Josias H. Hamman[1]

[1]Centre of Excellence for Pharmaceutical Sciences, North-West University, Potchefstroom, South Africa

[2]Post-Harvest and Wine Technology Division, Agricultural Research Council, Infruitec-Nietvoorbij, Stellenbosch, Cape Town

INTRODUCTION

One of the most enjoyable South African herbal teas with low tannin and no caffeine content is honeybush (*Cyclopia genistoides*) tea also familiar as "coastal tea", which emanates from the fynbos biome in the Eastern- and Western Cape region [1,2,3]. The honeybush plant is a woody shrub referred to as "the golden herb" mainly because it can be identified by its beautiful bright yellow flowers and trifoliate green leaves [4,5]. Some of the phytoconstituents present in the honeybush plant known as benzophenones and xanthones exhibited favourable biological activities that can contribute to prevent "diabesity" (diabetes and obesity) [6,7,8]. One mechanism of action against diabesity is enzyme (e.g. alpha-glucosidase and lipase) inhibition in the gastro-intestinal tract [9]. A multiple-unit pellet system (MUPS) can be produced by direct compression of beads into a tablet, which can be used for sustained drug release [10].

OBJECTIVES

To determine the inhibiting effects (i.e. α-glucosidase and lipase) of crude extracts, benzophenone rich fraction and xanthone enriched fraction from the honeybush (*Cyclopia genistoides*) plant on selected gastro-intestinal enzymes and to establish the bioavailability of the phytoconstituents present in honeybush from in vitro bi-directional transport to see whether the marker molecules present in honeybush permeate across the jejunum excised tissue of the pig. Moreover, to establish if a non-effervescent gastro-retentive MUPS dosage form to help produce a sustained release effect in the body to help with diseases such as "diabesity".

EXPERIMENTAL PROCEDURES

Preparation, extraction, fractionation and characterisation of honeybush extracts

Crude extracts and benzophenone and xanthone enriched fractions of honeybush were obtained through preliminary mini-scale extraction methods. The fractionations of phytomolecules were done with a XAD1180 polymeric resin whereafter they were chemically characterised by means of high performance liquid chromatography (HPLC) equipped with a diode-array detector (DAD). The analysis of selected marker molecules to determine their concentrations in the dissolution and transport samples was done with ultra-high performance liquid chromatography (UHPLC).

Enzyme inhibition

Fluorometric methods were utilized to determine the α-glucosidase and lipase enzyme activity of selected crude extracts (ARC188 and ARC189) and benzophenone as well as xanthone enriched fractions of honeybush.

Gastro-retentive drug delivery system development and characterisation

Non-effervescent floating MUPS gastro-retentive dosage forms were prepared with two bead formulations, each containing a low density polymeric excipient namely polypropylene (PP) or polystyrene divinylbenzene copolymer (PDC). The extrusion-spheronisation method was utilized for bead preparations. Thereafter, a multi-unit pellet system (MUPS) tablet was prepared through direct compression of the beads. The MUPS formulations were characterized by buoyancy, disintegration, friability, hardness, mass variation, content assay as well as dissolution studies.

***In vitro* bi-directional transport studies**

Bi-directional transport of the crude and rich fractions was determined in an *ex vivo* model where excised pig intestinal tissue was mounted in the Sweetana-Grass diffusion chamber apparatus. Solutions of the honeybush crude extracts as well as benzophenone and xanthone rich fractions were applied to the donor chambers and samples were withdrawn every 20 min for a total period of 2 h from the acceptor chambers. The samples were analysed by means of UHPLC and the apparent permeability coefficient values as well as efflux ratio values were calculated.

RESULTS AND DISCUSSION

The semi-logarithmic plots as well as the IC50 values of the honeybush crude extracts against α-glucosidase and lipase activity are shown in Figure 1 A-D. The ARC188 honeybush crude extract was more effective in terms of α-glucosidase and lipase inhibition activity than the ARC189 crude extract. Therefore, the ARC188 crude extract was chosen to be incorporated into a gastro-retentive MUPS dosage form. The dissolution profile of the marker molecules of honeybush extract showed a sustained release effect from the gastro-retentive MUPS formulations (Figure 2). Relative low transport across excised pig intestinal tissue was obtained for the marker molecules from both the honeybush crude extracts and the fractions. The relatively high efflux ratio (ER) values (> unity) confirmed that these marker molecules are susceptible to P-gp related efflux. This may indicate potential low bioavailability after oral administration, but this will potentially favour the enzyme inhibition effect of these molecules against enzymes in the lumen of the gastro-intestinal tract.

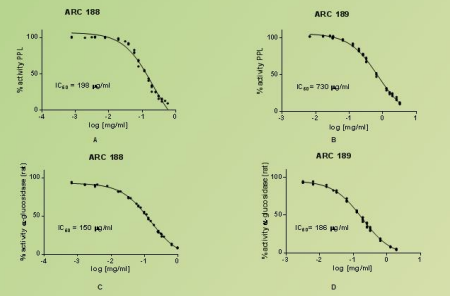

Figure 1: Semi-logarithmic plot of the percentage porcine pancreatic lipase activity as a function of concentration for A) ARC188 and B) ARC189 and of α-glucosidase inhibitory activity as a function of concentration for C) ARC188 and D) ARC189

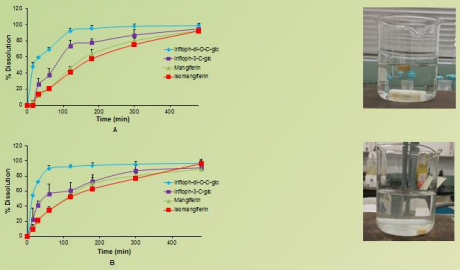

Figure 2: Percentage marker molecules released from MUPS tablets containing 50% w/w PP polymer (A) and 50% w/w PDC polymer (B) in 0.1 N HCl as a function of time and accompanying photographs showing the buoyance of each MUPS tablet after 24 hours

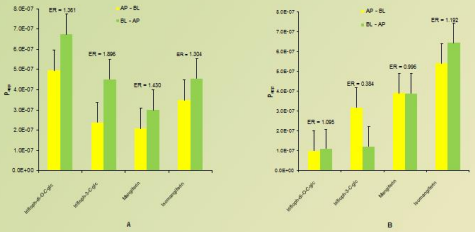

Figure 3: Apparent permeability coefficient (P_{app}) values for the bi-directional transport of marker molecules from the crude extract A) ARC188 and B) ARC189 with efflux ratio (ER) values indicated above the bar graphs

CONCLUSION

The moderate enzyme inhibition combined with the successful formulated gastro-retentive delivery system has the potential in preventing and alleviating diseases such as diabetes mellitus type 2 and obesity. The relatively low intestinal epithelial permeation of phytochemicals from honeybush may be beneficial in the treatment and prevention of "diabesity" due to the local enzyme inhibition action of honeybush phytochemicals in the gastrointestinal tract.

REFERENCES

[1] Iwu, M.M. 2014. Pharmacognostical profile of selected medicinal plants. Handbook of African medicinal plants. 2nd ed. Rosewood Drive, Danvers: Taylor & Francis Group, LLC. p. 199-202.
[2] Pheiffer, C., Dudhia, Z., Louw, J., Muller, C. & Joubert, E. 2013. *Cyclopia maculata* (honeybush tea) stimulates lipolysis in 3T3-L1 adipocytes. *Phytomedicine*, 20:1168-1171.
[3] SAHTA (South African Honeybush Tea Association). 2016. The honeybush plant. http://www.sahta.co.za/honeybush.html?layout=blog Date of access: 19 Sept. 2016.
[4] The Heights Tea Estate. 2016. Honeybush. http://www.heightsteaestate.co.za/ Date of access: 19 Sept. 2016.
[5] Van Wyk, B. & Wink, M. 2009. Medicinal plants of the world. South Africa: Briza Ltd. p. 119.
[6] Dudhia, Z., Louw, J., Muller, C., Joubert, E., De Beer, D., Kinnear, C. & Pheiffer, C. 2013. *Cyclopia maculata* and *Cyclopia subternata* (honeybush tea) inhibits adipogenesis in 3T3-L1 pre-adipocytes. *Phytomedicine*, 20:401-408.
[7] Kokotkiewicz, A., Bucinski, A. & Luczkiewicz, M. 2015. Xanthone, benzophenone and bioflavonoid accumulation in *Cyclopia genistoides* (L.) vent. (honeybush) shoot cultures grown on membrane rafts and in a temporary immersion system. *Journal of Plant Cell, Tissue and Organ Culture*, 120:373-378.
[8] Muller, C.J.F., Joubert, E., Gabuza, K., De Beer, D., Fey, S.J. & Louw, J. 2011. Assessment of the antidiabetic potential of an aqueous extract of honeybush (*Cyclopia intermedia*) in streptozotocin and obese insulin resistant Wistar rats. (*In* Rasooli, I., *ed.* Phytochemicals - bioactivities and impact on health. China, CN: InTech p. 313-332).
[9] You, Q., Chen, F., Wang, X., Jiang, Y. & Lin, S. 2012. Anti-diabetic activities of phenolic compounds in muscadine against alpha-glucosidase and pancreatic lipase. *LWT - Food Science and Technology*, 46:164-168.
[10] Martinez-Marcos, L. & Lanao, J.M. 2012. Multiple-unit pellet system for modified drug release. *Pharma & Drug Discovery*, 1:1-5.

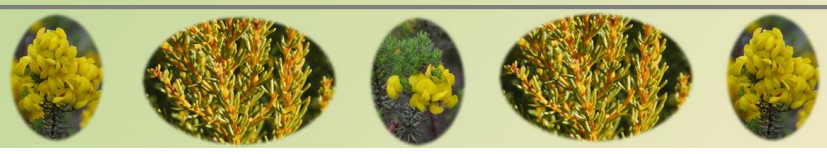

NORTH-WEST UNIVERSITY
YUNIBESITI YA BOKONE-BOPHIRIMA
NOORDWES-UNIVERSITEIT
POTCHEFSTROOM CAMPUS

ALL AFRICA CONGRESS
ON PHARMACOLOGY AND PHARMACY
2016

The All Africa Congress on Pharmacology and Pharmacy
hereby commends

MADELAINE RAATHS

As the

RUNNER-UP OF THE

BEST POSTER PRIZE - APSSA

held at Misty Hills Hotel and Conference Centre, Muldersdrift, Gauteng

5 – 7 October 2016

ALL AFRICA CONGRESS
ON PHARMACOLOGY AND PHARMACY
2016

The All Africa Congress on Pharmacology and Pharmacy
hereby commends

MADELAINE RAATHS

As the winner of the

SEPARATIONS PRIZE

FOR THE BEST POSTER WITH A CHROMATOGRAPHY ELEMENT

held at Misty Hills Hotel and Conference Centre, Muldersdrift, Gauteng

5 – 7 October 2016

NORTH-WEST UNIVERSITY
YUNIBESITI YA BOKONE-BOPHIRIMA
NOORDWES-UNIVERSITEIT

Private Bag X6001, Potchefstroom
South Africa 2520

Tel: (018) 299-4900
Faks: (018) 299-4910
Web: http://www.nwu.ac.za

Ethics Committee
Tel +27 18 299 4849
Email Ethics@nwu.ac.za

ETHICS APPROVAL OF PROJECT

The North-West University Research Ethics Regulatory Committee (NWU-RERC) hereby approves your project as indicated below. This implies that the NWU-RERC grants its permission that provided the special conditions specified below are met and pending any other authorisation that may be necessary, the project may be initiated, using the ethics number below.

Project title: Excised pig buccal and intestinal tissues as in vitro models for pharmacokinetic studies

Project Leader: Prof Sias Hamman

Ethics number: N W U - 0 0 0 2 5 - 1 5 - A 5
(Institution | Project Number | Year | Status)

Status: S = Submission; R = Re-Submission; P = Provisional Authorisation; A = Authorisation

Approval date: 2015-04-16 **Expiry date**: 2020-04-15

Special conditions of the approval (if any): None

General conditions:

While this ethics approval is subject to all declarations, undertakings and agreements incorporated and signed in the application form, please note the following:

- *The project leader (principle investigator) must report in the prescribed format to the NWU-RERC:*
  - *annually (or as otherwise requested) on the progress of the project,*
  - *without any delay in case of any adverse event (or any matter that interrupts sound ethical principles) during the course of the project.*
- *The approval applies strictly to the protocol as stipulated in the application form. Would any changes to the protocol be deemed necessary during the course of the project, the project leader must apply for approval of these changes at the NWU-RERC. Would there be deviated from the project protocol without the necessary approval of such changes, the ethics approval is immediately and automatically forfeited.*
- *The date of approval indicates the first date that the project may be started. Would the project have to continue after the expiry date, a new application must be made to the NWU-RERC and new approval received before or on the expiry date.*
- *In the interest of ethical responsibility the NWU-RERC retains the right to:*
  - *request access to any information or data at any time during the course or after completion of the project;*
  - *withdraw or postpone approval if:*
    - *any unethical principles or practices of the project are revealed or suspected,*
    - *it becomes apparent that any relevant information was withheld from the NWU-RERC or that information has been false or misrepresented,*
    - *the required annual report and reporting of adverse events was not done timely and accurately,*
    - *new institutional rules, national legislation or international conventions deem it necessary.*

The Ethics Committee would like to remain at your service as scientist and researcher, and wishes you well with your project. Please do not hesitate to contact the Ethics Committee for any further enquiries or requests for assistance.

Yours sincerely

Linda du Plessis

Digitally signed by Linda du Plessis
DN: cn=Linda du Plessis, o=NWU, Vaal Triangle Campus, ou=Vice-Rector: Academic, email=linda.duplessis@nwu.ac.za, c=US
Date: 2015.04.20 20:35:13 +02'00'

Prof Linda du Plessis
Chair NWU Research Ethics Regulatory Committee (RERC)

Annexure B

ENZYME INHIBITION

Figure B.1: Raw data of porcine pancreatic lipase results of ARC188 crude and rich fractions

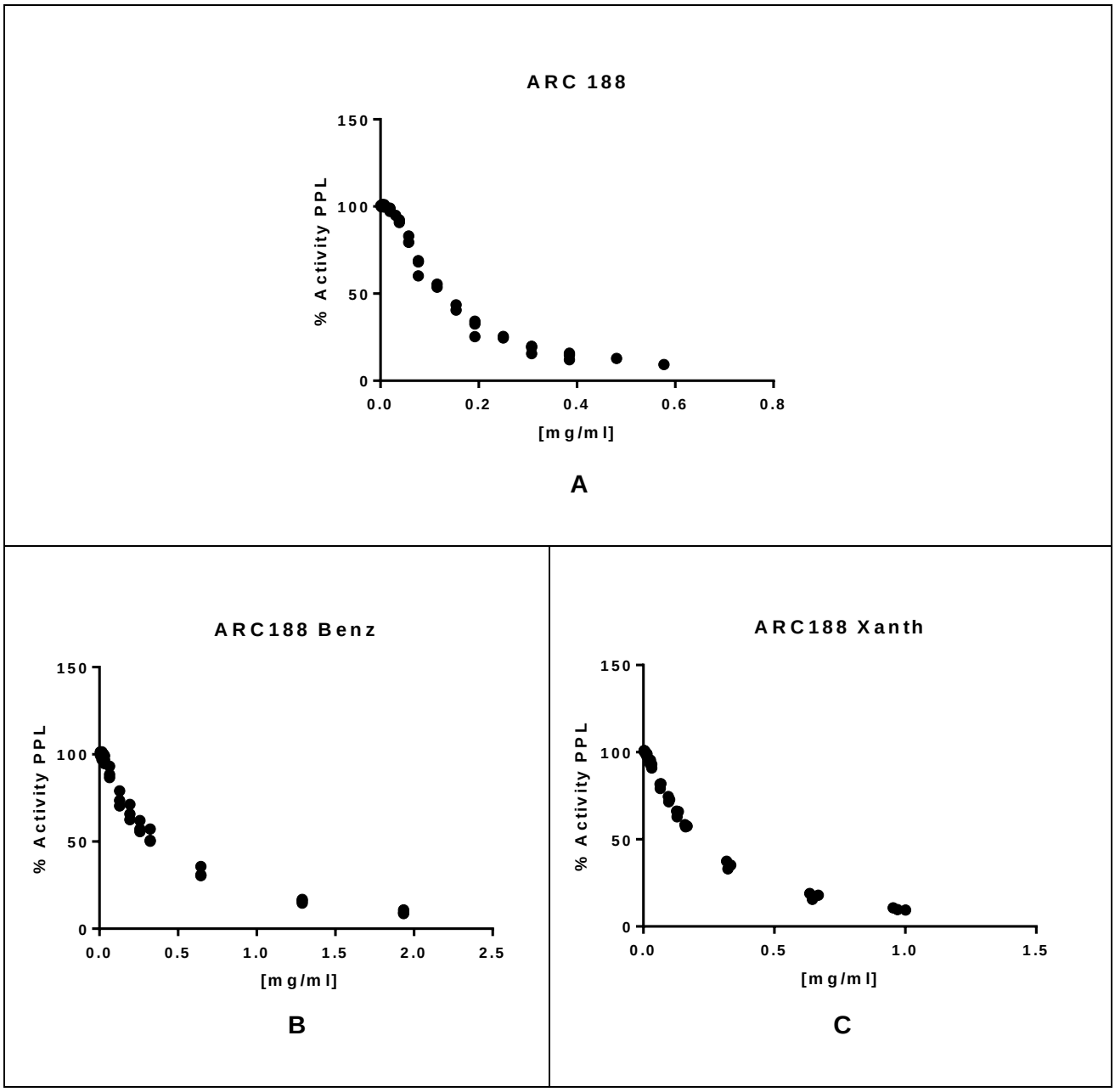

Figure B.2: Raw data of porcine pancreatic lipase results of ARC189 crude and rich fractions

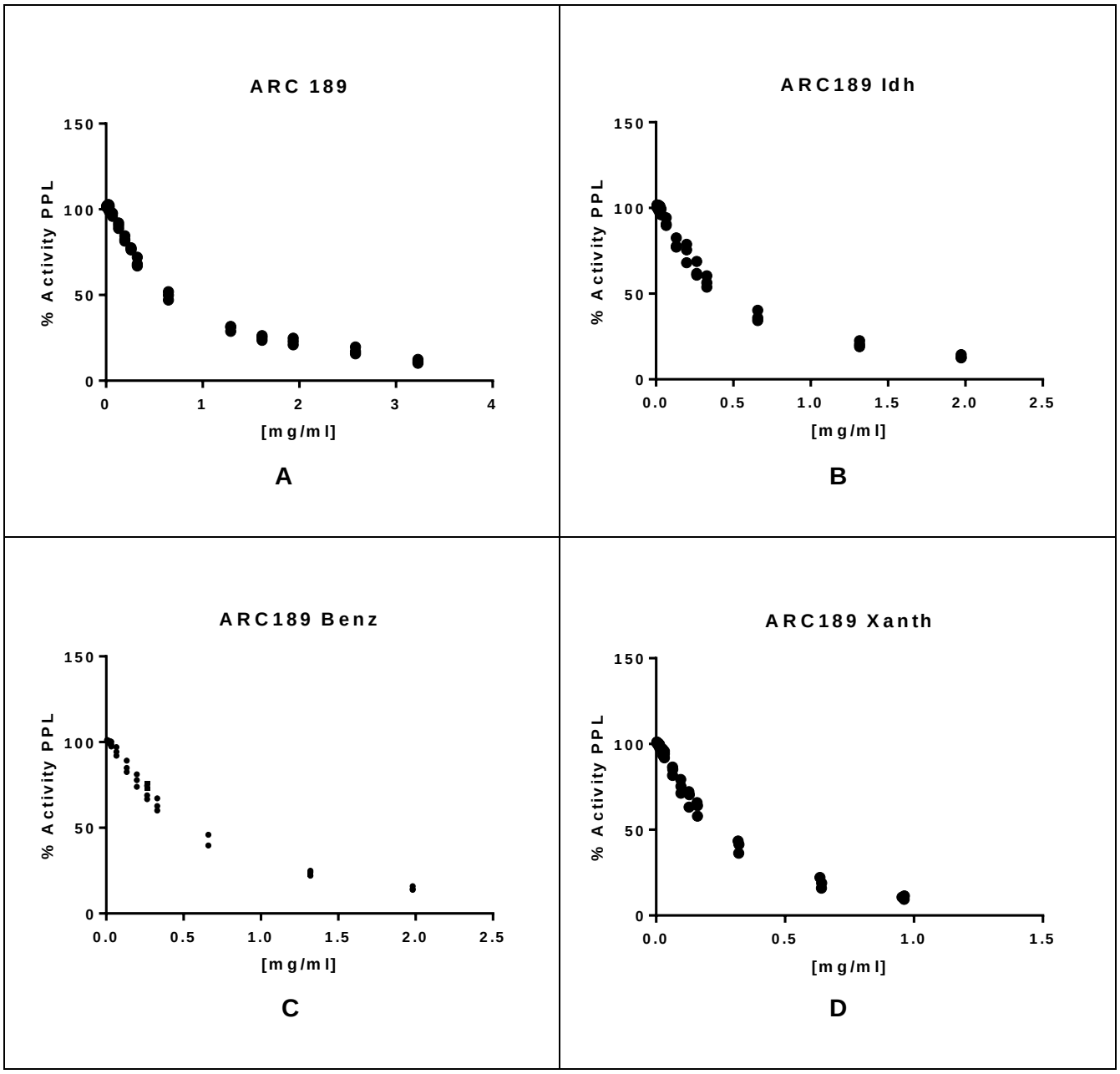

Figure B.3: Raw data of α-glucosidase of RIAP results of ARC188 crude and rich fractions

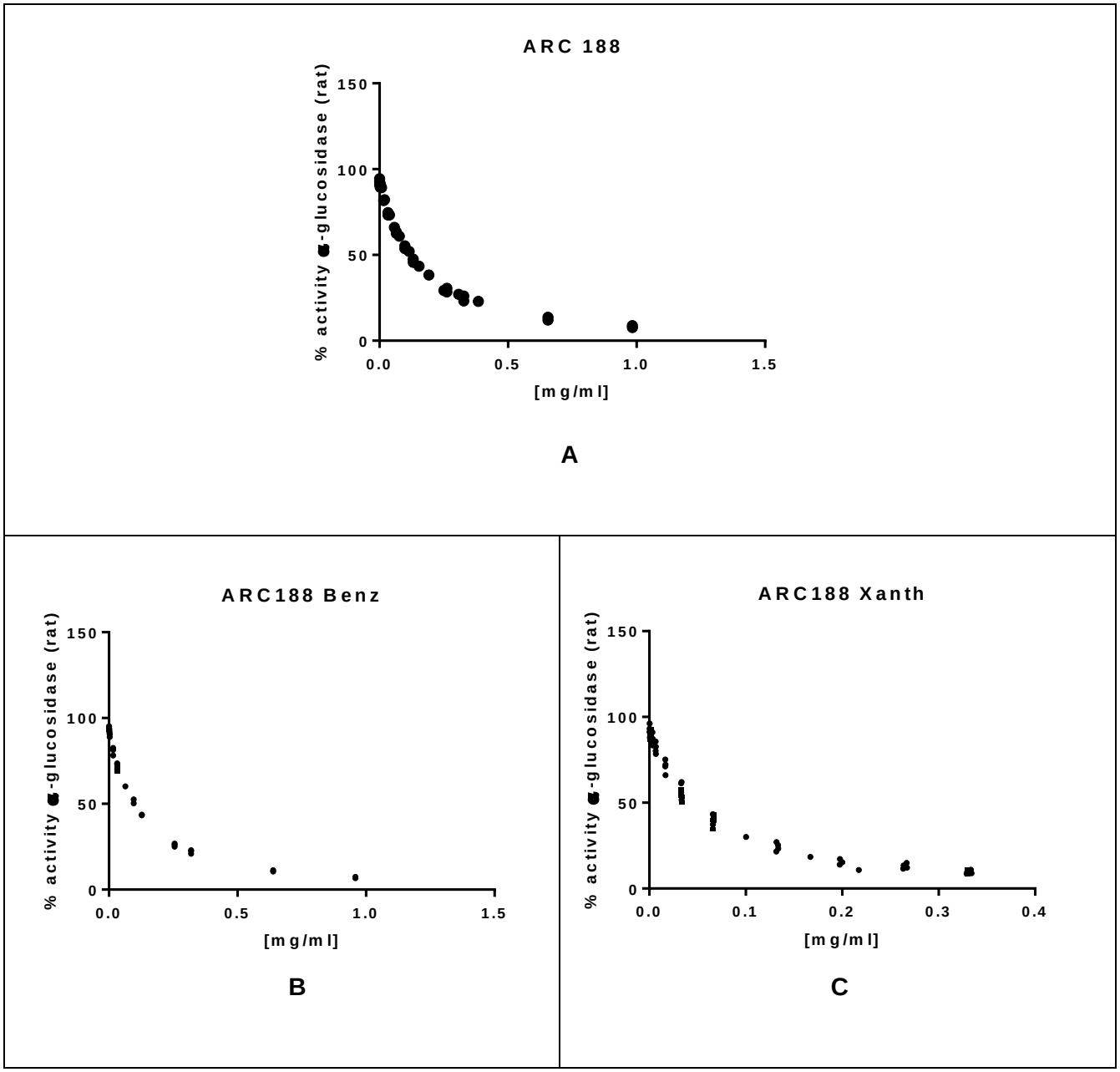

Figure B.4: Raw data of α-glucosidase of RIAP results of ARC189 crude and rich fractions

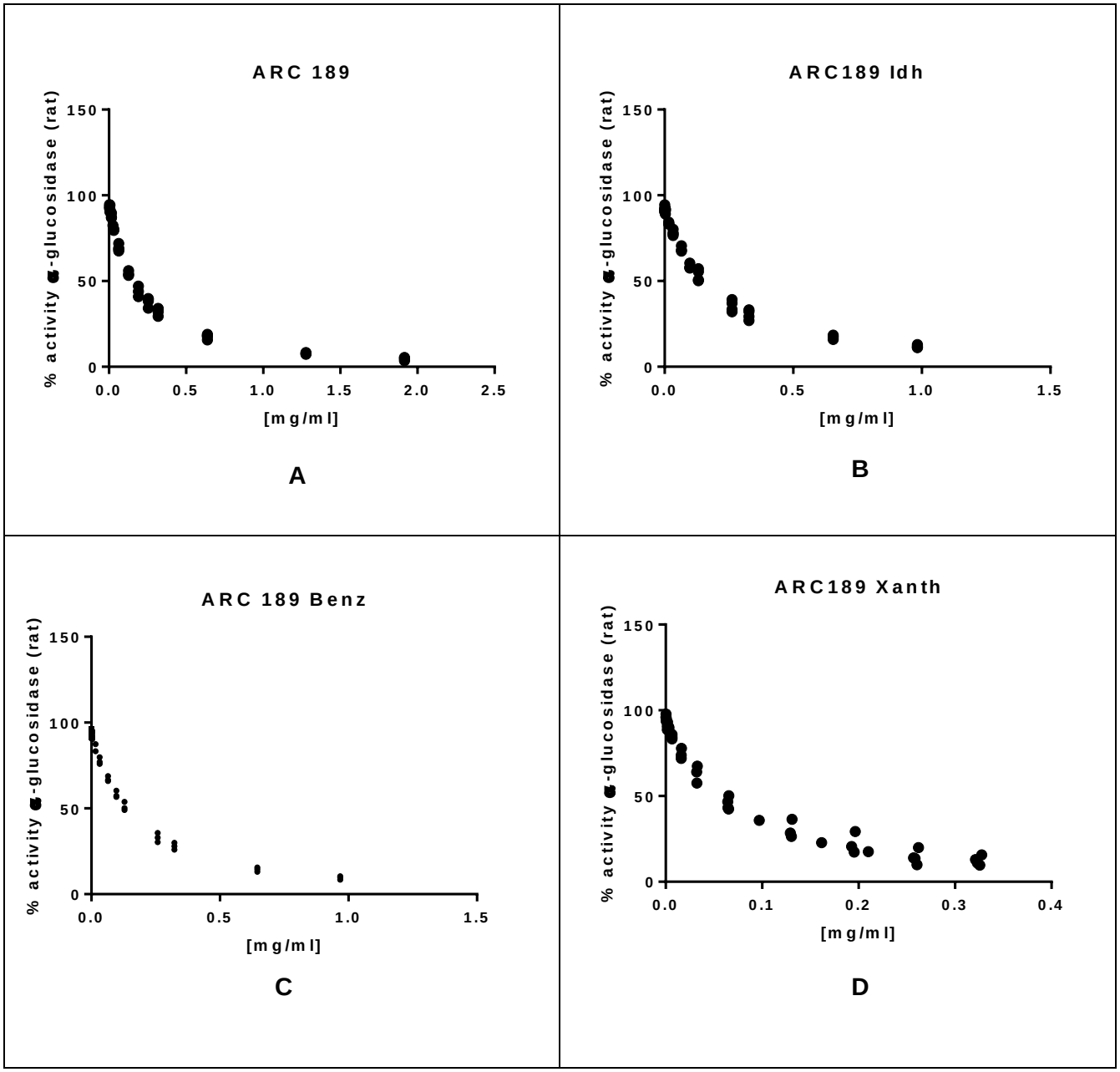

Annexure C

In vitro transport data

EXPERIMENTAL DATA

C.1. The transepithelial electrical resistance (TEER) values of the crude and rich fractions of honeybush (*C. genistoides*)

Table C.1.1: TEER value of ARC188 crude extract

TEER value Ω		
Side of administration	**0 min**	**120 min**
A-B	48	46
A-B	46	45
A-B	42	40
B-A	51	40
B-A	55	51
B-A	48	40

Table C.1.2: TEER value of ARC188 Xanth rich fraction

TEER value Ω		
Side of administration	**0 min**	**120 min**
A-B	46	38
A-B	49	41
A-B	51	45
B-A	47	39
B-A	41	32
B-A	60	46

Table C.1.3: TEER value of ARC189 crude extract

TEER value Ω		
Side of administration	**0 min**	**120 min**
A-B	59	37
A-B	40	37
A-B	51	49
B-A	54	43
B-A	43	52
B-A	49	45

Table C.1.4: TEER value of ARC189 IdH rich fraction

TEER value Ω		
Side of administration	**0 min**	**120 min**
A-B	56	43
A-B	56	42
A-B	46	38
B-A	52	44
B-A	51	41
B-A	57	44

Table C.1.5: TEER value of ARC189 Xanth rich fraction

TEER value Ω		
Side of administration	**0 min**	**120 min**
A-B	42	33
A-B	41	26
A-B	41	44
B-A	44	26
B-A	48	42
B-A	44	33

C.2. Apparent permeability coefficient (P_{app}) calculation results of the crude and rich fractions of honeybush (*C. genistoides*)

Table C.2.1: P_{app} values of ARC188

Cell	P_{app} (x 10^{-7}) cm/s				Efflux Ratio (ER)
	AP – BL	STD*	BL – AP	Stdev	
IDG	4.95	4.51	6.74	1.10	1.36
I3G	2.38	4.69	4.52	8.84	1.89
Mangiferin	2.09	2.72	2.99	9.58	1.43
Isomangiferin	3.49	4.22	4.55	1.14	1.30

Table C.2.2: P_{app} values of ARC189

Cell	Average Papp (x 10^{-7})				Efflux Ratio (ER)
	AP – BL	Stdev	BL – AP	Stdev	
IDG	1.00102E-07	1.48E-07	1.09628E-07	5.07E-07	1.095160044
I3G	3.18E-07	4.49E-07	1.21902E-07	2.17E-07	0.383701984
Mangiferin	3.92E-07	1.82E-07	3.90E-07	8.91E-07	0.996211029
Isomangiferin	5.40E-07	1.80E-07	6.44E-07	8.31E-07	1.192138675

Table C.2.3: P_{app} values of ARC189 IdH

Cell	Average Papp (x 10^{-7})				Efflux Ratio (ER)
	AP – BL	Stdev	BL – AP	Stdev	
IDG	1.692E-07	1.408E-07	2.556E-07	1.483E-07	1.510849423

Table C.2.4: P_{app} values of ARC188 Xanth

Cell	Average Papp (x 10^{-7})				Efflux Ratio (ER)
	AP – BL	Stdev	BL – AP	Stdev	
Mangiferin	5.31841E-07	6.27E-07	8.82511E-07	1.52199E-07	1.659351173
Isomangiferin	4.57218E-07	3.18E-07	7.94867E-07	1.44965E-07	1.738486187

Table C.2.5: P_{app} values of ARC189 Xanth

Cell	Average Papp (x 10^{-7})				Efflux Ratio (ER)
	AP – BL	Stdev	BL – AP	Stdev	
Mangiferin	6.42603E-07	4.91E-07	8.04284E-07	5.93E-07	1.251602577
Isomangiferin	7.21007E-07	5.09E-07	8.74948E-07	6.11E-07	1.213508463

Annexure D

Formulation section

Dose calculations

D.1 Dosage form

A person on average take 2.5g honeybush tea plant material in a cup of 250ml water, in other words 10 g plant material in 1000ml water.

Thus:

$$\frac{X\ g\ = 100\ ml\ water}{2.5\ g = 1000\ ml\ water}$$

X g = 0.25g/100 ml

= 0.25 % solid extract out of 1% plant material

Therefore: 2.5 g solid extract for each 10 g plant material

$\frac{2.5\ g}{10\ g} \times 100$ = 25% yield

$$25\%w/w = \frac{X\ g = 2.5\ g}{25\ g = 100\ g}$$

= 0.625 g of ARC188 per final batch of 50g beads

D.2 Dissolution

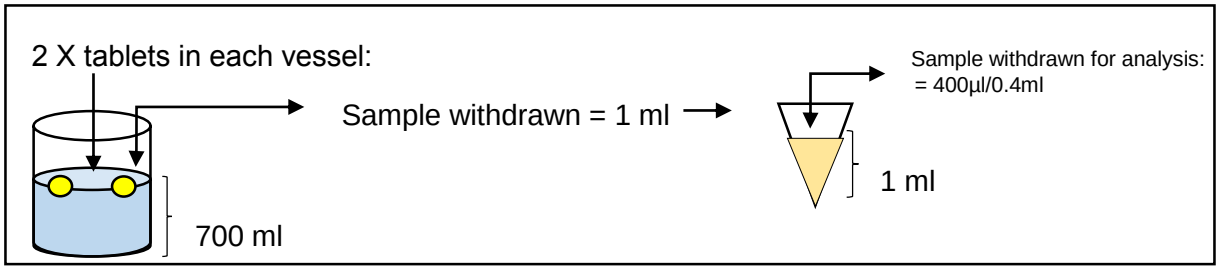

Figure D.2.1: Illustration of the dissolution sample and withdrawal

Thus: at 100%:

$$\frac{X\ mg\ =\ 0.4\ ml\ water}{0.333\ mg = 1000\ ml\ water}$$

X mg = 0.0001332 mg

$$\frac{X\ mg\ =\ 1\ ml\ water}{0.0001332\ mg = 0.4\ ml\ water}$$

X mg = 0.000333 mg

$$\frac{X\ mg\ =\ 700\ ml\ water}{0.000333\ mg = 1\ ml\ water}$$

X mg = 0.2331 mg from 2 tablets and 0.117 mg from 1 tablet

D.3 Assay

1 tablet was dissolved in 100 ml solution:

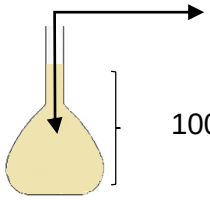

Table D.3.1: The assay results obtained from the UHPLC analysis

Assay UHPLC	**µg/ml mg compound / L undiluted sample**			
Sample	**IDG**	**I3G**	**Mangiferin**	**Isomangiferin**
A1 PP	0.664	0.462	1.545	0.463
A2 PP	0.794	0.733	1.552	0.468
A3 PP	0.890	0.813	0.308	0.175
Average	0.783	0.669	1.135	0.369
A1 PDC	0.828	0.879	0.442	0.200
A2 PDC	0.836	0.935	0.572	0.233
A3 PDC	0.736	0.770	0.506	0.205
Average	0.800	0.861	0.507	0.213

Sample	**Massa van tab (g)**
A1 PP	0.370
A2 PP	0.390
A3 PP	0.380
Average	0.380
A1 PDC	0.390
A2 PDC	0.380
A3 PDC	0.380
Average	0.383

Table D.3.2: The quantities of selected benzophenones and xanthones in the different crude extracts and fractions as measured by means of HPLC-DAD:

Crude extract and fractions	**(g/100g powder)**				
	Benzophenones			**Xanthones**	
	IDG	**M3G**	**I3G**	**Mangiferin**	**Isomangiferin**
ARC188	2.214	1.101	3.885	13.811	3.193
ARC188 Benz	23.267	11.384	28.272	0	0
ARC188 Xanth	0	0	5.804	54.016	14.352
ARC189	4.902	0.254	0.807	11.622	1.667
ARC189 IdH	74.966	2.389	0	0	0
ARC189 Benz	3.048	4.4	16.602	0	0
ARC189 Xanth	0	0	2.233	53.792	7.869

D.4.1 POLYPROPYLENE POLYMER

IDG

Average IDG from UHPLC analysis:

$$\frac{X\ \mu g = 100\ 000\ \mu l}{0.783\ \mu g = 1000\ \mu l}$$

= 78.3 µg per tablet

Formulation (theoretical):

$$\frac{x\ g\ (ARC188) = 0.38\ g\ (beads\ compressed\ into\ a\ MUPS)}{0.625\ g\ (ARC188) = 50\ g\ (powder\ of\ beads)}$$

x = 0.00475304 g / 4.75 mg

IDG:

$$\frac{x\ g\ (IDG) = 0.004753\ g\ (ARC188)}{2.214\ g\ (IDG) = 100\ g\ (ARC188)}$$

X = 0.000105 g / 105.23 µg

Thus:

$$\frac{Actual}{Theoretical}$$

$$\frac{78.3\ \mu g}{105.23\ \mu g} * 100$$

= 74.42%

I3G

Average I3G from UHPLC analysis:

$$\frac{X\ \mu g = 100\ 000\ \mu l}{0.669\ \mu g = 1000\ \mu l}$$

= 66.9 µg per tablet

Formulation (theoretical):

$$\frac{x\ g\ (ARC188) = 0.38\ g\ (beads\ compressed\ into\ a\ MUPS)}{0.625\ g\ (ARC188) = 50\ g\ (powder\ of\ beads)}$$

x = 0.00475304 g / 4.75 mg

I3G:

$$\frac{\text{x g (I3G) = 0.004753 g (ARC188)}}{\text{3.885 g (I3G) = 100 g (ARC188)}}$$

X = 0.0001846 g / 184.626 µg

Thus:

$$\frac{\text{Actual}}{\text{Theoretical}}$$

$$\frac{\text{66.9 µg}}{\text{184.626 µg}} * 100$$

= 36.24%

Mangiferin

Average mangiferin from UHPLC analysis:

$$\frac{\text{X µg = 100 000 µl}}{\text{1.135 µg = 1000 µl}}$$

= 113.5 µg per tablet

Formulation (theoretical):

$$\frac{\text{x g (ARC188) = 0.38 g (beads compressed into a MUPS)}}{\text{0.625 g (ARC188) = 50 g (powder of beads)}}$$

x = 0.00475304 g / 4.75 mg

Mangiferin:

$$\frac{\text{x g (mangiferin) = 0.004753 g (ARC188)}}{\text{13.811 g (mangiferin) = 100 g (ARC188)}}$$

X = 0.000656 g / 656.337 µg

Thus:

$$\frac{\text{Actual}}{\text{Theoretical}}$$

$$\frac{113.5\ \mu g}{656.337\ \mu g} * 100$$

= 17.29%

Isomangiferin

Average isomangiferin from UHPLC analysis:

$$\frac{X\ \mu g = 100\ 000\ \mu l}{0.369\ \mu g = 1000\ \mu l}$$

= 36.9 µg per tablet

Formulation (theoretical):

$$\frac{x\ g\ (ARC188) = 0.38\ g\ (beads\ compressed\ into\ a\ MUPS)}{0.625\ g\ (ARC188) = 50\ g\ (powder\ of\ beads)}$$

x = 0.00475304 g / 4.75 mg

Isomangiferin:

$$\frac{x\ g\ (isomangiferin) = 0.004753\ g\ (ARC188)}{3.193\ g\ (isomangiferin) = 100\ g\ (ARC188)}$$

X = 0.0001517 g / 151.74 µg

Thus:

$$\frac{Actual}{Theoretical}$$

$$\frac{36.9\ \mu g}{151.74\ \mu g} * 100$$

= 24.32%

D.4.2 PDC

IDG

Average IDG from UHPLC analysis:

$$\frac{X\ \mu g = 100\ 000\ \mu l}{0.800\ \mu g = 1000\ \mu l}$$

= 80 µg per tablet

Formulation (theoretical):

$$\frac{x\ g\ (ARC188) = 0.383\ g\ (beads\ compressed\ into\ a\ MUPS)}{0.625\ g\ (ARC188) = 50\ g\ (powder\ of\ beads)}$$

x = 0.0047875 g / 4.79 mg

IDG:

$$\frac{x\ g\ (IDG) = 0.0047875\ g\ (ARC188)}{2.214\ g\ (IDG) = 100\ g\ (ARC188)}$$

X = 0.0001059 g / 105.995 µg

Thus:

$$\frac{Actual}{Theoretical}$$

$$\frac{80\ \mu g}{105.995\ \mu g} * 100$$

= 75.47%

I3G

Average I3G from UHPLC analysis:

$$\frac{X\ \mu g = 100\ 000\ \mu l}{0.861\ \mu g = 1000\ \mu l}$$

= 86.1 µg per tablet

Formulation (theoretical):

$$\frac{x\ g\ (ARC188) = 0.383\ g\ (beads\ compressed\ into\ a\ MUPS)}{0.625\ g\ (ARC188) = 50\ g\ (powder\ of\ beads)}$$

x = 0.0047875 g / 4.7875 mg

I3G:

$$\frac{\text{x g (I3G)} = \text{0.0047875 g (ARC188)}}{\text{3.885 g (I3G)} = \text{100 g (ARC188)}}$$

X = 0.00018599 g / 185.994 µg

Thus:

$$\frac{\text{Actual}}{\text{Theoretical}}$$

$$\frac{\text{86.1 µg}}{\text{185.994 µg}} * 100$$

= 46.29%

Mangiferin

Average mangiferin from UHPLC analysis:

$$\frac{\text{X µg} = \text{100 000 µl}}{\text{0.507 µg} = \text{1000 µl}}$$

= 50.7 µg per tablet

Formulation (theoretical):

$$\frac{\text{x g (ARC188)} = \text{0.383 g (beads compressed into a MUPS)}}{\text{0.625 g (ARC188)} = \text{50 g (powder of beads)}}$$

x = 0.0047875 g / 4.7875 mg

Mangiferin:

$$\frac{\text{x g (mangiferin)} = \text{0.0047875 g (ARC188)}}{\text{13.811 g (mangiferin)} = \text{100 g (ARC188)}}$$

X = 0.000661 g / 661.202 µg

Thus:

$$\frac{\text{Actual}}{\text{Theoretical}}$$

$$\frac{50.7\ \mu g}{656.337\ \mu g} * 100$$

= 7.72%

Isomangiferin

Average isomangiferin from UHPLC analysis:

$$\frac{X\ \mu g = 100\ 000\ \mu l}{0.213\ \mu g = 1000\ \mu l}$$

= 21.3 µg per tablet

Formulation (theoretical):

$$\frac{x\ g\ (ARC188) = 0.383\ g\ (beads\ compressed\ into\ a\ MUPS)}{0.625\ g\ (ARC188) = 50\ g\ (powder\ of\ beads)}$$

x = 0.0047875 g / 4.7875 mg

Isomangiferin:

$$\frac{x\ g\ (isomangiferin) = 0.0047875\ g\ (ARC188)}{3.193\ g\ (isomangiferin) = 100\ g\ (ARC188)}$$

X = 0.0001528 g / 152.865 µg

Thus:

$$\frac{Actual}{Theoretical}$$

$$\frac{21.3\ \mu g}{152.865\ \mu g} * 100$$

= 13.93%

D.5 MUPS tablet tests

Table D.5.1: MUPS PDC polymer angle of repose and flow rate test

PDC polymer					
Tablet tests					
Angle of Repose	**Value 1**	**Value 2**	**Value 3**	**Average**	**Stdev**
h (height of the cone) (cm)	4.000	4.000	4.000	4.000	0.000
r (radius of the cone) (cm)	4.800	5.000	5.500	5.100	0.294
h/r	0.833	0.800	0.727	0.787	0.044
Angle Of Repose (Tan-1 h/r)	**39.806**	**38.660**	**36.027**	**38.164**	1.582
Flow rate	**Weight of sample beads (g)**	**Flow time of a pre-defined sample (s)**	**Flow time of a pre-weight sample (g/s)**	**Average**	**Stdev**
Replicate 1	20.005	1.100	18.200	20.005	0.000
Replicate 2	20.005	1.100	18.200	1.100	0.000
Replicate 3	20.005	1.100	18.200	18.200	0.000

Table D.5.2: MUPS PDC polymer hardness, diameter, thickness and friability tests

PDC polymer						
Tablet tests						
Tablet number	**Hardness (n=10)**	**Tablet weight (n=10) (mg)**	**Thickness (n=10)**	**Diameter (n=10)**	**DT (n=6)**	**Friability (n=10)**
1	23	390	5.17	10.18		3.820
2	23	370	5.16	10.21		3.810
3	35	380	5.20	10.09		
4	27	380	5.24	10.17		
5	33	370	5.24	10.26		
6	40	360	5.41	10.13		
7	34	380	5.23	10.18		
8	22	390	4.58	10.02		
9	26	390	4.61	10.05		
10	40	390	5.37	10.10		
Av	30.300	380.000	5.121	10.139	6min en 23s	0.262
Min	22.000	360.000	4.580	10.020		
Max	40.000	390.000	5.410	10.260		
Stdev	6.961	10.541	0.289	0.075		
%RSD		2.774				

Table D.5.3: MUPS PP polymer angle of repose and flow rate test

PP polymer					
Tablet tests					
Angle of Repose (beads)	**Replicate 1**	**Replicate 2**	**Replicate 3**	**Average**	**Stdev**
h (height of the cone) (cm)	4.000	4.000	4.000	4.000	0.000
r (radius of the cone) (cm)	5.000	5.500	5.500	5.333	0.236
h/r	0.800	0.727	0.727	0.752	0.034
Angle Of Repose (Tan-1 h/r)	**38.660**	**36.027**	**36.027**	**36.905**	1.241
Flow rate (beads)	**Weight of sample beads (g)**	**Flow time of a pre-defined sample (s)**	**Flow time of a pre-weight sample (g/s)**	**Average**	**Stdev**
Replicate 1	20.001	1.100	18.200	20.001	0.000
Replicate 2	20.001	1.100	18.200	1.100	0.000
Replicate 3	20.001	1.100	18.200	18.200	0.000

Table D.5.4: MUPS PP polymer hardness, diameter, thickness and friability tests

PP polymer						
Tablet tests						
Tablet number	**Hardness (Newton) (n=10)**	**Tablet weight (n=10) (mg)**	**Thickness (mm) (n=10)**	**Diameter (mm) (n=10)**	**DT (n=6)**	**Friability (n=10) (g)**
1	22	380	5.71	10.12		3.760
2	24	380	5.88	10.09		3.740
3	25	390	5.83	10.08		
4	22	370	5.70	10.11		
5	22	360	5.82	10.17		
6	21	380	5.73	10.10		
7	21	360	5.88	10.18		
8	23	370	5.84	10.11		
9	20	380	5.73	10.10		
10	27	370	5.86	10.11		
Av	22.700	374.000	5.798	10.117	3 min en 30s	0.532
Min	20.000	360.000	5.700	10.080		
Max	27.000	390.000	5.880	10.180		
Stdev	2.111	9.661	0.072	0.033		
%RSD		2.58				

Table D.5.5: The f_1 and f_2 fit factors of IDG rich fraction

IDG						f_1 = 10.417
Time	**Batch 1 PP**	**Batch 2 PDC**	**ABS(R-T)**	**$(R-T)^2$**		f_2 = 50.586
0	0	0	0	0		
15.0	47.7	54.1	6.354225	40.37618		
30.0	59.2	72.7	13.53154	183.1025		
60.0	69.5	90.0	20.43272	417.4959		Criterion:
120.0	92.4	92.6	0.261072	0.068159		f1<15
180.0	95.4	94.2	1.182236	1.397683		f2>50
300.0	98.2	95.9	2.332511	5.44061		
480	98.94104701	96.99906307	1.941984	3.771302		
	99.94116928	97.80700763	2.134162	4.554646		

Table D.5.6: The f_1 and f_2 fit factors of I3G rich fraction

I3G						f_1 = 27.187
Time	**Batch 1 PP**	**Batch 2 PDC**	**ABS(R-T)**	**$(R-T)^2$**		f_2 = 43.029
0	0	0	0	0		
15.0	0.0	22.2	22.16055	491.0898		
30.0	25.6	41.5	15.83927	250.8825		
60.0	37.3	56.3	18.94592	358.9479		Criterion:
120.0	74.0	60.9	13.12511	172.2684		f1<15
180.0	78.0	72.7	5.241554	27.47389		f2>50
300.0	87.1	86.9	0.234035	0.054772		
480	95.00461514	91.04286601	3.961749	15.69546		
	98.37107015	95.74622594	2.624844	6.889807		

Table D.5.7: The f_1 and f_2 fit factors of mangiferin rich fraction

Mangiferin						f_1 = 21.928
Time	**Batch 1 PP**	**Batch 2 PDC**	**ABS(R-T)**	**$(R-T)^2$**		**f_2 = 54.695**
0	0	0	0	0		
15.0	3.9	11.1	7.233947	52.32999		
30.0	11.8	19.9	8.156329	66.52571		
60.0	20.3	34.4	14.14513	200.0848		Criterion:
120.0	46.0	54.5	8.501895	72.28221		f1<15
180.0	64.0	70.4	6.368969	40.56376		f2>50
300.0	80.0	80.5	0.462733	0.214122		
480	92.89151776	89.0862392	3.805279	14.48014		
	99.35979508	98.4825787	0.877216	0.769509		

Table D.5.8: The f_1 and f_2 fit factors of isomangiferin rich fraction

Isomangiferin						f_1 = 26.243
Time	**Batch 1 PP**	**Batch 2 PDC**	**ABS(R-T)**	**$(R-T)^2$**		**f_2 = 53.203**
0	0	0	0	0		
15.0	0.0	9.5	9.49386	90.13344		
30.0	14.2	21.6	7.46855	55.77928		
60.0	20.7	34.2	13.5312	183.0947		Criterion:
120.0	40.8	52.3	11.4996	132.2427		f1<15
180.0	57.6	63.1	5.51694	30.43665		f2>50
300.0	75.4	76.8	1.46816	2.155496		
480	92.39766082	96.63993891	4.24227	17.99692		
	100.877193	102.4054983	1.52830	2.335717		

Table D.5.9: The dissolution data of IDG rich fraction for PP MUPS tablet

D1							
Time	**Irifloph-di-O,C-glc (mg/L)**	**Corr 1 (mg/1000 ml)**	**Corr 2 (mg/1000 ml)**	**Conc in 0.4 ml (sample)**	**Conc in 1 ml (sample)**	**Cumulative mg**	**% Dissolution**
0	**0**	**0**	**0**	**0**	**0**	**0**	**0**
15	0.140	0.14	0.14	0.000056	0.00014	0.098	41.96685929
30	0.190	0.189864465	0.189936244	0.0000759749	0.000189936	0.132955371	56.93591165
60	0.223	0.223447906	0.223496237	0.00008.93985	0.000223496	0.156447366	66.99596508
120	0.308	0.308745731	0.308868147	0.000123547	0.000308868	0.216207703	92.58732905
180	0.318	0.318862339	0.318877268	0.000127551	0.000318877	0.223214087	95.58769587
300	0.325	0.325931785	0.325942529	0.000130377	0.000325943	0.22815977	97.70560185
480	0.327	0.327117725	0.327120073	0.000130848	0.00032712	0.228984051	98.05858618
100%	0.333	0.333586643	0.333596563	0.000133439	0.000333597	0.233517594	100
D2							
Time	**Irifloph-di-O,C-glc (mg/L)**	**Corr 1 (mg/1000 ml)**	**Corr 2 (mg/1000 ml)**	**Conc in 0.4 ml (sample)**	**Conc in 1 ml (sample)**	**Cumulative mg Iri-O,C**	**% Dissolution**
0	**0.000**	**0**	**0**	**0**	**0**	**0**	**0**
15	0.183	0.18319766	0.18319766	0.00007327	0.00018319	0.12823836	54.9159342
30	0.198	0.19874557	0.19876782	0.00007950	0.00019876	0.13913747	59.5832941
60	0.233	0.23286739	0.23291658	0.00009316	0.00023291	0.16304161	69.8198397
120	0.319	0.31934192	0.31946603	0.00012778	0.00031946	0.22362622	95.7641880
180	0.332	0.33239986	0.33241901	0.00013296	0.00033241	0.23269331	99.6470156
300	0.341	0.34123730	0.34125059	0.00013651	0.00034125	0.23887541	102.294398
480	0.342	0.34242576	0.34242814	0.00013697	0.00034242	0.23969969	102.647382
100%	0.345	0.34536709	0.34537199	0.00013814	0.00034537	0.24176039	103.529843
D3							
Time	**Irifloph-di-O,C-glc (mg/L)**	**Corr 1 (mg/1000 ml)**	**Corr 2 (mg/1000 ml)**	**Conc in 0.4 ml (sample)**	**Conc in 1 ml (sample)**	**Cumulative mg Iri-O,C**	**% Dissolution**
0	**0.000**	**0**	**0**	**0**	**0**	**0**	**0**
15	0.155	0.1546432	0.1546432	0.00006.18573	0.0001546	0.1082502	46.356344
30	0.203	0.2034082	0.2034780	0.00008.13912	0.0002035	0.1424346	60.995232
60	0.239	0.2393414	0.2393931	0.00009.57572	0.0002394	0.1675752	71.761254
120	0.295	0.2958339	0.2959152	0.000118366	0.0002959	0.2071406	88.704501
180	0.303	0.3035577	0.3035692	0.000121428	0.0003036	0.2124984	90.998900
300	0.315	0.3159151	0.3159334	0.000126373	0.0003159	0.2211534	94.705235
480	0.320	0.3206362	0.320643583	0.000128257	0.000320644	0.224450508	96.11717236
100%	0.321	0.3212309	0.321232355	0.000128493	0.000321232	0.224862648	96.29366453

Table D.5.9.1: The average % dissolution data and standard deviation of IDG rich fraction for PP MUPS tablet

Average:	Time	% Dissolution	Stdev
	0	**0**	**0**
	15	47.74637904	5.377036646
	30	59.17147908	1.682599783
	60	69.52568611	1.956508505
	120	92.35200617	2.886904504
	180	95.4112037	3.532783619
	300	98.23507835	3.120802055
	480	98.94104701	2.737999742
		99.94116928	2.954450499

Table D.5.10: The dissolution data of I3G rich fraction for PP MUPS tablet

D1							
Time	**Irifloph-3-C-glc (mg/L)**	**Corr 1 (mg/1000 ml)**	**Corr 2 (mg/1000 ml)**	**Conc in 0.4 ml (sample)**	**Conc in 1 ml (sample)**	**Cumulative mg (Iri-3-C-glc)**	**% Dissolution**
0	**0.000**	**0**	**0**	**0**	**0**	**0**	**0**
15	0.000	0	0	0	0	0	0
30	0.155	0.154883	0.155105	0.0000620	0.0001551	0.10857352	36.0373547
60	0.211	0.211579	0.211660	0.0000847	0.0002117	0.14816189	49.1773888
120	0.344	0.344210	0.344400	0.0001378	0.0003444	0.24108002	80.0184606
180	0.353	0.353267	0.353281	0.0001413	0.0003533	0.24729638	82.0817717
300	0.373	0.373816	0.373846	0.0001495	0.0003739	0.26169214	86.8599659
480	0.388	0.388780	0.388803	0.0001555	0.0003888	0.27216179	90.3350163
100%	0.430	0.430341	0.430401	0.0001722	0.0004304	0.30128050	100
D2							
Time	**Irifloph-3-C-glc (mg/L)**	**Corr 1 (mg/1000 ml)**	**Corr 2 (mg/1000 ml)**	**Conc in 0.4 ml (sample)**	**Conc in 1 ml (sample)**	**Cumulative mg (Iri-3-C-glc)**	**% Dissolution**
0	**0.000**	**0**	**0**	**0**	**0**	**0**	**0**
15	0.000	0	0	0	0	0	0
30	0.096	0.09607581	0.09621326	0.00003849	0.00009621	0.06734928	22.3543440
60	0.130	0.12981743	0.12986570	0.00005195	0.00012987	0.09090599	30.1732073
120	0.334	0.33429201	0.33458473	0.00013383	0.00033459	0.23420931	77.7379588
180	0.342	0.34205169	0.34206306	0.00013683	0.00034206	0.23944414	79.4754839
300	0.412	0.41207146	0.41217231	0.00016487	0.00041217	0.28852062	95.7647824
480	0.442	0.44250875	0.44255299	0.00017702	0.00044255	0.30978709	102.823478
100%	0.439	0.43975172	0.43974862	0.00017590	0.00043975	0.30782403	102.171907
D3							
Time	**Irifloph-3-C-glc (mg/L)**	**Corr 1 (mg/1000 ml)**	**Corr 2 (mg/1000 ml)**	**Conc in 0.4 ml (sample)**	**Conc in 1 ml (sample)**	**Cumulative mg (Iri-3-C-glc)**	**% Dissolution**

0	**0.000**	**0**	**0**	**0**	**0**	**0**	**0**
15	0.000	0	0	0	0	0	0
30	0.080	0.07970162	0.07981564	0.00003193	0.00007982	0.05587095	18.5444943
60	0.140	0.14052877	0.14061579	0.00005625	0.00014062	0.09843105	32.6708997
120	0.277	0.27689989	0.27709514	0.00011084	0.00027710	0.1939666	64.3807340
180	0.311	0.31116567	0.31121498	0.00012449	0.00031122	0.21785049	72.3081926
300	0.338	0.33875126	0.33879129	0.00013552	0.00033879	0.23715390	78.7153167
480	0.395	0.39526461	0.39534609	0.00015814	0.00039535	0.27674226	91.8553508
100%	0.399	0.40001256	0.40002004	0.00016001	0.00040002	0.28001403	92.941304

Table D.5.10.1: The average % dissolution data and standard deviation of I3G rich fraction for PP MUPS tablet

Average:	**Time**	**% Dissolution**	**Stdev**
	0	**0**	**0**
	15	0	0
	30	25.64539767	7.511028208
	60	37.34049859	8.431828363
	120	74.04571779	6.897299244
	180	77.95514942	4.132333867
	300	87.113355	6.962720965
	480	95.00461514	5.563501372
		98.37107015	3.940479224

Table D.5.11: The dissolution data of mangiferin rich fraction for PP MUPS tablet

D1							
Time	**Mangiferin (mg/L)**	**Corr 1 (mg/1000 ml)**	**Corr 2 (mg/1000 ml)**	**Conc in 0.4 ml (sample)**	**Conc in 1 ml (sample)**	**Cumulative mg (Mangiferin)**	**% Dissolution**
0	**0.000**	**0**	**0**	**0**	**0**	**0**	**0**
15	0.031	0.030698	0.0306984	0.0000123	0.0000307	0.02148890	2.4176484
30	0.186	0.185991	0.1862121	0.0000745	0.0001862	0.13034850	14.665100
60	0.285	0.285721	0.2858636	0.0001143	0.0002859	0.20010451	22.513128
120	0.546	0.546602	0.5469756	0.0002188	0.0005470	0.38288292	43.076952
180	0.841	0.842143	0.8425662	0.0003370	0.0008426	0.58979633	66.356128
300	0.961	0.961807	0.9619797	0.0003848	0.0009620	0.67338581	75.760517
480	1.186	1.187868	1.1881927	0.0004753	0.0011882	0.8317349	93.575875
100%	1.268	1.269645	1.2697639	0.0005079	0.0012698	0.88883476	100
D2							
Time	**Mangiferin (mg/L)**	**Corr 1 (mg/1000 ml)**	**Corr 2 (mg/1000 ml)**	**Conc in 0.4 ml (sample)**	**Conc in 1 ml (sample)**	**Cumulative mg (Mangiferin)**	**% Dissolution**
0	**0.000**	**0**	**0**	**0**	**0**	**0**	**0**
15	0.076	0.0763602	0.0763602	0.0000305	0.00007636	0.05345212	6.01372930

30	0.133	0.1335715	0.1336534	0.0000535	0.00013365	0.09355735	10.5258431
60	0.226	0.2260244	0.2261568	0.0000905	0.00022616	0.15830977	17.8109336
120	0.614	0.6141158	0.6146713	0.0002459	0.00061467	0.43026992	48.4083137
180	0.875	0.8758290	0.8762038	0.0003505	0.00087620	0.61334266	69.0052514
300	1.056	1.0571658	1.0574265	0.0004230	0.00105743	0.74019853	83.2774059
480	1.263	1.2648399	1.2651388	0.0005061	0.00126514	0.88559714	99.6357455
100%	1.283	1.2852899	1.2853213	0.0005141	0.00128532	0.89972494	101.225220
D3							
Time	**Mangiferin (mg/L)**	**Corr 1 (mg/1000 ml)**	**Corr 2 (mg/1000 ml)**	**Conc in 0.4 ml (sample)**	**Conc in 1 ml (sample)**	**Cumulative mg (Mangiferin)**	**% Dissolution**
0	**0.000**	**0**	**0**	**0**	**0**	**0**	**0**
15	0.041	0.0405008	0.0405008	0.0000162	0.00004.050	0.02835055	3.18963114
30	0.128	0.1276421	0.1277668	0.0000511	0.00012777	0.08943674	10.0622465
60	0.261	0.2608652	0.2610558	0.0001044	0.00026106	0.18273909	20.5593996
120	0.591	0.5910728	0.5915455	0.0002366	0.00059155	0.41408181	46.5870411
180	0.718	0.7183449	0.7185275	0.0002874	0.00071853	0.50296922	56.5874834
300	1.028	1.0292295	1.0296754	0.0004119	0.00102968	0.72077281	81.0918788
480	1.084	1.0850961	1.0851775	0.0004341	0.00108518	0.75962426	85.4629331
100%	1.228	1.2296104	1.2298193	0.0004919	0.00122982	0.86087349	96.8541654

Table D.5.11.1: The average % dissolution data and standard deviation of mangiferin rich fraction for PP MUPS tablet

Average:	Time	% Dissolution	Stdev
	0	**0**	**0**
	15	3.873669606	1.545721186
	30	11.75106289	2.069208494
	60	20.29448719	1.928780763
	120	46.02410225	2.212619777
	180	63.98295412	5.340050179
	300	80.04326725	3.157065514
	480	92.89151776	5.806227191
		99.35979508	1.841000755

Table D.5.12: The dissolution data of isomangiferin rich fraction for PP MUPS tablet

D1							
Time	**Isomangiferin (mg/L)**	**Corr 1 (mg/1000 ml)**	**Corr 2 (mg/1000 ml)**	**Conc in 0.4 ml (sample)**	**Conc in 1 ml (sample)**	**Cumulative mg (Isomangiferin)**	**% Dissolution**
0	**0.000**	**0**	**0**	**0**	**0**	**0**	**0**
15	0.000	0	0	0	0	0	0
30	0.044	0.0438731	0.0439359	0.0000176	0.0000439	0.030755124	14.661654
60	0.066	0.0660599	0.0660916	0.0000264	0.0000661	0.046264118	22.055138
120	0.116	0.1163393	0.1164113	0.0000465	0.0001164	0.081487936	38.847118
180	0.175	0.1749086	0.1749925	0.0000610	0.0001750	0.122494768	58.395990
300	0.223	0.2229901	0.2230591	0.00008.9	0.0002231	0.156141399	74.436090
480	0.277	0.2774314	0.2775096	0.0001110	0.0002775	0.194256724	92.606516
100 %	0.299	0.2996331	0.2996653	0.0001199	0.0002997	0.209765718	100
D2							
Time	**Isomangiferin (mg/L)**	**Corr 1 (mg/1000 ml)**	**Corr 2 (mg/1000 ml)**	**Conc in 0.4 ml (sample)**	**Conc in 1 ml (sample)**	**Cumulative mg (Isomangiferin)**	**% Dissolution**
0	**0.000**	**0**	**0**	**0**	**0**	**0**	**0**
15	0.000	0	0	0	0	0	0
30	0.042	0.041623	0.0416828	0.0000167	0.0000417	0.029177938	13.909774
60	0.057	0.057057	0.0570791	0.0000228	0.0000571	0.039955375	19.047619
120	0.129	0.129451	0.1295546	0.0000518	0.0001296	0.090688186	43.233083
180	0.182	0.182052	0.1821274	0.0000729	0.0001821	0.127489189	60.776942
300	0.225	0.224875	0.2249367	0.0000900	0.0002249	0.157455721	75.062657
480	0.284	0.284559	0.2846445	0.0001139	0.0002846	0.199251146	94.987469
100 %	0.303	0.303393	0.3034205	0.0001214	0.0003034	0.212394361	101.25313
D3							
Time	**Isomangiferin (mg/L)**	**Corr 1 (mg/1000 ml)**	**Corr 2 (mg/1000 ml)**	**Conc in 0.4 ml (sample)**	**Conc in 1 ml (sample)**	**Cumulative mg (Isomangiferin)**	**% Dissolution**
0	**0.000**	**0**	**0**	**0**	**0**	**0**	**0**
15	0.000	0	0	0	0	0	0
30	0.042	0.041808	0.041867	0.000017	0.0000419	0.029307136	13.971366
60	0.063	0.063057	0.063087	0.000025	0.0000631	0.044161204	21.052632
120	0.121	0.120835	0.120918	0.000048	0.0001209	0.084642307	40.350877
180	0.160	0.160291	0.160347	0.000064	0.0001604	0.11224306	53.508772
300	0.229	0.229344	0.229443	0.000092	0.0002294	0.160610092	76.566416
480	0.268	0.268441	0.268497	0.000107	0.0002685	0.18794798	89.598998
100 %	0.303	0.303746	0.303796	0.000122	0.0003038	0.212657225	101.37845

Table D.5.12.1: The average % dissolution data and standard deviation of isomangiferin rich fraction for PP MUPS tablet

Average:	Time	% Dissolution	Stdev
	0	**0**	**0**
	15	0	0
	30	14.1809315	0.340850964
	60	20.71846282	1.250344991
	120	40.81035923	1.819801246
	180	57.56056809	3.025450119
	300	75.3550543	0.893940458
	480	92.39766082	2.204785835
		100.877193	0.622375289

Table D.5.13: The dissolution data of IDG rich fraction in PDC MUPS tablet

D4							
Time	**Irifloph-di-O-C-glc (mg/L)**	**Corr 1 (mg/1000 ml)**	**Corr 2 (mg/1000 ml)**	**Conc in 0.4 ml (sample)**	**Conc in 1 ml (sample)**	**Cumulative mg (Iri-di-O,C-glc)**	**% Dissolution**
0	**0.000**	**0**	**0**	**0**	**0**	**0**	**0**
15	0.188	0.187901	0.187901	0.0000752	0.0001879	0.13153078	55.253162
30	0.251	0.251078	0.251169	0.0001005	0.0002512	0.17581796	73.857223
60	0.303	0.303494	0.303569	0.0001214	0.0003036	0.21249844	89.265880
120	0.317	0.317679	0.317700	0.0001271	0.0003177	0.22238981	93.421023
180	0.318	0.318287	0.318289	0.0001273	0.0003183	0.22280195	93.594154
300	0.329	0.329459	0.329475	0.0001318	0.0003295	0.23063261	96.883642
480	0.335	0.335942	0.335952	0.0001344	0.0003360	0.23516616	98.788083
100%	0.340	0.340067	0.340073	0.0001360	0.0003401	0.23805113	100
D5							
Time	**Irifloph-di-O-C-glc (mg/L)**	**Corr 1 (mg/1000 ml)**	**Corr 2 (mg/1000 ml)**	**Conc in 0.4 ml (sample)**	**Conc in 1 ml (sample)**	**Cumulative mg (Iri-di-O,C-glc)**	**% Dissolution**
0	**0.000**	**0**	**0**	**0**	**0**	**0**	**0**
15	0.186	0.1855494	0.1855494	0.00007422	0.00018555	0.12988457	54.5616274
30	0.247	0.2469593	0.2470471	0.00009882	0.00024705	0.17293298	72.6453057
60	0.292	0.2923173	0.2923825	0.00011695	0.00029238	0.20466778	85.9763909
120	0.303	0.3035526	0.3035692	0.00012143	0.00030357	0.21249844	89.2658795
180	0.306	0.3065082	0.3065131	0.00012261	0.00030651	0.21455914	90.1315343
300	0.310	0.3106280	0.3106345	0.00012425	0.00031063	0.21744412	91.3434512
480	0.314	0.3147493	0.3147559	0.00012590	0.00031476	0.22032911	92.5553680
100%	0.315	0.3159311	0.3159334	0.00012637	0.00031593	0.22115339	92.9016300
D6							
Time	**Irifloph-di-O-C-glc (mg/L)**	**Corr 1 (mg/1000 ml)**	**Corr 2 (mg/1000 ml)**	**Conc in 0.4 ml (sample)**	**Conc in 1 ml (sample)**	**Cumulative mg (Iri-di-O,C-glc)**	**% Dissolution**
0	**0.000**	**0**	**0**	**0**	**0**	**0**	**0**
15	0.178	0.1784942	0.17849422	0.00007140	0.00017849	0.12494596	52.4870237

30	0.243	0.2434216	0.24351448	0.00009741	0.00024351	0.17046013	71.6065198
60	0.321	0.3217088	0.32182113	0.00012873	0.00032182	0.22527479	94.6329397
120	0.323	0.3235843	0.32358744	0.00012944	0.00032359	0.22651121	95.1523327
180	0.336	0.3365213	0.33654042	0.00013462	0.00033654	0.23557830	98.9612141
300	0.338	0.3383035	0.33830674	0.00013532	0.00033830	0.23681472	99.4806071
480	0.338	0.3388940	0.33889551	0.00013556	0.00033890	0.23722686	99.6537381
100%	0.341	0.3418345	0.34183937	0.00013674	0.00034184	0.23928756	100.519393

Table D.5.13.1: The average % dissolution data and standard deviation of IDG rich fraction for PDC MUPS tablet

Average:	Time	% Dissolution	Stdev
	0	**0**	**0**
	15	54.10060436	1.175382784
	30	72.70301601	0.919751241
	60	89.95840335	3.567786564
	120	92.61307833	2.470109801
	180	94.22896744	3.632542966
	300	95.90256689	3.393641943
	480	96.99906307	3.161978177
		97.80700763	3.475100942

Table D.5.14: The dissolution data of I3G rich fraction for PDC MUPS tablet

D4							
Time	**Irifloph-3-C-glc (mg/L)**	**Corr 1 (mg/1000 ml)**	**Corr 2 (mg/1000 ml)**	**Conc in 0.4 ml (sample)**	**Conc in 1 ml (sample)**	**Cumulative mg (Iri-3-C-dlc)**	**% Dissolution**
0	**0.000**	**0**	**0**	**0**	**0**	**0**	**0**
15	0.139	0.139482	0.1394815	0.0000558	0.0001395	0.09763702	30.96157
30	0.184	0.184487	0.1845509	0.0000738	0.0001846	0.12918565	40.96592
60	0.193	0.193418	0.1934314	0.0000774	0.0001934	0.13540201	42.93718
120	0.239	0.239637	0.2397035	0.0000959	0.0002397	0.16779248	53.20849
180	0.280	0.280308	0.2803669	0.0001122	0.0002804	0.19625684	62.23479
300	0.403	0.403582	0.4037592	0.0001615	0.0004038	0.28263144	89.62494
480	0.445	0.445764	0.4458248	0.0001783	0.0004458	0.31207733	98.96249
100%	0.450	0.450491	0.4504987	0.0001802	0.0004505	0.31534910	100
D5							
Time	**Irifloph-3-C-glc (mg/L)**	**Corr 1 (mg/1000 ml)**	**Corr 2 (mg/1000 ml)**	**Conc in 0.4 ml (sample)**	**Conc in 1 ml (sample)**	**Cumulative mg (Iri-3-C-dlc)**	**% Dissolution**
0	**0.000**	**0**	**0**	**0**	**0**	**0**	**0**
15	0.160	0.16001746	0.16001746	0.00006401	0.00016002	0.11201222	35.5200700
30	0.216	0.21672006	0.21680118	0.00008672	0.00021680	0.15176083	48.1247066
60	0.234	0.23453638	0.23456219	0.00009383	0.00023456	0.16419354	52.0672289

120	0.240	0.24016244	0.24017093	0.00009607	0.00024017	0.16811965	53.3122359
180	0.328	0.32791518	0.32804120	0.00013122	0.00032804	0.22962884	72.8173463
300	0.349	0.34979423	0.34982602	0.00013993	0.00034983	0.24487821	77.6530574
480	0.363	0.36354289	0.36356323	0.00014543	0.00036356	0.25449426	80.7023909
100%	0.408	0.40836831	0.40843315	0.00016337	0.00040843	0.28590321	90.6624472
D6							
Time	**Irifloph-3-C-glc (mg/L)**	**Corr 1 (mg/1000 ml)**	**Corr 2 (mg/1000 ml)**	**Conc in 0.4 ml (sample)**	**Conc in 1 ml (sample)**	**Cumulative mg (Iri-3-C-dlc)**	**% Dissolution**
0	**0.000**	**0**	**0**	**0**	**0**	**0**	**0**
15	0.000	0	0	0	0	0	0
30	0.159	0.1590840	0.15931159	0.00006373	0.00015931	0.11151811	35.3633844
60	0.332	0.3324671	0.33271515	0.00013309	0.00033272	0.23290061	73.8548521
120	0.343	0.3434492	0.34346524	0.00013739	0.00034347	0.24042567	76.2411156
180	0.374	0.3742685	0.37431331	0.00014973	0.00037431	0.26201932	83.0886544
300	0.420	0.4205186	0.42058542	0.00016823	0.00042059	0.29440980	93.3599624
480	0.420	0.4210513	0.42105282	0.00016842	0.00042105	0.29473697	93.4637130
100%	0.434	0.4350538	0.43507467	0.00017403	0.00043508	0.30455227	96.5762306

Table D.5.14.1: The average % dissolution data and standard deviation of I3G rich fraction for PDC MUPS tablet

Average:	**Time**	**% Dissolution**	**Stdev**
	0	**0**	**0**
	15	22.16054524	15.77999397
	30	41.48466904	5.222685413
	60	56.28641943	12.96988387
	120	60.9206123	10.83331459
	180	72.71359567	8.513872023
	300	86.87932037	6.699778237
	480	91.04286601	7.648669521
		95.74622594	3.856955101

Table D.5.15: The dissolution data of mangiferin rich fraction for PDC MUPS tablet

D4							
Time	**Mangiferin (mg/L)**	**Corr 1 (mg/1000 ml)**	**Corr 2 (mg/1000 ml)**	**Conc in 0.4 ml (sample)**	**Conc in 1 ml (sample)**	**Cumulative mg (Mangiferin)**	**% Dissolution**
0	**0.000**	**0**	**0**	**0**	**0**	**0**	**0**
15	0.164	0.16411291	0.1641129	0.0000657	0.0001641	0.11487903	11.390
30	0.284	0.28443005	0.2846022	0.0001138	0.0002846	0.19922152	19.752
60	0.431	0.43113607	0.4313463	0.0001725	0.0004314	0.30194240	29.936
120	0.696	0.69670297	0.6970835	0.0002788	0.0006971	0.48795843	48.378
180	0.953	0.95404223	0.9544113	0.0003818	0.0009544	0.66808788	66.237

300	1.196	1.19705194	1.1974010	0.0004790	0.0011974	0.83818071	83.101
480	1.375	1.37630499	1.3765634	0.0005506	0.0013766	0.96359437	95.535
100%	1.439	1.44080062	1.4408953	0.0005764	0.0014409	1.00862673	100.000
D5							
Time	**Mangiferin (mg/L)**	**Corr 1 (mg/1000 ml)**	**Corr 2 (mg/1000 ml)**	**Conc in 0.4 ml (sample)**	**Conc in 1 ml (sample)**	**Cumulative mg (Mangiferin)**	**% Dissolution**
0	**0.000**	**0**	**0**	**0**	**0**	**0**	**0**
15	0.211	0.211138297	0.2111383	0.0000845	0.0002111	0.14779681	14.653
30	0.327	0.327323923	0.3274901	0.0001310	0.0003275	0.22924310	22.728
60	0.455	0.455129819	0.4553131	0.0001821	0.0004553	0.31871916	31.599
120	0.716	0.716471032	0.7168456	0.0002867	0.0007169	0.50179191	49.750
180	0.911	0.912503333	0.9127847	0.0003651	0.0009128	0.63894930	63.348
300	1.061	1.062676281	1.0628926	0.0004252	0.0010629	0.74402481	73.766
480	1.100	1.101938284	1.1019963	0.0004408	0.0011020	0.77139742	76.480
100%	1.337	1.338800502	1.3391415	0.0005357	0.0013391	0.93739907	92.938
D6							
Time	**Mangiferin (mg/L)**	**Corr 1 (mg/1000 ml)**	**Corr 2 (mg/1000 ml)**	**Conc in 0.4 ml (sample)**	**Conc in 1 ml (sample)**	**Cumulative mg (Mangiferin)**	**% Dissolution**
0	**0.000**	**0**	**0**	**0**	**0**	**0**	**0**
15	0.105	0.104896181	0.1048962	0.0000420	0.0001049	0.07342733	7.280
30	0.248	0.24823667	0.2484417	0.0000994	0.0002484	0.17390922	17.242
60	0.601	0.601551532	0.6020572	0.0002408	0.0006021	0.42144004	41.784
120	0.942	0.942570193	0.9430586	0.0003772	0.0009431	0.66014100	65.449
180	1.172	1.173565033	1.1738967	0.0004696	0.0011739	0.82172771	81.470
300	1.218	1.219660113	1.2197280	0.0004879	0.0012197	0.85380959	84.651
480	1.370	1.372138145	1.3723584	0.0005489	0.0013724	0.96065108	95.243
100%	1.475	1.476903399	1.4770558	0.0005908	0.0014771	1.03393904	102.510

Table D.5.15.1: The average % dissolution data and standard deviation of mangiferin rich fraction for PDC MUPS tablet

Average:	Time	% Dissolution	Stdev
	0	**0**	**0**
	15	11.108	3.016752443
	30	19.907	2.242377317
	60	34.440	5.237152169
	120	54.526	7.744339998
	180	70.352	7.9496086
	300	80.506	4.807614479
	480	89.086	8.914774402
		98.483	4.052158026

Table D.5.16: The dissolution data of isomangiferin rich fraction for PDC MUPS tablet

D4							
Time	**Isomangiferin (mg/L)**	**Corr 1 (mg/1000 ml)**	**Corr 2 (mg/1000 ml)**	**Conc in 0.4 ml (sample)**	**Conc in 1 ml (sample)**	**Cumulative mg (Isomangiferin)**	**% Dissolution**
0	**0.000**	**0**	**0**	**0**	**0**	**0**	**0**
15	0.042	0.0423732	0.0423732	0.0000170	0.000042	0.029661233	12.925381
30	0.071	0.0713075	0.0713489	0.0000285	0.000071	0.049944219	21.764032
60	0.106	0.1058473	0.1058968	0.0000424	0.000106	0.074127735	32.302406
120	0.158	0.1580193	0.1580941	0.0000632	0.000158	0.110665874	48.224513
180	0.206	0.2064667	0.2065362	0.0000826	0.000207	0.144575369	63.001146
300	0.258	0.2579086	0.2579825	0.0001032	0.000258	0.18058778	78.694158
480	0.327	0.3277290	0.3278293	0.0001311	0.000328	0.229480541	100
100 %	0.327	0.3278287	0.3278293	0.0001311	0.000328	0.229480541	100
D5							
Time	**Isomangiferin (mg/L)**	**Corr 1 (mg/1000 ml)**	**Corr 2 (mg/1000 ml)**	**Conc in 0.4 ml (sample)**	**Conc in 1 ml (sample)**	**Cumulative mg (Isomangiferin)**	**% Dissolution**
0	**0.000**	**0**	**0**	**0**	**0**	**0**	**0**
15	0.051	0.0509978	0.0509978	0.0000204	0.000051	0.035698475	15.556210
30	0.076	0.0758196	0.0758551	0.0000303	0.000076	0.05309859	23.138603
60	0.106	0.1062287	0.1062723	0.0000425	0.000106	0.074390599	32.416953
120	0.168	0.1681444	0.1682332	0.0000673	0.000169	0.11776321	51.317297
180	0.182	0.1824822	0.1825029	0.0000730	0.000183	0.127752054	55.670103
300	0.223	0.2237508	0.2238102	0.0000895	0.000224	0.156667128	68.270332
480	0.290	0.2901819	0.2902773	0.0001161	0.000291	0.20319411	88.545246
100 %	0.341	0.3416495	0.3417236	0.0001367	0.000342	0.23920652	104.23826
D6							
Time	**Isomangiferin (mg/L)**	**Corr 1 (mg/1000 ml)**	**Corr 2 (mg/1000 ml)**	**Conc in 0.4 ml (sample)**	**Conc in 1 ml (sample)**	**Cumulative mg (Isomangiferin)**	**% Dissolution**
0	**0.000**	**0**	**0**	**0**	**0**	**0**	**0**
15	0.000	0	0	0	0	0	0
30	0.066	0.065622	0.0657161	0.0000263	0.000066	0.04600125	20.0458
60	0.124	0.124588	0.1246728	0.0000499	0.000125	0.08727100	38.0298
120	0.188	0.188045	0.1881357	0.0000753	0.000188	0.13169502	57.3883
180	0.231	0.231259	0.2313206	0.0000925	0.000231	0.16192441	70.5613
300	0.273	0.273693	0.2737544	0.0001095	0.000274	0.19162808	83.5052
480	0.332	0.332251	0.3323356	0.0001329	0.000332	0.23263491	101.375
100 %	0.337	0.337585	0.3375929	0.0001350	0.000338	0.23631501	102.978

Table D.5.16.1: The average % dissolution data and standard deviation of isomangiferin rich fraction for PDC MUPS tablet

Average:	Time	% Dissolution	Stdev
	0	**0**	**0**
	15	9.49386352	6.798548847
	30	21.64948454	1.265218902
	60	34.24971363	2.673321277
	120	52.31004200	3.806396258
	180	63.07751050	6.079538522
	300	76.82321497	6.358735454
	480	96.63993891	5.751254795
		102.40549828	1.777025778

D.6 Graphic illustration of the MUPS tests

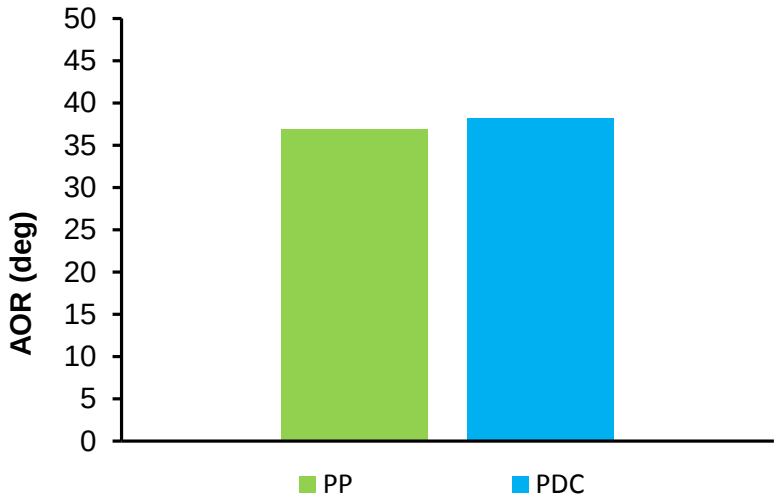

Figure D.6.1: Graphic illustration of the angle of repose data for PP and PDC

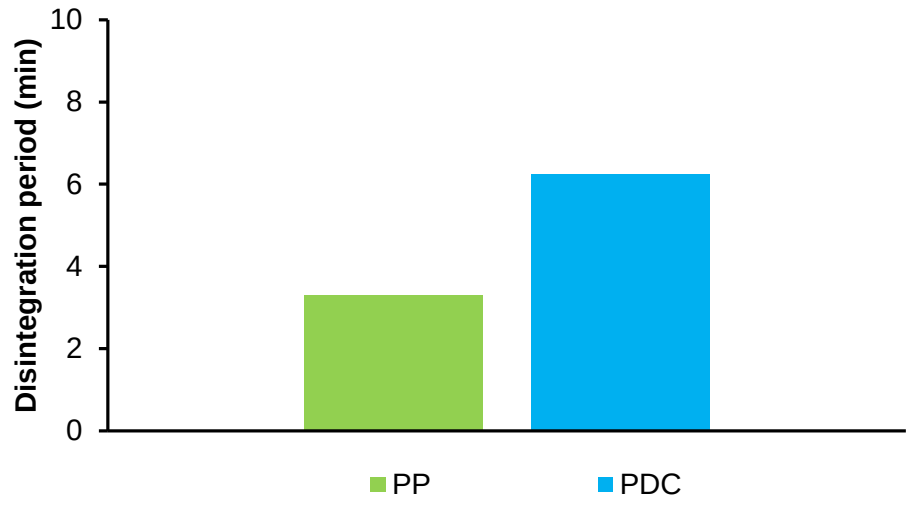

Figure D.6.2: Graphic illustration of MUPS PP and PDC polymers disintegration period data

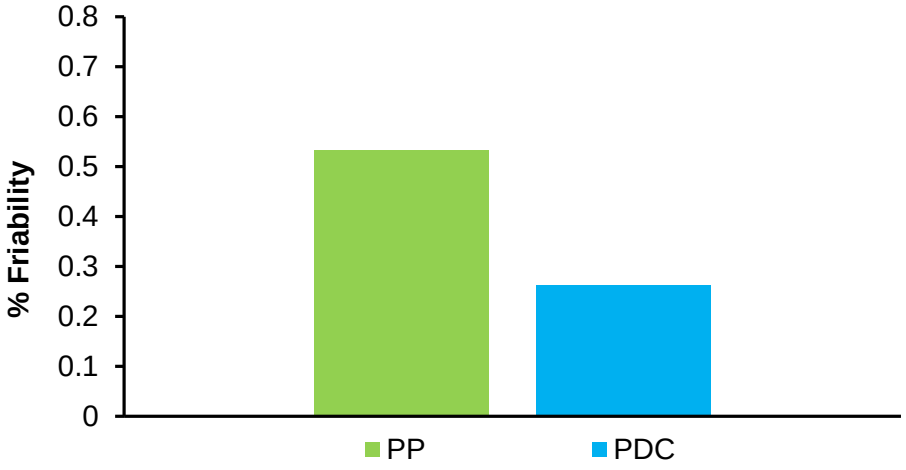

Figure D.6.3: Graphic illustration of MUPS PP and PDC polymers percentage friability data

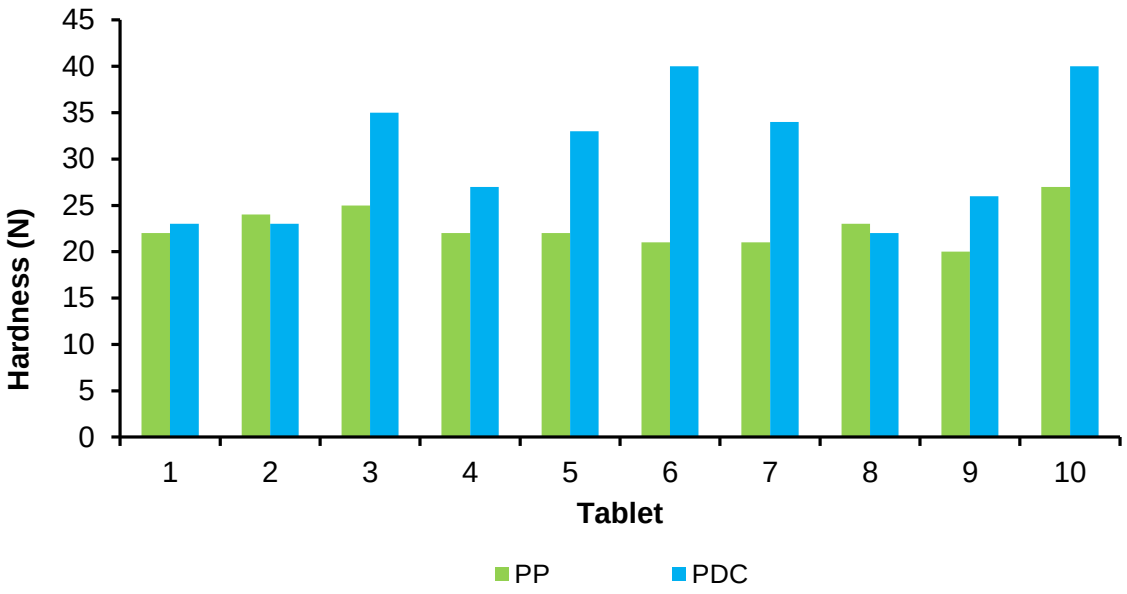

Figure D.6.4: Graphic illustration of MUPS PP and PDC hardness data